DEVELOPMENT AND GAS PERMEATION STUDY OF FLAT ASYMMETRIC POLYPHENYLENE OXIDE MEMBRANES

Sylvie M. Gagné

A thesis submitted to the School of Graduate Studies and Research
in partial fulfillment of the requirements for the degree of
MASTER OF APPLIED SCIENCE
in the Department of Chemical Engineering
University of Ottawa

January 1996

ISBN 0-612-15718-0

UNIVERSITÉ D'OTTAWA
UNIVERSITY OF OTTAWA

Abstract

Natural gas is a mixture of hydrocarbon gases and impurities. Processing is required to recover valuable hydrocarbon liquids, remove water vapor, and increase the heating value of the gas before it can be sold to consumers. In addition, the removal of acid gases such as hydrogen sulfide and carbon dioxide is necessary to prevent hydrate formation and corrosion.

When compared to other gas separation processes such as cryogenics, adsorption and absorption, membrane separation for gases must compete primarily on the basis of overall economics and convenience. The use of membrane separation for natural gas processing would reduce the size and weight of the processing units and should require less maintenance and operator supervision, at a lower capital cost. For these reasons, membrane processing systems are particularly well suited for remote sites such as off-shore platforms.

Asymmetric gas separation membranes were prepared from polyphenylene oxide (PPO) and modified PPO and tested for CO_2/CH_4 separation. Using a fractional factorial design, a study of membrane casting conditions was completed in order to optimize the flux and the selectivity of the membrane. A membrane with a CO_2/CH_4 pure gas permeation rate ratio of 119 and a CO_2 permeation rate of 6.8×10^{-9} moles/(m^2 s Pa) was obtained.

Acknowledgments

I wish to thank my family and friends for their constant support, Dr. T. Matsuura for his encouragement, guidance and advice. I also acknowledge everyone at the Industrial Membrane Research Institute for their helpful discussions and suggestions.

The financial support of British (Consumer) Gas is gratefully acknowledged.

Contents

List of Tables

List of Figures

Nomenclature

A	species or factor
a	treatment
B	species or factor
b	treatment
C	factor
c	treatment, concentration
D	diffusion coefficient, cm^2/s or factor
D_0	preexponential factor, dimensionless
d	treatment
E	enrichment, dimensionless
E_D	activation energy, J/mol
E_s	enthalpy of sorption, J/mol
$E(Y)$	predicted value of the response
I	identity element
J	flux, kg/m^2s
J_v	volumetric flux, m/s
L	thickness of the active layer, m
P	permeability coefficient, Barrer=10^{-10} cm^3 (STP)·cm/(cm^2·s·cm Hg)
p	pressure or partial pressure, $kg/(m\ s^2)$

R gas constant, = 82.0567 cm^3 atm/ deg. mole

R^2 coefficient of multiple determination, dimensionless

S solubility, cm^3 (STP)/(cm^3 polymer· atm)

S_0 preexponential factor, dimensionless

SS single degree of freedom sum of square

T temperature, K

T_g glass transition temperature, K

T_m melting temperature, K

v local volume fraction, dimensionless or specific volume, m^3

v_0 volume of the molecules, m^3

v_f fractional free volume, dimensionless

v_{fs}° fractional free volume at reference temperature and pressure, dimensionless

x position coordinate or mole fraction in feed, dimensionless

Y response

y mole fraction in permeate, dimensionless

Greek Letters

α thermal expansion coefficient, dimensionless

α_{ij} separation factor, dimensionless

β compressibility, dimensionless or parameters for factors

γ plasticization parameter, dimensionless

δ solubility parameter, $(J/m^3)^{1/2}$

σ standard deviation

ϕ local volume fraction of penetrant, dimensionless

subscripts

D Henry

d dispersive

E error

f feed

H Langmuir

h hydrogen bonds

i species i

j species j

p polar, permeate

s reference

T total

t total

superscript

k number of factors in factorial design

1. Introduction

1.1 Membranes and the Membrane Industry

The most general definition of a membrane is given by Ho and Sirkar (1992):

> *The membrane is an interphase between two bulk phases which controls the exchange of mass between the two bulk phases.*

The membrane phase may be one or a combination of solids, liquids or a gel. A membrane can be thick or thin. Its structure can be homogeneous or heterogeneous. Membranes can be biological or synthetic, neutral or charged. Synthetic membranes can be further subdivided into organic or inorganic membranes (Mulder, 1991).

In membrane separation processes, the bulk phases are mixtures. The membrane is selective to one or more of the species in the feed mixture. These species are exchanged preferentially through the membrane so that one of the bulk phases becomes enriched with the species while the other becomes depleted.

The movement of any species across the membrane is caused by one or more driving forces. These driving forces arise from a gradient in chemical potential or electrical potential across the membrane.

Generally, membrane processes are operated in cross-flow mode (Figure 1.1): the feed is separated into two streams, one that goes through the membrane, the permeate, and a fraction of the feed that does not go through the membrane, the retentate or concentrate (residue gas). Either the permeate or the retentate is the desired product stream (Ho and Sirkar, 1992).

Membrane separation technology is based on the principle that components in gaseous or liquid mixtures pass through, or permeate, membrane structures at different rates due to their molecular characteristics. Different types of membranes and membrane processes (Table 1.1) have been developed for

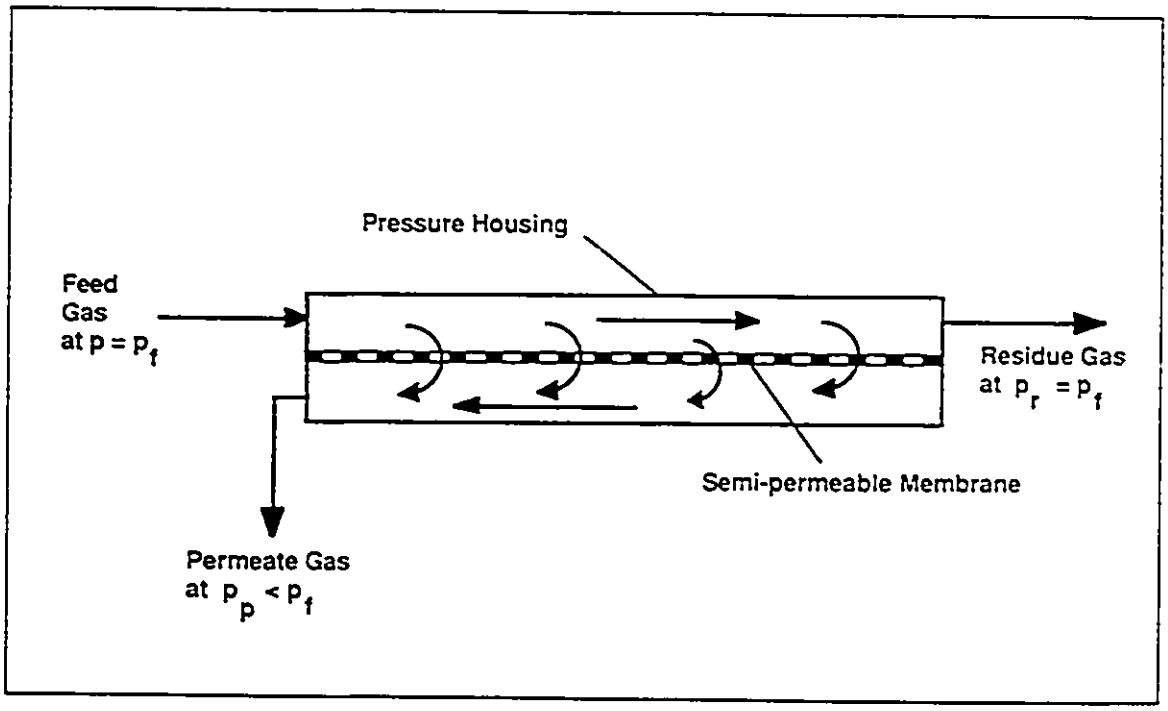

Figure 1.1 *Schematic diagram of cross-flow filtration mode for the membrane separation of gases (Zolandz and Fleming, 1992).*

different applications (Franken and Fane, 1990).

Table 1.1 Membrane processes and some applications

Membrane Process	Driving Force	Example of Applications
Electrodialysis (ED)	Electrical potential difference	desalination of brackish water removal of metals in wastewater
Microfiltration (MF)	Pressure difference (10-100 kPa)	removal of colloids from waste streams removal of dust particles from air
Ultrafiltration (UF)	Pressure difference (0.1-1 MPa)	separation of oil/water emulsions recovery of proteins recovery of electrophoretic paints
Nanofiltration (NF)	Pressure difference (0.5-2 MPa)	treatment of electroplating rinse water
Reverse Osmosis (RO)	Pressure difference (2-10 MPa)	desalination of sea water removal of nitrate from ground water
Liquid Membranes (LM)	Concentration difference	recovery of plating chemicals
Gas Separation (GS)	Pressure difference (2-10 MPa)	air separation removal of CO_2 from methane
Vapor Permeation (VP)	Partial pressure difference	removal of condensable solvents from air
Pervaporation (PV)	Partial pressure difference	dehydration of solvents removal of organics from wastewater
Membrane Distillation (MD)	Temperature difference	desalination of brine

Membrane separation was not considered a technically important separation process until 30 years ago (Mulder, 1991). Today, membrane systems are replacing a number of older, more costly separation technologies such as distillation, cryogenics, pressure swing adsorption, and mercury or asbestos diaphragm electrolytic processes. Generally, membrane systems offer lower costs, less maintenance, and more flexibility than the older technologies. For example, they are often smaller in size and have a modular design, making them easy to fit in an existing plant without requiring new construction. This reduces the capital cost and construction time. They also offer flexibility of operation as membrane modules can be turned on or off depending on the plant output. In addition, most membrane separations do not involve a phase change and therefore are energy efficient (Weber and Bowman, 1986, Franken and Fane, 1990).

Potential disadvantages of membranes are concentration polarization and fouling which can reduce the performance of the membrane in liquid separations. Membranes prepared from polymeric materials may be damaged by high temperatures, extreme pH, and the use of chlorine and organic solvents. Because they are usually operated in split flow mode, a complete separation cannot be achieved using solely a membrane process (Franken and Fane, 1990).

Gas permeation was first discovered by J. K. Mitchell in 1830, when he observed hydrogen permeation through natural rubber. Around the same time, A. Fick formulated what is known today as Fick's first law after studying gas transport across nitro-cellulose membranes. In 1866, Sir Thomas Graham made quantitative measurements of gas permeation rates and proposed the "solution-diffusion" mechanism of transport of the gases through the membranes. He was the first to separate gases by membrane and attempted gas permeation across a variety of membrane materials, including metals.

In the 1950s and 1960s, many synthetic polyolefins and other vinylic-type polymers were developed and their gas permeability was studied, mostly for packaging applications. A breakthrough in membrane separation came in 1962 with the development of asymmetric reverse osmosis membranes made of cellulose acetate by Loeb and Sourirajan (1963). Interest in gas separation materials intensified in the 1970s, leading to the first commercial membrane separator, the Prism® which was developed by Monsanto (Henis, 1994).

One of the first applications of gas separation membranes was in H_2 separation and recovery in ammonia purge and recycle streams. In petrochemical and refinery applications, membranes have been used to recover H_2 from hydrotreaters, hydrodesulfurization processes and purge gases to recycle back to the plant, and for syngas ratio adjustment. Membranes are also used for air separation to produce nitrogen for inert gas blanketing and O_2

enriched air for medical applications. There are three major carbon dioxide membrane separation applications: CO_2 recovery from landfill gas, separation of CO_2 used in enhanced oil recovery from hydrocarbons, and natural gas processing. Also, gas separation membranes can be used for solvent vapor recovery, air dehydration, and helium recovery (Spillman, 1989).

1.2 Present Separation Technology in the Natural Gas Industry

Natural gas occurs usually in the gaseous state under pressure in sedimentary, porous underground rock layers (Medici, 1974). It is a mixture of hydrocarbon gases and impurities. Each gas stream produced has its own composition which may change as the natural gas reservoir becomes depleted. The hydrocarbons most commonly found in natural gas are methane, ethane, propane, butanes, pentanes and small amounts of heavier hydrocarbons. The impurities found in natural gas include carbon dioxide, hydrogen sulfide, nitrogen, and water vapor (Ikoku, 1984).

Field processing is required to remove undesirable components. This consists of four basic processes (Figure 1.2):

1) Separation of the gas from free liquids such as crude oil, hydrocarbon condensate, water and entrained solids

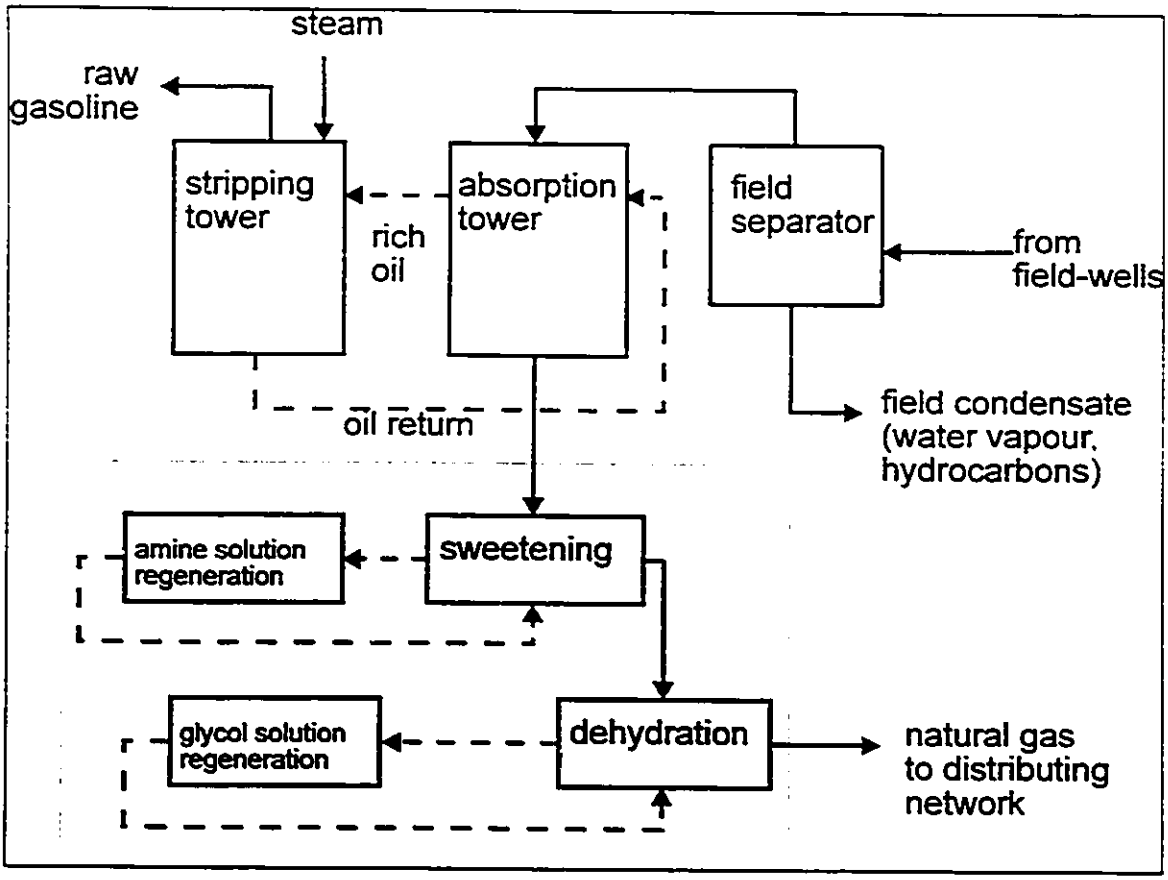

Figure 1.2 *Natural gas processing (Medici, 1974).*

2) Processing the gas to remove condensable and recoverable hydrocarbon vapors

3) Processing the gas to remove condensable water vapor

4) Processing the gas to remove other undesirable compounds, such as hydrogen sulfide or carbon dioxide (Ikoku, 1984).

These processing steps are important to recover valuable hydrocarbon liquids, decreasing the volume of the gas, increasing its heating value as well as preventing the formation of gas hydrates. Gas hydrates are solid crystalline

compounds formed by the chemical composition of natural gas and water under pressure at temperatures above the freezing point of water. The presence of H_2S or CO_2 is conductive to hydrate formation since these acid gases are more soluble in water than hydrocarbons. Hydrates may block lines and other equipment (Ikoku, 1984).

In addition, hydrogen sulfide and carbon dioxide in the presence of water are very corrosive and can cause failure of valves, pipelines, and pressure vessels. Hydrogen sulfide is also toxic and poisonous and must be removed if the gas is to be used as a domestic fuel. Carbon dioxide removal is required if the gas is going to a cryogenic plant to prevent the solidification of CO_2. Furthermore, carbon dioxide has no heating value (Ikoku, 1984).

Some of the processes for removing acid gases and water from natural gas include: cryogenics, iron-sponge sweetening, hot potassium carbonate process, alkanolamine sweetening, glycol/amine process (Figure 1.2) and the sulfinol process (Ikoku, 1984).

According to Astarita, et al. (1983) 50 to 70% of the natural gas treatment plant investment is directly associated with the magnitude of the solvent circulation rate, for processes involving physical solvent absorption. Another 10 to 20% of the initial investment is dependent of the regeneration energy requirements.

1.3 Membrane Separation of Natural Gas

When compared to other gas separation processes such as cryogenics, adsorption and absorption, membrane separations must compete primarily on the basis of overall economics and convenience. The main advantages of membranes include low capital investment, ease of operation, low energy consumption, cost effectiveness and good weight and space efficiency. The extent of the benefits from using membrane technology are highly dependent on the nature of the separation problem.

For natural gas sweetening, the most common process is amine absorption. However, amine plants are large and heavy, requiring tall structures which present problems for use on offshore platforms. They are very complex and require constant operator supervision and maintenance. Also, the presence of a regenerator which burns some of the methane is a fire safety hazard on off-shore platforms. Membrane treatment of natural gas would eliminate these problems, usually at a lower capital cost. Small membrane units can also be used to treat the gas right at the well-head, eliminating the corrosion and safety problems associated with "feeder" lines to a centrally located processing plant. Table 1.2 illustrates the relative merits of membranes for a specific gas treating application (Spillman, 1990).

Natural gas is typically produced at high pressure which is ideal for membrane separation. The carbon dioxide, hydrogen sulfide and moisture

permeate through the membrane leaving a methane stream with essentially no pressure drop (Spillman, 1990).

Table 1.2 Process comparison for natural gas treating

Process Description	Overall Operating Cost	Overall Capital Cost	Overall Space	Overall Weight
Si tage M	1	1	1	1
M DEA amin (dietha)	0.44	4.6	1.19	5.39
Two-Stage Membrane plus Compression	0.85	1.43	1.65	1.47
Selexol (dimethyl ether of polyethylene glycol) solvent	0.13	6.18	1.74	7.79
DEA amine process	0.087	6.36	1.96	8.1
Activated MDEA (methyldiethanolamine)	0.068	6.25	1.58	7.91

Another benefit of membrane systems is that they can be easily modified to handle unexpected variations in processing conditions such as an increase in flow or a change in compositions (Spillman, 1990). Membrane systems are extremely reliable since the process is continuous with few control components

which can cause a shutdown. When required, changing membrane modules is a simple operation, with minimum downtime (Gurr, 1991).

Membrane separation of natural gas impurities, in particular acid gases is a low energy process. It is also simple, requiring reduced operator attention and easy turn-up and turn-down capabilities. They offer an alternative to adsorption processes for gas treating facilities. For these reasons, a membrane separation unit is particularly well suited for remote sites (Stookey et al., 1985).

1.4 Polyphenylene Oxide Membranes

Polyphenylene oxide (PPO) was synthesized by General Electric by oxidizing 2,6-dimethylphenol. It is used commercially in a mixture with polystyrene to form Noryl® resin which is one of the most important engineering thermoplastics (Hay, 1986).

As a gas membrane material, PPO has a high permeability to gases when compared to other glassy polymers (Stern, 1994). Because of its high glass transition temperature (T_g), and its aromatic groups in the main polymer chain, it is expected to give membranes with excellent chemical and thermal stability (Mulder, 1991). The preparation of gas separation membranes from PPO and modified PPO was studied by many research groups.

A study of the formation of PPO membranes by Wijmans et al. (1985) found that the porosity of the top layer of PPO membranes decreases when the PPO concentration increases and that this porous structure is the result of liquid-liquid demixing during membrane formation. In the case of homogeneous PPO membranes the interplay of precipitation rate and crystallization kinetics determines the mechanical stability of the film. If the evaporation rate is slowed down or if the casting thickness is increased, the film becomes stiff and brittle due to its higher degree of crystallinity.

A study (Smid et al. 1991) of asymmetric hollow fiber membranes prepared from a range of poly (2,6-dimethyl-1,4-phenylene ether) of different intrinsic viscosities found that increasing the intrinsic viscosity of the polymer reduces the minimum skin thickness of the membrane, thus increasing the permeability, while the selectivity remains the same. This was attributed to a decrease of the number of imperfections in the skin of the membranes prepared from high intrinsic viscosity polymer. A change in the morphology of the sublayer was also identified as a possible cause of the increased permeability.

By a series of plasma-etching experiments, Bauer et al. (1991) determined that the resistance of the sublayer of skinned asymmetric hollow fiber PPO membranes has a significant influence on the overall membrane properties. In addition, it was found that the molecular weight of the PPO has a large effect on the resistance of the sublayer: the higher the molecular weight, the lower the

gas resistance of the sublayer will be. The gas resistance of the sublayer was also found to depend, to a lesser extent, on membrane preparation. By decreasing the sublayer resistance, the overall selectivity of the membrane can be improved.

Tsujita et al. (1991) suggest that the solubility and permeability coefficients of PPO membranes can be controlled by the holding temperature after quenching the polymer film from a temperature above T_g. The results were associated with changes in the microvoid content, unrelaxed volume, or frozen free volume in the polymer by quenching from liquid to glass state.

Non-solvent additives were used in the casting mixtures by some researchers. Wijmans et al. (1985) and Perego et al. (1991) used octanol as the non-solvent additive. This leads to membranes with a more open pore structure. It was used to control the skin thickness of asymmetric Silyl-PPO and increased the gas permeability of the membranes without loss of selectivity. Similarly, Smid et al. (1991) used 2-ethyl-1-hexanol as the non-solvent additive in the preparation of PPO membranes.

In order to increase the selectivity of PPO membranes, chemical modifications of the polymer were attempted by various researchers. A wide range of substituents can be attached on the aromatic ring or on the methyl group of the polymer.

For example, three chemical modifications of PPO were investigated with respect to gas permeation properties, polymer solubility and thermal behavior by Percec and Li (1988). For brominated PPO (100% substitution on the ring), the glass transition temperature, T_g, increases to 273°C. When compared to PPO, the CO_2 permeability increases by 2.47 times and the CO_2/CH_4 selectivity increases by 1.45 times, for brominated PPO with 100% degree of substitution. There is no change in the solution properties of the polymer. Similar results were obtained by Story and Koros (1992) and Sisto et al. (1994).

Sulphonylation of PPO (Percec and Li, 1988) leads to a twofold increase in the CO_2/CH_4 separation factor. An increase in T_g is also observed. In addition, sulfonylated and acylated PPOs become soluble in polar aprotic solvents, which greatly expands the possible solvent systems for PPO membrane making. Increases in permeability and selectivity for CO_2/CH_4 are also obtained. It was found that the substitution degree, main chain rigidity, bulkiness and the flexibility and polarity of the side chains are major parameters controlling the gas permeation properties of the PPO membrane.

The sorption and permeability of CO_2 and CH_4 in PPO and chemically modified PPO were studied by Story and Koros (1992). It was found that the introduction of carboxylic acid substituents to the methyl side chain position of PPO increases the solubility selectivity of the material but significantly reduces the overall permeability.

Asymmetric flat sheet membranes were prepared from silylated polyphenylene oxide (Silyl-PPO) by Perego et al. (1991). An increase in gas permeability is observed for Silyl-PPO with respect to PPO, with the same selectivity. This effect is attributed to an increased interchain distance in the silylated polymer.

Bulky groups such as aryl trimethylsilylethynyl (Me_3C-C≡C) and 3,3-dimethylbutynyl (Me_3C-C≡C) were attached on the aromatic backbone of PPO, by Sisto et al. (1994). An overall increase of gas permeability was observed when compared to unmodified PPO due to a decrease in the packing density. However, the modified PPO membranes have lower permselectivities. Correlations between the gas transport properties and the polymer composition were also performed.

A study by Ilinitch et al. (1992) found that PPO and some PPO-based copolymers possess rather high selectivities and permeabilities for the separation of gaseous mixtures containing methane and ethane, ethylene and ethane, or propene and propane.

Chern and Ghosal (1992) prepared PPO and nitrated PPO membranes. The nitration of PPO (15% substitution) increases the glass transition temperature to 233 °C while the packing density remains essentially the same. The large increase in T_g was attributed to an increase in inter-chain attraction and an increase in the rotational energy barrier caused by the presence of the -

NO_2 group. The permeability to all gases decreases upon nitration with very small increases in the permselectivity for CO_2/CH_4 and O_2/N_2 pairs. The decrease in permeability was attributed to restriction of torsionnal motion among the polymer chains. Aryl-nitration was not found to reduce the packing density of the polymer.

Sulphonated PPO was studied by Fu et al. (1994a, 1994b). The sulphonated polymer was found to be soluble in aprotic solvents, its density and glass transition temperature increase with the degree of sulphonation. These effects are attributed to H-bonds formed between $-SO_3H$ groups. These bulky groups may lead to chain stiffness by suppressing the torsionnal motions in the polymer. However, sulphonated PPO was not as thermally stable as the base PPO. Sulphonated PPO membranes had higher water vapor permeability than PPO.

Although they were prepared and tested under different conditions, a summary of CO_2 permeability and selectivity of different PPO and modified PPO membranes is presented in Table 1.3. All of these membranes are homogenous.

Table 1.3 Carbon dioxide permeability and carbon dioxide/methane pure gas permeation rate ratio for PPO and modified PPO

Polymer (degree of substitution in parentheses)	CO_2 permeability (Barrer)	CO_2/CH_4 pure gas permeation rate ratio	Reference
unmodified PPO			
PPO	52.3	13.8	Ghosal and Chern (1992)
PPO	64	16.4 *	Percec and Li (1988)
PPO	42	15.1	Story and Koros (1992)
PPO	82.0	12.8	Perego et al. (1991)
PPO	51.8	18.5	Sisto et al. (1994)
nitrated PPO			
PPO-NO_2 (15%)	40.4	16.6	Ghosal and Chern (1992)
brominated PPO			
PPOBr (6.5%)	64	16.72*	Percec and Li (1988)
PPOBr (21.5%)	67.2	17.71*	Percec and Li (1988)
PPOBr (46%)	78.08	19.35*	Percec and Li (1988)
PPOBr (61%)	99.84	18.04*	Percec and Li (1988)
PPOBr (100%)	158.08	23.73*	Percec and Li (1988)
PPOBr (85%)	146	16.0	Sisto et al. (1994)
PPOBr (100%)	104.0	15.0	Story and Koros (1992)
sulphonylated PPO			
PPO-$SO_2C_6H_4CH_3$ (60%)	89.60	21.81*	Percec and Li (1988)
PPO-$SO_2C_6H_3(CH_3)_2$ (23%)	72.96	20.00*	Percec and Li (1988)
PPO-$SO_2C_6H_5$ (38%)	99.20	27.38*	Percec and Li (1988)
PPO-$SO_2C_6H_4C_2H_5$ (31%)	73.60	16.40*	Percec and Li (1988)
PPO-SO_2OH	19.84	32.80*	Percec and Li (1988)
carboxylated PPO			
CPPO-22 (22%)	22	19.5	Story and Koros (1992)
CPPO-45 (45%)	12.9	23.2	Story and Koros (1992)
methyl-ester carboxylated (95%)	18.0	17.0	Story and Koros (1992)

Table 1.3 (continued) *Carbon dioxide permeability and carbon dioxide/methane pure gas permeation rate ratio for PPO and modified PPO*

Polymer (degree of substitution in parentheses)	CO_2 permeability (Barrer)	CO_2/CH_4 pure gas permeation rate ratio	Reference
silylated PPO			
Silyl-PPO	80.2	14.3	Perego et al. (1991)
Silyl-PPO	294	9.8	Perego et al. (1991)
alkynylated PPO			
PPO-$Me_3SiC{\equiv}C$ (80%)	596	6.1	Sisto et al. (1994)
PPO-Me_3C-$C{\equiv}C$ (70%)	462	8.7	Sisto et al. (1994)
PPO-Me_3Si-CH_2CH_2 (80%)	194	7.4	Sisto et al. (1994)

* separation factor determined using gas mixtures

1.5 Membrane Making by Phase Inversion

Gas separation membranes can be made in hollow fiber or flat sheet form. The most common method of preparing flat sheet polymeric membranes is by a phase inversion process. Ideally membranes should have a defect-free selective layer, as thin as possible, to obtain a high selectivity and maximum flux. The substructure supporting the selective layer should not contribute any resistance to gas transport but should provide sufficient mechanical strength to withstand high-pressure operation.

There are various types of membrane structures that satisfy these criteria (Figure 1.3): a) integrally skinned asymmetric, b) multicomponent ("caulked"), c) single-layer composite, d) multilayer composite and e) asymmetric composite.

In integrally skinned asymmetric membranes, the selective skin layer is formed at the same time and from the same material as the porous sublayer.

Multicomponent membranes are integrally skinned membranes that are coated or "caulked" with a highly permeable but comparatively unselective polymer, such as poly(dimethyl siloxane), which plugs the defects present in the skin of the asymmetric membrane.

In thin-film composite membranes, the selective layer is formed from a small amount of high-performance polymer on the surface of a more porous support material. The selective layer can be formed by solution coating, interfacial polymerization or plasma polymerization. The multilayer composite and the asymmetric composite are extensions of this type of membrane.

Integrally skinned membranes are formed by phase inversion. The term "phase inversion" is used to describe the transformation of a polymer from a liquid to a solid state. This phase separation in a membrane-forming system consisting of a polymer, solvent(s), and nonsolvent(s) can be induced by a change in temperature, solvent evaporation, or solvent depletion and/or nonsolvent addition during a quench step. This can be represented on a ternary phase diagram.

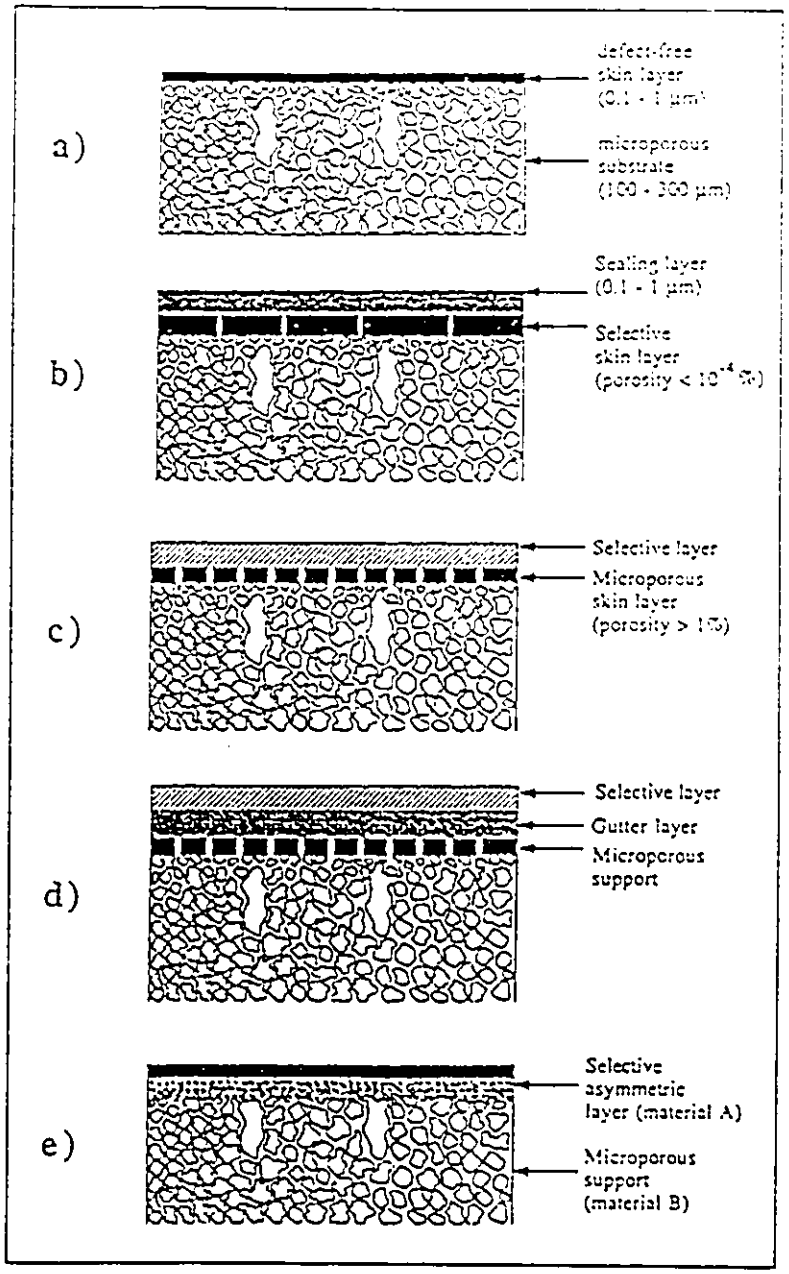

Figure 1.3 *Structure of gas separation membranes a) integrally skinned asymmetric; b) multicomponent; c) single-layer thin-filmed composite; d) multilayer thin-film composite; e) asymmetric composite (Koros and Pinnau, 1994).*

A typical isothermal ternary phase diagram is illustrated in Figure 1.4, representing the solvent-polymer casting solution and the non-solvent quench bath. The diagram shows the stable region, the metastable region, located between the binodal and spinodal and the unstable region. The tie lines connect points on the binodal that are in equilibrium. A composition in the two-phase region always lies on a tie-line and splits into two phases represented by the intersections between the tie line and the binodal: a polymer-rich region and a polymer-poor region.

When preparing membranes, a solution of polymer with a composition in the miscible region of the diagram is spread (cast) on a support and immersed in a non-solvent bath. For wet casting, the outlet of the casting knife that transfers the polymer from a closed reservoir is submerged directly in a liquid coagulation medium that is a nonsolvent for the polymer. In dry casting, the outlet of the casting knife is exposed to air. During dry/wet casting, evaporation

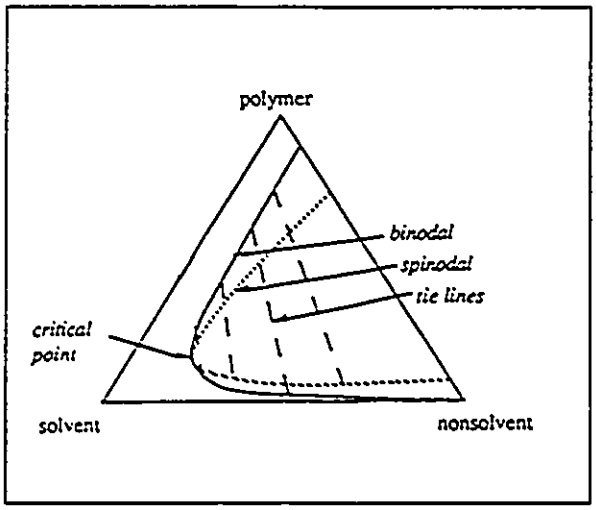

***Figure 1.4** Isothermal phase diagram for ternary membrane-forming system (Mulder, 1991).*

of the solvent occurs before the membrane is immersed in the non-solvent bath, thereby producing a more concentrated polymer region near the air-solution interface to promote the formation of a skin layer. This technique of membrane making requires multicomponent casting solutions consisting of polymer, at least one volatile solvent and one less volatile nonsolvent. It was found (Pesek and Koros, 1994) that the use of two solvents of different volatility allowed finer control of the solvent evaporation and polymer coagulation rates.

During the quench step, the non-solvent diffuses into the nascent membrane, causing spinodal decomposition of the polymer solution into polymer-rich and polymer-poor regions, which give the membrane its sponge-like structure.

Different mechanisms of phase separation can occur. Very slow quench rates will favor nucleation and growth of the polymer over spinodal decomposition. Gelation, the formation of a three-dimensional network by physical crosslinking (Figure 1.5), is also an important phenomenon in the formation of the

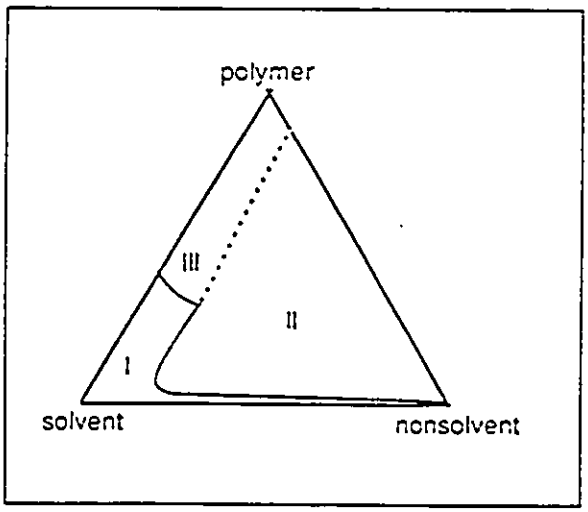

Figure 1.5 Isothermal ternary diagram of system containing a one-phase region (I); a two-phase region (II); and a gel region (III) (Mulder, 1991).

skin layer of the membrane. It is believed that the acceleration of the kinetics of the sol-to-gel transition increases the free volume and gives membranes with thinner effective separating layers (Fritzsche et al., 1985). Sol-gel transition has been observed in PPO membrane making by Wijmans et al. (1985).

The quench liquid and any solvent remaining from the membrane formation process must be removed from the membrane before it can be used for gas processing. Sometimes, evaporative drying is suitable, other times, a series of solvent exchange steps is necessary to prevent densification or collapse of the membrane structure.

After casting and drying, gas separation membranes are often post-treated to minimize the effect of surface defects on the selectivity of the membrane. The most common post-treatment is coating the membrane with a highly permeable polymer to block surface defects. Another method is solvent treatment, either by solvent liquid or vapor to induce swelling in the membrane and eliminate the defects (Rezac et al., 1994).

Most of the polymers used for gas separation membranes are glassy polymers. Since the glassy state is a not an equilibrium state, *d*-spacing (free volume), orientation, and the crystalline fraction in the membrane can be profoundly influenced by environmental factors during membrane making. The choice and concentration of solvent, nonsolvent additive, and coagulation bath will affect the kinetics of the phase separation, and therefore the membrane

structure. The concentration of the polymer is also important. To some extent, the performance of gas separation membranes can be controlled by the membrane making process.

1.6 Scope of Research

The objective of the present research was to develop a membrane for natural gas (CO_2 -CH_4) separation, using polyphenylene oxide (PPO) as the base polymer. Various experiments were used to identify PPO membranes which have good mechanical strength and gas separation capabilities. Membrane strength and selectivity depend on the interplay of the precipitation rate and the crystallization of the PPO. Some of the factors that affect the membrane formation and performance include the polymer, solvents and additives selected as well as their concentration, the casting thickness, the evaporation time before gelation, and the temperature of the casting solution. All of these factors were studied to varying degrees.

The membrane performance will be modeled and optimized to approach the target values of 3.4×10^{-8} moles/(m^2 s Pa) CO_2 permeation rate and 50 CO_2/CH_4 pure gas permeation rate ratio. These targets were selected by British (Consumer) Gas. They represent a membrane two times as CO_2 permeable as a cellulose acetate membrane, the most CO_2 permeable commercial membrane. The CO_2/CH_4 pure gas permeation rate ratio target is two times the CO_2/CH_4

pure gas permeation rate ratio of the most selective commercial membrane for this gas pair, which is made of polysulfone.

The experiments are limited to asymmetric flat sheet membranes as they usually have a greater permeability than homogeneous membranes. Considering the large number of factors studied, the flat sheet configuration was selected because flat sheet membranes are easier to prepare and test than hollow fiber or tubular membranes.

The results obtained will serve as the basis for the development of asymmetric hollow fiber membranes for natural gas separation.

2. Theoretical Aspects

2.1. Polymers

Gas separation membranes can be made from a number of different organic and inorganic materials. However, only polymeric membranes are currently being used for industrial separations (Stern, 1994). The choice of a given polymer as a membrane material is not arbitrary but based on very specific properties, originating from structural factors such as molecular weight, chain flexibility and chain interactions. These structural factors determine the thermal, chemical and mechanical properties of the polymers as well as the permeability (Mulder, 1991). The ideal gas separation polymer should offer high productivity, selectivity and durability (Pixton and Paul, 1994).

2.1.1. Chemical Structure

The chemical structure is the combination of steric and polar properties of polymeric membranes at the submacromolecular level, including chain segments and functional groups (Kesting and Fritzsche, 1993).

Polymers are high molecular weight molecules composed of a number of basic units, the monomers. Polymers can be linear or branched. Copolymers are formed when the repeating units are not the same. It is also possible to connect two or more polymer chains to each other by crosslinking by chemical

reaction. Physical crosslinks can also exist in semi-crystalline polymers where the crystallites act as crosslinks or in block copolymers where the domains of the dispersed phases act as crosslinks. Stereoisomerism also affects the regularity of the structure of the polymer, determining the degree of crystallinity of the polymer (Mulder, 1991).

The size and shape of bulky side groups in both the polymer main chain and side chains determine some of the fundamental polymer characteristics such as packing density ($1/v_f$), the rigidity of the polymer chain segments, and the accessibility and hence participation of functional groups in membrane-permeant interaction. Structural regularity generally favors close packing and can lead to increased density and rigidity in both crystalline and amorphous phases (Kesting and Fritzsche, 1993).

Polarity is the term used to define the unevenness in the distribution of electrons about atoms, functional groups, and molecules. The high-electron density regions of polar groups are attracted to the low-electron density regions of other accessible polar groups to a degree proportional to the difference between their electron densities. The more polar the groups, the greater the force of attraction between them. Because of these net forces of attraction between macromolecules, interchain displacement (d-spacing) and the free volume (v_f) in polar polymers tends to be smaller than they are in nonpolar

polymers leading to lower permeability and higher selectivity (Kesting and Fritzsche, 1993).

One of the ways of expressing polarity is the solubility parameter, δ, which is defined as $\delta = (CED)^{1/2}$, where CED is the cohesive energy density. The solubility parameter can be treated as a total parameter δ_t which includes polar forces, dispersive (non-polar) forces, and Lewis acid-Lewis base interaction forces.

The polar forces (δ_p) are due to the presence of permanent dipoles which are the result of charge separation between atoms in a group. Permanent dipoles exert a strong attraction on other permanent dipoles and can also influence neutral groups in which they can induce a dipole. Examples of some groups with permanent dipoles are hydroxyl (-OH), carbonyl (-C=O) or halide (-I, -Br, -Cl, or -F) (Mulder, 1991).

Dispersive forces (δ_d) are due to random fluctuations in the electron density. These dispersion forces are much weaker than dipole forces but are very common in hydrocarbons. δ_d increases with increasing length of aliphatic chains and degree of saturation (Kesting and Fritzsche, 1993).

Polymer-polymer and polymer-solvent interactions can be explained in terms of Lewis acid/base theory. Polymers containing halogen or nitro groups are acidic (electron pair acceptor) and polymers with aromatic or olefin groups are primarily basic (electron pair donor), some polymers can be considered

amphoteric. These Lewis acid-Lewis base interaction forces include hydrogen bonding (δ_h) (Kesting and Fritzsche, 1993).

2.1.2. Macromolecular Architecture

The macromolecular architecture of polymers include properties such as molecular weight and molecular weight distribution, conformation, configuration and copolymer composition and arrangement (Kesting and Fritzsche, 1993).

The chain length is an important parameter in determining the properties of a polymer. There is usually a distribution in molecular weight, so the length of the macromolecular chain is usually expressed by the average molecular weight. The molecular weight distribution curve also influences the characteristics of the polymers. With increasing chain length the number of interaction sites between the various chains increases and consequently the chemical, physical and mechanical properties of the polymer vary. In addition, the coiled polymer chains are not situated separately from each other but are entangled. The number of entanglements increases with the increasing chain length (Mulder, 1991).

The polymer concentration required to achieve the minimum viscosity consistent with a defect free membrane (macrovoid-free substructure, defect-free skin layer) will also decrease with increasing molecular weight. When membranes are prepared from equal viscosity sols, porosity and v_f will increase with polymer molecular weight. The glass transition temperature increases with increasing molecular weight, indicating increased chain stiffness. High molecular

weight polymers usually yield membranes with good mechanical properties (Kesting and Fritzsche, 1993).

Chain flexibility is a one of the main structural characteristics of the polymer. It is determined by two factors: the character of the main chain and the presence and nature of the side chains or side groups. In polymers where the main chain consists entirely of -C-C- bonds, rotation around each -C-C- bond is possible, which makes the chain rather flexible. When heterocyclic or aromatic groups are introduced in the main chain, such as in the case of PPO, there results a substantial decrease in flexibility.

Chain flexibility is also determined by the character of the side groups which determine to some extent whether rotation around the main chain can take place readily or whether steric hindrance occurs. In addition, the character of the side group has a strong effect on inter-chain interaction (Mulder, 1991). It was found by Chern (1991) that the gas diffusivity in polymers correlates very strongly with polymer packing density.

The state of the polymer is important relative to its mechanical, chemical, thermal and permeation properties. The state of the polymer, glassy or rubbery, depends on the actual temperature relative to the glass transition temperature, T_g. The mobility of the polymeric chains is very restricted in the glassy state, since the segments cannot rotate freely around the main chain bonds. On increasing the temperature, some motions can occur in the side chains or in a

few segments of the main chain. At the T_g, the thermal energy is just sufficient to overcome the restriction in rotation due to bulky side groups or to overcome the interactions between the chains. Many physical properties change at the glass transition temperature. The tensile modulus of the polymer in the rubbery state is often three or four orders of magnitude lower than the tensile modulus in the glassy state. Other physical properties also change at the T_g such as the specific volume, the specific heat, the refractive index and the permeability. The glassy state is considered the ideal condition for gas separation membranes (Kesting and Fritzsche, 1993).

Glassy polymers have heterogeneous structure consisting regions with ordered and disordered structures. The free volume has a non-equilibrium nature and exists in the glassy polymer as a interconnected microporous network (Volkov, 1991). Since the glassy state is a non-equilibrium condition, *d*-spacing (free volume), orientation and the crystalline fraction can be influenced by environmental factors before, during and after the sol to gel transition during membrane making (Kesting and Fritzsche, 1993).

Several models of order in amorphous polymers have been developed. The "random-coil" folded chain model is described by Kesting and Fritzsche (1993). Polymer chains in a folded configuration form crystalline nodules. Each nodule (approximately 200 Å in diameter) contains several tens of macromolecules. The chain segments within the folded mass are parallel to one

another over distances of at least 10 Å. These nodules have been observed in the surface of asymmetric integrally skinned gas separation membranes of polysulfone. The interstices between nodules are thought to be domains of lower polymer density. The nodules form nodular aggregates and supernodular aggregates (aggregates of nodular aggregates) which form the macrovoid structure in the membrane.

When the temperature increases, the physical and chemical properties of polymers change and they finally degrade. The extent of such a change depends on the type of polymer and the glass transition temperature and melting point (T_m) of the polymer. The following factors which lead to and increase in thermal stability generally also increase the chemical stability: those that increase T_g and T_m and those that increase the crystallinity. The presence of resonance structures such as in aromatic polymers also increases thermal stability (Mulder, 1991).

The tensile modulus and the brittleness of the membrane material are important parameters of mechanical strength. Mechanical properties are important for gas separation membranes because high pressures are applied and particularly in the case of hollow fibres which are self-supporting (Mulder, 1991).

2.2. *Gas Permeation*

In all membrane gas separations, the driving force for the permeation of gas across the membrane is the pressure difference between the high pressure feed stream and the permeate stream which is usually at atmospheric pressure. The separation is achieved because of differences in the relative transport rates of the molecules in the feed. Components that diffuse more rapidly through the membrane become enriched in the permeate stream. The slower components are concentrated in the retentate stream. The degree to which the components of the feed are separated is determined by the characteristics of the membrane as well as the relative driving force of each component (Zolandz and Fleming, 1992).

There are various mechanisms by which the components of the feed gas stream are separated by the membrane (Figure 2.1). In the case of a membrane with very large pores, no separation occurs as the molecules pass through it in convective flow.

If the size of the pores is smaller than the mean free path of the gas molecules, the gas molecules interact with the pore walls more frequently than with one another so that low molecular weight gases are able to diffuse more rapidly than heavier ones and separation occurs. The difference in transport rates of two components is inversely proportional to the square root of the ratio of their molecular weight, at zero permeate pressure. This type of process,

called Knudsen diffusion, is not an economically feasible separation in most cases.

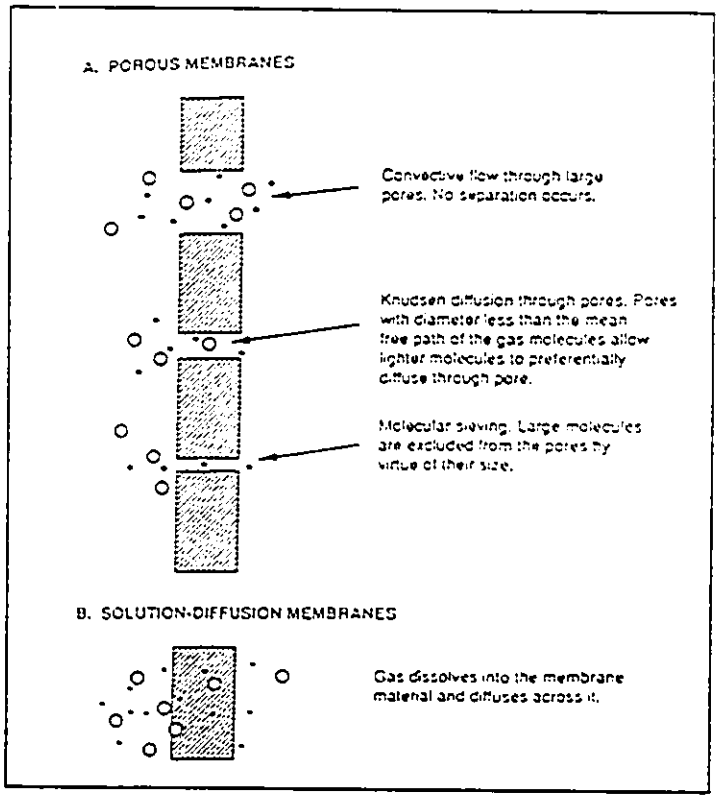

Figure 2.1 *Mechanisms for gas separation using membranes (Zolandz and Fleming, 1992).*

Generally, the membranes used for commercial separation of gases are polymeric and have a solution-diffusion mechanism. The solution-diffusion mechanism is usually considered to consist of three steps: (1) sorption (absorption and/or adsorption) upon the upstream boundary, (2) activated diffusion through the membrane, and (3) dissolution or evaporation from the downstream boundary. This solution-diffusion mechanism is driven by a

difference in the thermodynamic activity existing at the upstream and downstream faces of a membrane. The activity difference causes a concentration difference that leads to diffusion in the direction of decreasing activity (Kesting and Fritzsche, 1993).

The driving force for the separation through the membrane is a partial pressure, or fugacity, difference. From Fick's law of diffusion, the flux of a given component across the membrane is derived as:

$$J_v = (P / l)(p_f - p_p) \qquad \text{Eq. 2-1}$$

where J_v is the volumetric flux of the component gas across the membrane, P is the permeability of the component in the membrane polymer, l is the thickness of the active layer, and p_f and p_p are, respectively, the partial pressures of the component on the feed (f) and permeate (p) sides of the membrane. The permeability (P) is usually taken as a product of two parameters, the diffusivity (D) and the solubility (S):

$$P = DS \qquad \text{Eq. 2-2}$$

There are various models used to describe gas transport in polymers: the matrix model, the free-volume theory, the dual mode sorption model.

The matrix model is based on the assertion that gas molecules exist in a glassy material as a single population. The concentration dependence of the sorption and permeability is thought to be due to gas/polymer interactions. The

parameters of this model do not have easily definable physical significance (Zolandz and Fleming, 1992).

The free-volume theory of gas diffusion in polymers is based on free-volume transport in liquids. According to the free-volume theory, the movement of molecules depends on the free volume available as well as the availability of energy sufficient to overcome polymer-polymer attractive forces. The flux (J) of the penetrant gas can be written in terms of the local volume fraction of penetrant in the polymer, ϕ, and the mutual diffusion coefficient, D:

$$J = -\frac{D}{1-\phi}\frac{d\phi}{dx} \qquad \textit{Eq. 2-3}$$

where the diffusion coefficient D is assumed to be a function of the local concentration, all at a position coordinate x in the flux direction, perpendicular to the membrane area (Zolandz and Fleming, 1992).

The fractional free volume is defined as:

$$v_f = \frac{v - v_0}{v} \qquad \textit{Eq. 2-4}$$

where v is the specific volume of the sample and v_0 is the volume occupied by the sample molecules themselves. The specific volume is the reciprocal of the density. v_0 can be estimated by molecular group contribution methods, by fitting the theoretical equation of state for a polymer to pressure-volume-temperature data and deducing the occupied volume or by positron annihilation spectroscopy (PAS) (Pixton and Paul, 1994). The fractional free volume, v_f, in a polymer can

also be expressed as a function of absolute temperature (T) , penetrant gas pressure (p), and concentration:

$$v_f = v_{fs}^{\circ} + \alpha (T - T_s) - \beta (p - p_s) + \gamma\phi \qquad \textit{Eq. 2-5}$$

where v_{fs}° is the fractional free volume of the pure polymer at the reference temperature and pressure, T_s and p_s. Usually the reference temperature is chosen as the glass transition temperature, T_g, and the reference pressure is 1 atm. α [$=(\partial v_f / \partial T)_s$] is the "thermal expansion" coefficient, β [$=-(\partial v_f / \partial p)_s$] is the "compressibility" and γ [$=(\partial v_f / \partial \phi)_s$] is a concentration coefficient which defines the effectiveness of the penetrant as a plasticizer (Stern and Kulkarni, 1983).

The dual mode sorption model refers to the existence of two thermodynamically distinct populations of the penetrant gas, namely, mobile molecules dissolved in the polymer by an ordinary dissolution mechanism obeying Henry's law and molecules residing in a limited number of preexisting microcavities in the polymer matrix, obeying a Langmuir type of isotherm, with rapid exchange between the two populations. (Zolandz and Fleming, 1992).

The Henry's mode sites are small and correspond to the normally densified regions of the polymer. Sorption in these sites is analogous to the sorption of low pressure gases in rubbery polymers.

The Langmuir sorption sites or "holes" are larger and more variable in size. They are associated with the microvoids or excess free volume formed from intersegmental packing defects which are fixed in the glassy state during the glass transition. Permanent Langmuir sites cease to exist at temperatures

slightly above T_g. This is probably due to relaxation in the polymer matrix and small interchain displacement or micropores expanding upon heating i such a way that the distinction between intra- and internodular micropores disappears giving a rubbery polymer. The penetrant molecules sorbed in the Langmuir sites are much less mobile than those in the Henry's law sorption sites (Kesting and Fritzsche, 1993).

The dual mode sorption model accounts for these two distinct molecular environments with different inherent mobilities by expressing Fick's law as:

$$J = -D_D \frac{dC_D}{dx} - D_H \frac{dC_H}{dx} \qquad \text{Eq. 2-6}$$

where J is the diffusive flux and the coefficients D_D and D_H characterize diffusion due to local concentration gradients in the respective Henry (subscript D) and Langmuir (subscript H) environments. Both are dependent on temperature, but are assumed to be independent of concentration (Kesting and Fritzsche, 1993).

The dual mode sorption model is consistent with permeation results to date and appears capable of accommodating the time, temperature and pressure dependence of permeation as well as a certain degree of independence between Henry's mode and Langmuir site sorption and permeation (Kesting and Fritzsche, 1993).

The temperature dependence of the permeability can be obtained from these two Arrhenius relations:

$$D = D_0 e^{-E_D/RT} \qquad \text{Eq. 2-7}$$

and

$$S = S_0 e^{-E_S/RT} \qquad \text{Eq. 2-8}$$

where D and S are the diffusivity and solubility, D_0 and S_0 are preexponential factors, E_D is the activation energy, and E_s is the enthalpy of sorption.

The presence of secondary components in the feed gas can have profound effects on the transport rate of penetrants in glassy polymers. In general the transport rate of a penetrant A is depressed by the second penetrant B. The total sorption level for A is depressed by B due to exclusion of A from some Langmuir sorption sites that would be available in the pure gas case.

The concentration dependence of the diffusion coefficient for penetrant transport in polymers can be evaluated from steady-state permeability and equilibrium solubility. Some polymers exposed to high levels of strongly interacting gases such as CO_2 and H_2S experience a depression in their glass transition temperature (plasticization). This is thought to increase the size of the segmental motions that participate in the diffusion process and usually results in a drop in selectivity. The effect of CO_2 on glassy polymer plasticization is dependent on the material properties of the membrane and the CO_2 pressure. Currently, the suitable process conditions for a membrane material cannot be predicted and must be determined by experiment (Zolandz and Fleming, 1992).

Also, there can be a significant time-dependent or history effect on the membrane, particularly for gases like CO_2 at extremely high pressure (Pixton and Paul, 1994).

There are several equipment designs for the measurement of gas permeation through polymer film. Some employ a sweep of carrier gas on the downstream side of the membrane, combined with an appropriate detector for analyzing the composition of this stream. For pure gases it is sufficient to measure either the volume of permeate at a fixed pressure or the rise of permeate pressure in a fixed volume. These methods were described and compared by Stern et al. (1963).

The ability of the membrane to separate a mixture of gases, *i* and *j*, is described by the separation factor (α_{ij}):

$$\alpha_{ij} = \frac{y_i / y_j}{x_i / x_j} \qquad \textit{Eq. 2-9}$$

where y_i, x_i and y_j, x_j refer to the mole fraction of components *i* and *j* in the product and the feed streams, respectively (Zolandz and Fleming, 1992).

Often, mixed gas permeation behavior in glassy polymers can be adequately predicted from pure gas measurements, and pure gas permeation rate ratios. However, CO_2 is a known plasticizer and the prediction of mixed gas permeation from pure gas measurements may not be accurate at high CO_2 partial pressure in the upstream. It is very important to calculate pure gas

permeation rate ratio from measurements made on the same film, because a variety of factors related to the equipment calibration, sample preparation and mounting can increase the errors associated with independently measuring absolute permeability coefficients (Pixton and Paul, 1994).

2.3. *Factorial Design*

The use of factorial experimental design for membrane research and development is fairly recent. A factorial design was used by Pesek and Koros (1994) to study and optimize the permeation properties of asymmetric polysulfone hollow fiber membranes for gas separation.

Factorial designs are a statistical experimental method used to study the effects and interactions of several factors on a response. The statistical design of an experiment is the process of planning the experiments so that appropriate data will be collected, which may be analyzed by statistical methods, resulting in valid and objective conclusions (Montgomery, 1984). This approach is necessary when the data is subject to experimental error. In a factorial experiment, several factors are investigated simultaneously, with each factor studied at two or more levels. Levels of the factors may be quantitative such as a temperature or qualitative such as the type of polymer. It provides the smallest number of runs while testing all possible combinations of the levels and factors.

Typically, letters are used to identify the factors. For example, an experiment testing four treatment factors would assign the letters A, B, C, and D to the factors. For exploratory work, usually two levels are used: a "high" level and a "low" level, identified by +1 and -1. A 2-level, four factor factorial design is denoted as a 2^4 design. Such a design involves 16 runs as shown in Table 2.1 (Milliken and Johnson, 1984).

Table 2.1 *A 2^4 factorial design.*

	Level of the factors				
Runs	**A**	**B**	**C**	**D**	**treatment combination**
1	-1	-1	-1	-1	(1)
2	+1	-1	-1	-1	a
3	-1	+1	-1	-1	b
4	+1	+1	-1	-1	ab
5	-1	-1	+1	-1	c
6	+1	-1	+1	-1	ac
7	-1	+1	+1	-1	bc
8	+1	+1	+1	-1	abc
9	-1	-1	-1	+1	d
10	+1	-1	-1	+1	ad
11	-1	+1	-1	+1	bd
12	+1	+1	-1	+1	abd
13	-1	-1	+1	+1	cd
14	+1	-1	+1	+1	acd
15	-1	+1	+1	+1	bcd
16	+1	+1	+1	+1	abcd

The factors are treatments that may have a significant impact on the response. Some prior knowledge is required in order to choose the factors and their levels. The experimental runs are performed in random order, often in replicates. The treatment combinations are denoted by lower case letters. For example the *abc* treatment combination indicates that factors *A*, *B*, and *C* are at the high (+1) level while factor *D* is at the low level (-1) for that run. The run with all the factors at the low level is denoted by (1).

It is important to determine which factors have significant impact on the response. This is accomplished by estimating the main effects and interaction effects, which are denoted by capital letters. The main effect of a factor, for example *A*, is defined as the change in response produced by a change in the level of the factor. The interaction effects, such as *AB* or *ABC*, are found when the difference in response between the levels of one factor is not the same at all levels of the other factors (Montgomery, 1984).

The following complete model for the 2^4 design presented in Table 2.1 can be obtained:

$$E(Y) = \beta_0 + \beta_1 A + \beta_2 B + \beta_3 C + \beta_4 D + \beta_5 AB + \beta_6 AC + \beta_7 AD + \beta_8 BC + \beta_9 BD + \beta_{10} CD + \beta_{11} ABC + \beta_{12} ABD + \beta_{13} ACD + \beta_{14} BCD + \beta_{15} ABCD \qquad \textit{Eq. 2-10}$$

Where $E(Y)$ is the expected value of Y at a given value of the factors A, B, C, and D, and β_i are the parameters for the factors. These parameters can be estimated by least squares analysis. Two level factorial designs do not give information on pcssible quadratic behavior (Draper and Smith, 1981).

As the number of factors in a 2^k design increases, the number of runs increases rapidly, becoming expensive and time-consuming to perform. If we can assume that third order and higher order interactions are negligible, then a fractional factorial design can be used to obtain information on the main effects and low-order interactions. This is often done ..hen $k \geq 4$. (Hines and Montgomery, 1980). Fractional factorial designs are usually used for scanning purposes, to identify the factors that have large effects on the response.

A one-half fraction of the 2^k design contains 2^{k-1} runs and is called a 2^{k-1} fractional factorial design. The 2^{4-1} design is a one-half fraction of the 2^4 design. We can choose the 8 treatment combinations so that the $ABCD$ effect has the value of +1, as shown in Table 2.2. $ABCD$ is called the generator of this fraction of the full factorial design and $I = ABCD$ is the defining relation for the design, where I is the identity element (Montgomery, 1984).

The information from a fractional factorial design is available only as mixtures of information, consisting of one potentially important piece of information and one or more piece of information judged to be unimportant,

Table 2.2 A 2^{4-1} fractional factorial design

Runs	Levels of the factors			
	A	B	C	D
1	-1	-1	-1	-1
2	1	-1	-1	1
3	-1	1	-1	1
4	1	1	-1	-1
5	-1	-1	1	1
6	1	-1	1	-1
7	-1	1	1	-1
8	1	1	1	1

usually high order interactions. In the design presented in Table 2.2, changes in the variable *A* coincide with changes in the treatment combination *bcd*.

The resulting effect of these changes is the sum of the individual effects of *a* and *bcd*. *a* and *bcd* are said to be confounded and *a* is an alias of *bcd*. When selecting a fractional factorial design, care must be exercised so that effects of potential importance are not aliased with each other. For the half fraction of the 2^4 design presented in Table 2.2, the defining relation was chosen to give a resolution IV design. A resolution IV design is one in which no main effect is aliased with any other main effect or two-factor interaction, but two-factor

interactions are aliased with other 2-factor interactions. Since 3-factor and 4-factor interactions are assumed negligible, this type of design can be used to gain valuable information on the main effects *A*, *B*, *C*, and *D*. Alternatively, the defining relation *I=-ABCD* could also have been used to yield a resolution IV design but any other defining relations would have aliased the main effects with 2-factor interactions or other main effects (Montgomery, 1984).

The alias structure of a design may be determined by using the defining relation *I=ABCD*. Multiplying any effect by the defining relation yields the aliases for that effect. For example, for the alias of *A*:

$$A \cdot I = A \cdot ABCD$$
$$A = A^2BCD = BCD \qquad \textit{Eq. 2-11}$$

since any effect times the identity *I* is just the original effect and $A^2 = I$ (Montgomery, 1984). The complete alias structure for the 2^{4-1} design shown in Table 2.2 is represented in Table 2.3.

Assuming the interactions involving more than two operating variables are negligible, the 2^{4-1} design of Table 2.2 can be used to get valuable information on the main effects (*A*, *B*, *C*, *D*).

Various methods of statistical analysis can be used for factorial and fractional factorial designs. For non-replicated fractional factorial experiments, Milliken and Johnson (1989) recommend a half-normal plotting method. The plotting technique can be used to make judgments about which effects are likely

to be significant and to estimate the experimental error in nonreplicated experiments.

Table 2.3 *Aliases of the effects for a 2^{4-1} fractional factorial design, I=ABCD*

Effect	Alias
A	BCD
B	ACD
C	ABD
D	ABC
AB	CD
AC	BD
AD	BC

An ANOVA procedure is used to generate single-degree-of-freedom sums of squares for each of the 7 effects from one of the alias sets in Table 2.3. Analysis of variance involves the partitioning of the degrees of freedom and the sum of squared deviation between the "error" (SS_E) and the "treatment" ($SS_{treatments}$) or effect (Montgomery, 1984). The total sum of squares (SS_T) is a measure of the overall variability of the data so that

$$SS_T = SS_{treatments} + SS_E \qquad Eq.\ 2\text{-}12$$

If the effect exists, it will inflate its own mean squared deviation but not that of the error. By removing the SS_E and using only the $SS_{treatments}$ for the half-normal plot, the differences within treatments due to random error are eliminated.

The square root of the single-degree-of-freedom sum of squares is calculated for each effect. These square roots are ranked in order from small to large. The probit value for each of these square root is plotted against it. This is the half-normal plot.

Examination of the half-normal plot will reveal which effects appear to be significant. If none of the effects are significant, all the effects will fall on a straight line, passing through the origin. Effects that do not fall on this straight line are assumed to be significant. When these are removed, the remaining effects are plotted and an estimate of the standard deviation, σ, can be obtained graphically.

The response variables can also be modeled as linear functions of the effects using a least squares regression procedure. Several assumptions are made in fitting a regression model, therefore the validity of the model must be assessed. A normal probability plot or a histogram of the residuals can be used to check the assumption that the errors are normally distributed, with a mean of zero. Plots of the residuals against the expected value of the response and against the independent variables are a simple way to check for lack of fit.

The lack-of-fit test is used to verify whether the assumed order of the model is correct. The coefficient of multiple determination (R^2) is often used to judge the adequacy of a regression. R^2 can be viewed as the amount of variability in the data accounted for by the regression model (Hines and Montgomery, 1980).

Contour plots of the models are recommended by Miliken and Johnson (1984) as a way to determine the combinations of factors that will give near-optimum responses.

3. Properties of Materials

3.1. Polymers

The polymers used in the research were 2,6-dimethyl polyphenylene oxide (PPO) and chemically modified PPO. The chemical structure of PPO is shown in Figure 3.1. The polymer has a high softening point, good chemical resistance, electrical insulation and dimensional stability (Alger, 1989). It is used commercially mostly in a blend with polystyrene known as Noryl® (Hay, 1986). Of the many aromatic polymers which possess a high T_g, PPO shows the highest permeability to gases (Percec and Li, 1988). However, the ideal separation factor for gas mixtures is usually lower than for other membrane materials such as cellulose acetate.

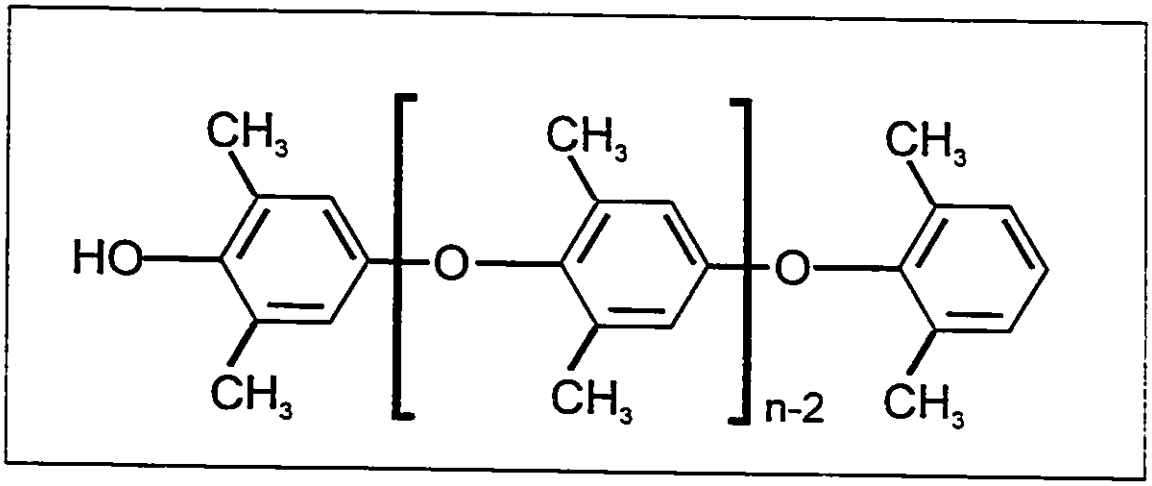

Figure 3.1 *Structure of poly-(2,6-dimethyl-1,4-phenylene oxide).*

The chemical structure of PPO allows for a wide range of substituents that can be attached to the aromatic ring, or on the methyl group, or on both. These reactions can lead to a wide range of gas separation materials with improved permeability, permselectivity or broader solvent solubility (Sisto et al., 1994).

The polymer used in the experiments is PPO Blendex Modifier Resin BHPP 820 from General Electric. It has an intrinsic viscosity of 0.4 dL/g and a T_g of 215 °C. Two chemically modified PPOs were prepared from this material: acylated PPO, and brominated PPO with 100% substitution on the aromatic ring. High molecular weight PPO with an intrinsic viscosity of about 1.0 dL/g was also obtained from General Electric.

3.2. *Solvents and Additive*

A summary of the solvents used for casting solution preparation of PPO membranes are presented in Table 3.1. Chemically modified PPO membranes and high molecular weight PPO membranes were prepared with chloroform as the solvent. All solvents were used as received from the manufacturer, without further purification.

For some membranes, a non-solvent additive, 2-ethyl-1-hexanol, was also used in the preparation of the casting solution. This additive was obtained from Kodak and used as received.

Table 3.1 Summary of solvents used for solution preparation.

Solvent	Supplier	Density at room temperature (g/ml)	Boiling point (°C)
chloroform	BDH	1.498	61.7
1,1,2-trichloroethene	Fisher Scientific Company	1.456	87.1
tetrachloroethene	Matheson Coleman & Bell	1.623	121.1
chlorobenzene	Fisher Scientific Company	1.106	131.7

The non-solvent used as the gelation bath for all the membranes was methanol, from BDH. Used methanol from the gelation bath was filtered and reused for gelling other membranes. Some trials with ethanol, from BDH, as the gelation bath were also attempted.

3.3 Gases

The gases for permeation tests were H_2, CH_4, CO_2, O_2, N_2 and mixtures of 49.2% CO_2 in CH_4 and 20.4% CO_2 in CH_4, all supplied by Air Products. Helium from Air Products was used as the carrier gas for the gas chromatograph.

4. Experimental Method

4.1. Preparation of Casting Solutions

The polymers were dried in a vacuum oven or a conventional oven for at least one hour at 60°C before solution preparation. The solution was prepared by adding the solvent to 8 to 15 g of dry polymer, in a glass bottle. When additive was used, it was added to the polymer with the solvent. Sometimes, it was necessary to stir the contents with a magnetic stirrer and/or heat the solutions to ensure complete dilution of the polymer.

Table 4.1 gives the exact casting solution composition of the membranes. All the membranes were asymmetric, unless otherwise indicated. Casting thickness was 152 μm. The additive was 2-ethyl-1-hexanol. The additive concentration is indicated as a fraction on the total non-polymer components in the casting solution. The * represents the coupon number, since many coupons of the same membrane were prepared.

The solutions were filtered through nylon fabric or a 3 μm Millipore filter, depending on availability, using a Millipore pressure filter cartridge. Nitrogen gas at pressures of 69 to 276 kPa (10 to 40 psig) was used to force the polymer solution through the filter. The solutions were left to de-gas for at least 12 hours before membrane casting.

Table 4.1 Composition of casting solutions

Membrane Code	Type of PPO	Polymer Concentration	Solvent	Additive as wt% of Solvent
2-20C-6-*	BHPP 820	20 wt%	chloroform	0%
2-15C-6-*	BHPP 820	15 wt%	chloroform	0%
2-20CCT-6-*	BHPP 820	20 wt%	70 wt% chloroform, 30 wt% 1,1,2-trichloroethene	0%
2-20CT-6-*	BHPP 820	20 wt%	50 wt% chloroform, 50 wt% 1,1,2-trichloroethene	0%
2-20CTT-6-*	BHPP 820	20 wt%	30 wt% chloroform, 70 wt% 1,1,2-trichloroethene	0%
2-20T-6-*	BHPP 820	20 wt%	1,1,2-trichloroethene	0%
2-15T-6-*	BHPP 820	15 wt%	1,1,2-trichloroethene	0%
2-20B-6-*	BHPP 820	20 wt%	chlorobenzene	0%
2-20TA-6-*	BHPP 820	20 wt%	1,1,2-trichloroethene	16.7%
2-20T2A-6-*	BHPP 820	20 wt%	1,1,2-trichloroethene	14.3%
2-20T3A-6-*	BHPP 820	20 wt%	1,1,2-trichloroethene	12.5%
2-H20T-6-* (homogeneous)	BHPP 820	20 wt%	chloroform	0%
2-H20CT-6-* (homogeneous)	BHPP 820	20 wt%	50 wt% chloroform, 50 wt% 1,1,2-trichloroethene	0%
2-H20T-6-* (homogeneous)	BHPP 820	20 wt%	1,1,2-trichloroethene	0%
5-20C-6-*	Acylated BHPP 820	20 wt%	chloroform	0%

Table 4.1 (continued) Composition of casting solutions

Membrane Code	Type of PPO	Polymer Concentration	Solvent	Additive as wt% of Solvent
6-15C-6-*	high molecular weight PPO	15 wt%	chloroform	0%
8-20C-6-*	100% brominated on ring BHPP 820	20 wt%	chloroform	0%
7-F1-6-*	high molecular weight PPO	10 wt%	chloroform	0%
7-F2-6-*	high molecular weight PPO	15 wt%	chloroform	0%
7-F3-6-*	high molecular weight PPO	10 wt%	chloroform	14%
7-F4-6-*	high molecular weight PPO	15 wt%	chloroform	14%
7-F5-6-*	high molecular weight PPO	10 wt%	chloroform	0%
7-F6-6-*	high molecular weight PPO	15 wt%	chloroform	0%
7-F7-6-*	high molecular weight PPO	10 wt%	chloroform	14%
7-F8-6-*	high molecular weight PPO	15 wt%	chloroform	14%
7-F0-6-*	high molecular weight PPO	12.5 wt%	chloroform	7 %
7-OP1-6-*	high molecular weight PPO	12.5 wt%	chloroform	8.75 %
7-OP2-6-*	high molecular weight PPO	10 wt%	chloroform	9.8 %

4.2. *Preparation of Membranes*

A brass casting bar was used to spread the polymer solution on glass plates during membrane preparation. The casting bar was designed to cast membranes of four different wet thicknesses: 102 μm (4 mil), 152 μm (6 mil), 203 μm (8 mil), and 254 μm (10 mil).

The membranes were prepared at room conditions (relative humidity, temperature, pressure) in a dust-free glovebox. The solutions were poured on a glass plate and spread with the casting bar in one continuous, smooth motion. In some cases the casting solution was heated (30 to 60 °C) in an oven before casting. Immediately after casting, the glass plate was immersed in a gelation bath for one hour. For some membranes, a longer length of time for partial evaporation of the solvent was allowed before gelation.

When removed from the bath, the membranes were visually examined for defects such as dirt and pinholes, and coupons were cut and numbered. For some casting conditions, the membranes did not spontaneously detach from the glass plate during gelation. These membranes were removed from the glass plate by allowing the gelation media to evaporate from the membrane for 10 minutes, then immersing the glass plate in a water bath. The membrane could then be easily peeled off the glass plate.

All coupons were dried in a vacuum oven or a vacuum desiccator for at least 12 hours prior to testing to ensure complete evaporation of traces of solvents or gelation media. The content of the gelation bath was filtered and stored to be reused for the next casting session, without further treatment.

Some of the membranes were laminated with a silicon rubber membrane of thickness 25 μm obtained from General Electric.

4.3. Gas Permeation Testing

The membranes were tested in the gas permeation apparatus described below (Figure 4.1). Three permeation cells were connected in series to a gas cylinder. A purge line was attached to allow flushing of the cell when changing

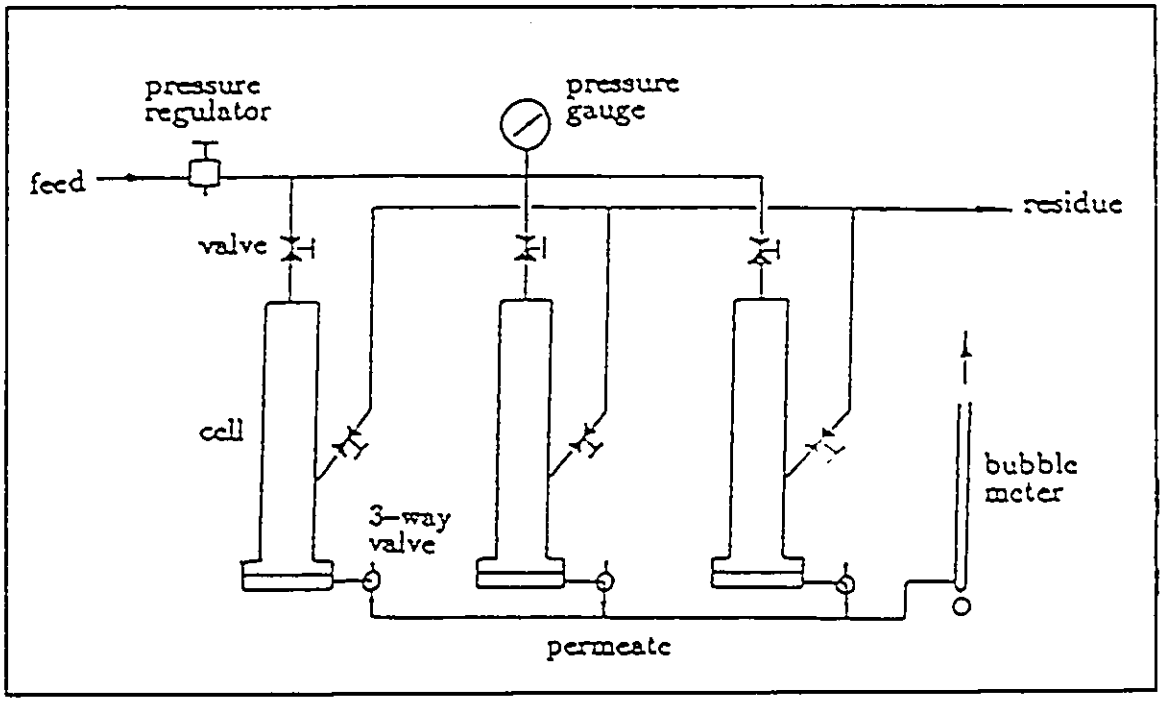

Figure 4.1 Gas permeation testing apparatus.

the feed gas. A permeate line from each of the cells permitted the measurement of the exit gas flow rate, using a bubble flowmeter. All lines were 6.35 mm (1/4 inch) stainless steel tubing except for the permeate line (3.18 mm (1/8 inch) stainless steel) and the feed to the gas chromatograph (1.59 mm (1/16 inch) stainless steel) and lines to the flowmeters which were made from flexible rubber and Nalgene tubing. Fittings were supplied by Swagelok and the valves were supplied by Whitey.

The gas permeation cells (Figure 4.2) were composed of a stainless steel pressure chamber, in two detachable parts. The membrane was supported by a stainless steel porous plate in the bottom of the cell. Gas that permeated through the membrane exited the cell by the permeate collection line which connected the area below the porous metal plate to a 3-way valve in order to feed the permeate either to a bubble flowmeter or to the gas chromatograph. The upper part of the cell contained the feed gas under pressure. It was fitted with control valves to the feed gas inlet and purge lines. The membrane was maintained in the cell by two rubber "O" rings. The two halves of the cell were held together by nuts and bolts. The magnetic stirrer was not used when the feed is a gas. The test cell is described in details in Agrawal and Sourirajan (1970).

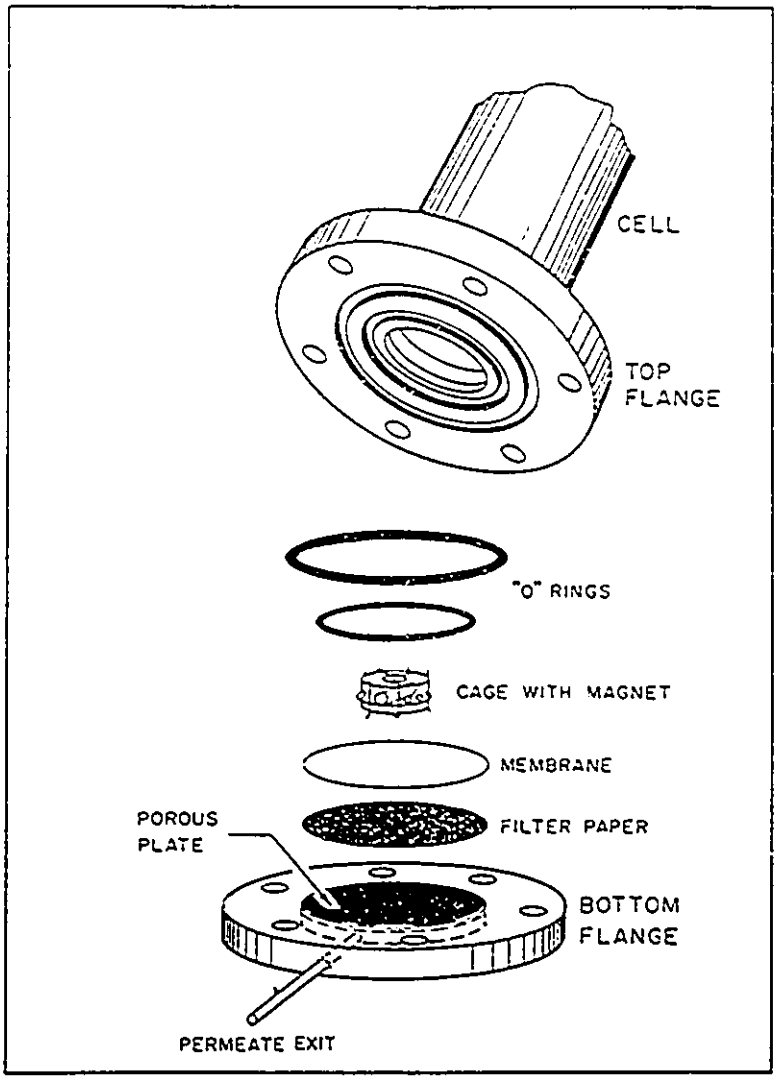

Figure 4.2 *Gas permeation test cell (Agrawal and Sourirajan, 1970).*

The bubble flowmeters used were Varian Optiflow 420, Varian 0 to 60 ml and Supelco 0 to 0.5 ml models. The smallest gas flowrate that could be detected using the capillary bubble flowmeter was 0.005 ml/min.

For a permeation test, a membrane was installed in a cell by placing a filter paper on the porous metal plate to prevent ruptures due to sharp edges.

The membrane was taped on top of the filter paper with the selective layer of the membranes exposed to the feed gas. A second filter paper was sometimes placed on top of the membrane in such a way as to cover the permeation area but not interfere with the seal of the two "O" rings. This was done to reduce the ruptures due to suction on the membrane when the pressure was released, during the purging of the cell. The filter paper held the membrane down tightly in the cell, preventing the membrane from stretching or moving with the change in pressure. The upper and lower part of the cell were then closed by means of nuts and bolts to ensure that there were no gas leaks. The actual permeation area of the membrane coupon depends on the cell in which it is tested.

After purging the test cell with the feed gas, the pressure was adjusted using a pressure regulator. The operating pressures were in the range from 414 to 1379 kPa (60 to 200 psig). About every hour, three permeate flow rates were measured and recorded for each membrane, until steady state was reached. As well, the temperature and atmospheric pressure were also recorded. Using this method, the gas permeation test usually took five to six hours for each gas tested.

The usual order of the gas testing was CH_4, CO_2, N_2, and O_2, all at 690 kPa (100 psig) feed pressure. By testing CH_4 first, it was possible to determine if the membrane was too open to be selective. CO_2 was then tested followed by N_2. The permeation rate of N_2 should be close to that of CH_4. Therefore it was possible to know if the high permeation rate of CO_2 was due to a membrane

rupture during the permeation test. If a rupture had occurred, the N_2 permeation rate would become as high as that of CO_2 . Oxygen was also tested to obtain data on the O_2/N_2 gas pair, since separation of air is of industrial importance. In some cases, the permeation rate of H_2 was also determined. For some membranes, the feed pressure was increased to 1034 or 1379 kPa(150 or 200 psig) to test the mechanical strength of the membrane coupon.

4.4. Separation Experiment

When membranes with very high CO_2/CH_4 pure gas permeation rate ratio were identified, they were tested for the separation of CO_2-CH_4 gas mixtures. In addition to measuring the flowrate, the permeate was analyzed by gas chromatography to determine the separation factor of the membrane. A Varian 3300 gas chromatograph fitted with a molecular sieve 5A column was used. The thermal response factors for the thermal conductivity detector were determined according to the method of Dietz (1967). Helium was used as the carrier gas for the gas chromatograph.

The settings for the gas chromatograph can be found in Appendix D.

5. Methodology

5.1. General Experimental Strategy

The objective of the research was to develop a membrane for CO_2-CH_4 separation, using PPO as the base polymer. The scope of the research was limited to asymmetric membranes as they usually have higher permeation rates than homogeneous membranes. The target value for the CO_2 permeation of the membrane was 3.37×10^{-8} moles/(m^2 s Pa) and the target for CO_2/CH_4 pure gas permeation rate ratio was 50.

In order to obtain a membrane that had good mechanical strength to withstand gas permeation testing, a series of membranes with different thicknesses were cast from 20wt% PPO in chloroform. They were then gelled in methanol. From this experiment, the casting thickness which enabled sufficiently high mechanical strength was found. Then other factors affecting membrane performance and mechanical strength were studied.

Of these factors, different solvents, solvent combinations, and gelation bath media were explored. The effect of PPO concentration and concentration of 2-ethyl-1-hexanol additive were studied as well as the effect of the evaporation time before gelation. The lamination of the membranes with a silicone rubber film was attempted. Membranes prepared from various chemically modified PPO

and high molecular weight PPO were also prepared and tested for gas permeation.

When a membrane coupon had a very high CO_2/CH_4 pure gas permeation rate ratio, it was tested for the separation of CO_2-CH_4 gas mixtures. Some coupons were subjected to increased feed pressures to test their mechanical strength.

After this preliminary gathering of information, the ranges of the casting conditions which gave a membrane film strong enough to withstand gas testing were identified.

Further screening of some of these conditions was done using a fractional factorial design. The effects and relative importance of polymer concentration, additive concentration, temperature and evaporation time before gelation on the performance of the gas separation membrane were studied. Mathematical models were developed and the optimum casting conditions to obtain the target values of permeation rate and CO_2/CH_4 pure gas permeation rate ratio were determined from the models. Membranes were cast under these conditions and tested.

Scanning electron microscope observation of some membrane coupons was performed in order to confirm that the membranes were asymmetric.

5.2. *Analysis of Permeation Data*

Each membrane coupon was tested with different gases. Once the membrane coupon was in the cell and under pressure, at least three permeate flow rate measurements done and recorded. The measurement of the permeate flow rate in triplicate was done every hour until the membrane reached steady state. To determine the permeate flow rate at steady state, the three permeation rate results for each hour were averaged and, using the ambient temperature and atmospheric pressure, converted to standard temperature and pressure (STP, 0°C, 101.3 kPa), according to the ideal gas law. These permeation rate at STP were plotted against the time. The plots exhibited a plateau after steady-state was reached. This permeation rate at steady state was converted from cm^3/s to moles/s, and further divided by the membrane area and the test pressure to give the permeation rate in units of moles/(m^2 s Pa). The permeation rate at steady state is used in all graphs, tables and calculations in this report.

For some coupons, the CH_4 permeation could not be detected even by the most sensitive bubble flowmeter. In these cases, an approximate value of 5.6×10^{-12} mole/(m^2 s Pa), was used as the CH_4 permeation rate for these coupons. This value is the smallest flowrate that can be detected by the capillary bubble flowmeter.

Some membranes had permeation rates that were larger than the measurable range for the available bubble flowmeters. For these membranes,

the permeation rates were measured at many lower feed pressures. The permeation rate as a function of feed pressure could be approximated by a straight line which was extrapolated to obtain the permeation rate at the desired feed pressure. These plots can be found in Appendix A.

5.3. *Analysis of Gas Mixture Permeation Results*

For membranes that were tested for the separation of CO_2-CH_4 gas mixtures, the data were collected and converted to STP values, according to the method described in section 5.2. The permeate was also analyzed by gas chromatography (GC) to determine the separation factor for these membranes.

The permeate was fed to the gas chromatograph and one peak was obtained for each component gas in the feed mixture. The area of each peak was calculated by integration.

To obtain accurate results from the GC analysis of gas mixtures, the area underneath each chromatographic peak must be divided by a "thermal response factor" (Dietz, 1967). The thermal response factors for the thermal conductivity detector of the GC were calculated by analyzing four CO_2-CH_4 mixtures of known composition. The thermal response factors were determined to be 37.8 for CH_4 and 47 for CO_2. These factors are in the same range as those found by Dietz.

The concentration of the CO_2 and the CH_4 in the permeate was determined from the corrected area of the peaks obtained. The separation factor (α_{ij}) for each membrane was calculated using the equation:

$$\alpha_{ij} = \frac{c_{pi} / c_{pj}}{c_{fi} / c_{fj}} \qquad \textit{Eq. 5-1}$$

where the subscript *i* refers to the most permeable gas (CO_2) and *j* to CH_4. c_p is the concentration in the permeate and c_f is the concentration in the feed. The enrichment (*E*) is given by:

$$E = \frac{c_{pi}}{c_{fi}} \qquad \textit{Eq. 5-2}$$

using the same notation as above.

5.4. *Analysis of Fractional Factorial Design Results and Modeling of Data*

A fractional factorial experiment was performed to determine the effect of polymer concentration, presence of additive, evaporation time before gelation and temperature of casting solution on the performance of high molecular weight PPO membranes. A linear model was fitted to the results obtained. This model was used to identify the optimal casting conditions to achieve the target values of

3.37×10^{-8} moles/(m^2 s Pa) CO_2 permeation rate and a CO_2/CH_4 permeation rate ratic of 50.

Two response variables are selected: CO_2 permeation rate and CO_2/CH_4 pure gas permeation rate ratio, at 690 kPa (100 psig) feed pressure. One half of the full 2^4 design was performed, based on the assumptions that 4-factor and 3-factor interactions are not significant compared to 2-factor interactions and single factor effects. Accordingly the combined effect *AB* of polymer concentration *A* and additive concentration *B* are confounded with the combined effect of the evaporation time before gelation *C* and the casting solution temperature *D*. Similarly, the *AC* effect is confounded with the *BD* effect, the *AD* effect with the *BC* effect, the single factor effect *A* is confounded with the *BCD* 3-factor interaction, *B* with *ACD*, *C* with *ABD* and *D* with *ABC*. The total effect (1) is confounded with the 4-factor interaction *ABCD*.

No replicates were performed, but usually the data from two or more membrane coupons which gave similar results were used for calculations. These membrane coupons are not replicates since these were cast from the same solution batch and often came from the same membrane sheet. These data were not averaged for the modeling. The order of membrane casting and testing is randomized by pulling the run number from a hat.

The data were analyzed using SAS® statistical software. All the programs can be found in Appendix B. The data were scaled before analysis.

The response variables of CO_2 permeation rate and CO_2/CH_4 pure gas permeation rate ratio were analyzed by the half-normal plotting method and modeled using backward stepwise elimination from the most general model using linear regression.

The models were checked for adequacy using residual analysis, lack-of-fit and the coefficient of multiple determination (R^2). Since heteroscedasticity was present in the data, weighing and model fitting of the data by Tukey biweight robust regression (Beaton and Tukey, 1974) was attempted but the model accuracy did not improve.

Also using SAS®, contour plots of the modeled CO_2 permeation rate and CO_2/CH_4 permeation rate ratio were plotted in order to determine the casting conditions that would give a membrane which would have both the targeted CO_2 permeation rate of 3.37×10^{-8} moles/(m^2 s Pa) and CO_2/CH_4 pure gas permeation rate ratio of 50. By overlaying the two contour plots it was possible to determine graphically the optimum casting conditions for the desired membrane.

6. Results and Discussion

In order to identify a PPO membrane with the desired gas separation capabilities and mechanical strength, a series of preliminary tests were performed to determine the casting solution composition and casting conditions most likely to yield a membrane suitable for CO_2/CH_4 separation. When these were completed, the membrane casting conditions were modeled and optimized in an effort to obtain a membrane with the target CO_2 permeation rate of 3.37×10^{-8} moles/(m^2 s Pa) and pure gas permeation rate ratio of 50.

The permeation test results for each membrane tested can be found in Appendix A.

6.1. Effects of Membrane Casting Conditions

Preliminary casting tests of membranes cast at wet thicknesses of 101.6 μm (4 mil), 152.4 μm (6 mil), 203.2 μm (8 mil), and 254 μm (10 mil) revealed that a wet casting thickness of 6 mil yielded permeable membranes that had enough mechanical strength to withstand permeation testing.

6.1.1. Effect of Forced Solvent Evaporation

The rate of evaporation of the solvent from the membrane is a very important factor in membrane formation but this was difficult to evaluate due to the poor mechanical strength and surface defects of the membranes.

The purpose of solvent evaporation from the cast membrane before immersing it in the gelation bath is to promote the formation of the skin layer. A series of 20 wt% PPO membranes in 1,1,2-trichloroethene were left in an oven at 60 °C to test the effect of forced solvent evaporation on the properties of the membranes (Table 6.1). The coupon codes are explained in Section 4.1. It was observed that most of the solvent was evaporated in the oven before the gelation step and the membranes seemed homogeneous. The membranes also had many surface defects due to dust in the oven.

By immersing the membrane in the gelation bath immediately after casting the formation of a thin selective layer is promoted. The membranes are less open to gas flow but much more selective, as demonstrated by coupons 2-20T-6-1 and 2-20T-6-10.

Table 6.1 Effect of forced solvent evaporation before gelation on membranes prepared from 20 wt% PPO in trichloroethene

Coupon	Evaporation time in oven (min)	CH_4 permeation (moles/ (m^2 s Pa)) at 690 kPa	CO_2 permeation (moles/ (m^2 s Pa)) at 690 kPa	CO_2/CH_4 permeation rate ratio
2-20T-6-6	10	3.54×10^{-9}	1.48×10^{-9}	0.42
2-20T-6-7	10	ruptured	N/A	N/A
2-20T-6-2	3	ruptured	1.69×10^{-8}	N/A
2-20T-6-3	3	ruptured	N/A	N/A
2-20T-6-4	1	5.04×10^{-8}	ruptured	N/A
2-20T-6-7	1	ruptured	N/A	N/A
2-20T-6-1	0	5.6×10^{-12}	6.91×10^{-10}	123
2-20T-6-10	0	5.6×10^{-12}	6.29×10^{-10}	112

6.1.2. Effect of Gelation Bath Composition

Most membranes in this study were prepared with a methanol gelation bath. In general, these membranes had a white or translucent color characteristic of asymmetric membranes and were mechanically strong.

Ethanol was used as the gelation bath for membranes prepared from 20 wt% PPO in trichloroethene (coupons 2-20T-6-21, 2-20T-6-22). These membranes were clear and too brittle to be tested for gas permeation.

6.1.3. Effect of Silicon Rubber Membrane Lamination

When membrane coupons were laminated with a thin (25 μm) silicon rubber membrane, the mechanical strength of the coupon was increased, steady state permeation was achieved faster and fluctuations in the flow rate were minimized. The lamination increased the CO_2/CH_4 permeation rate ratio by blocking pinholes and other defects that prevented the separation. Consequently, the permeation rates also decreased.

A comparison of two membranes (Figures 6.1 and 6.2) prepared under similar conditions demonstrates that the minimization of surface defects by

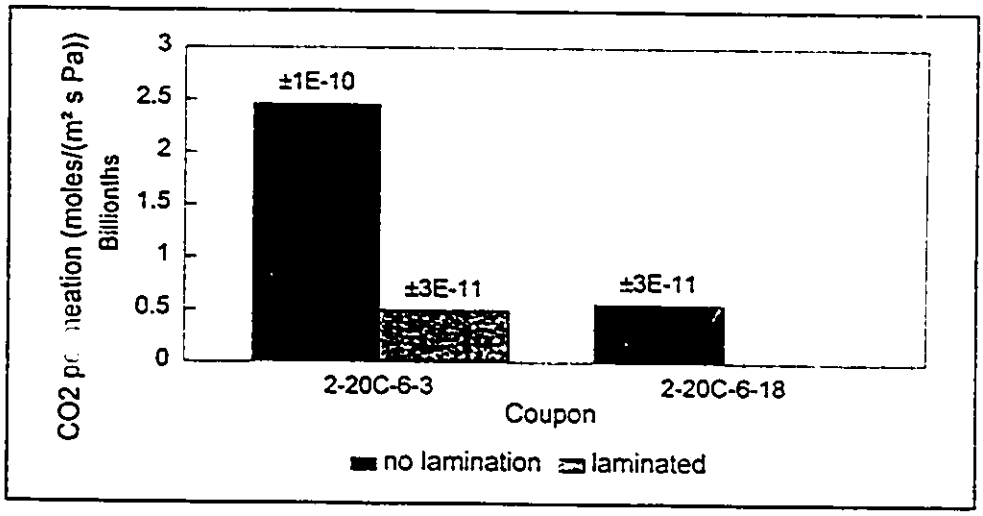

Figure 6.1 *Effect of silicon rubber lamination on the CO_2 permeation rate of a coupon with surface defects (2-20C-6-3) and a defect-free coupon (2-20C-6-18) prepared under similar conditions.*

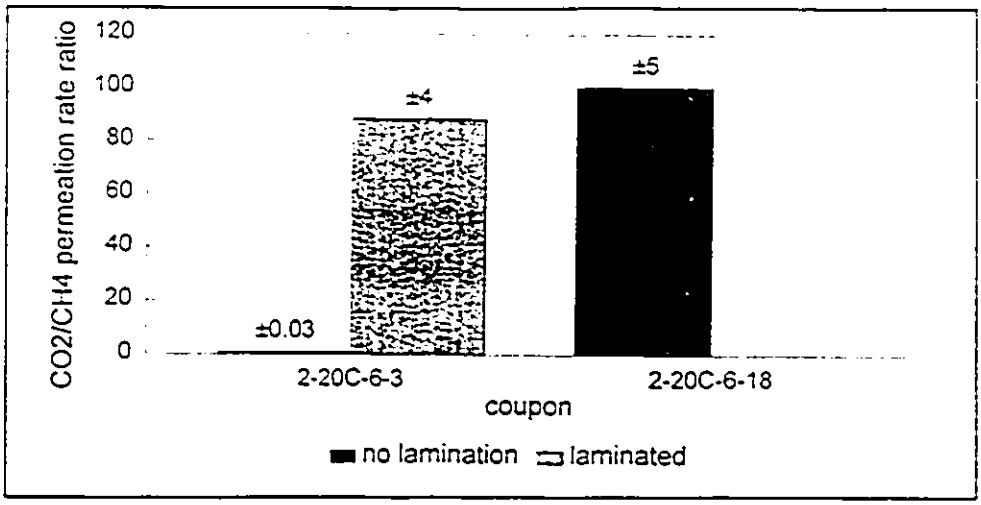

Figure 6.2 *Effect of silicon rubber lamination on the CO_2/CH_4 pure gas permeation rate ratio of a coupon with surface defects (2-20C-6-3) and a defect-free coupon (2-20C-6-18) prepared under similar conditions.*

lamination brought the CO_2 permeation rates and CO_2/CH_4 permeation rate ratio of the membrane (coupon 2-20C-6-3) to the same order of magnitude as a similar but defect-free membrane (coupon 2-20C-6-18). The errors indicated are two times the standard deviation of the pure gas permeation rates at steady state. The errors on the pure gas permeation rate ratio are calculated by multiplying the relative error from the permeation rates by the pure gas permeation rate ratio.

The effect of lamination on a defect free membrane was negligible. Therefore, lamination was not used for most of the membranes tested.

6.2. *Effects of Casting Soiution Composition*

6.2.1. Effect of Solvent for PPO

PPO membranes were prepared from 20% polymer by weight using a variety of solvents: chloroform, 1,1,2-trichloroethene, tetrachloroethene and chlorobenzene. Membranes prepared with solvent mixtures of chloroform and 1,1,2-trichloroethene were also tested. All the chemicals tested were solvents for the polymer but chloroform dissolved PPO faster and did not require heating.

While tetrachloroethene is a solvent for PPO, it was not possible to obtain membranes prepared from solutions using this solvent. Membranes prepared from mixtures of PPO and chlorobenzene were not mechanically strong and many had visible surface defects such as pinholes and cracks. Lamination with silicone rubber to block these surface defects gave membranes with permeation rates higher than those prepared from chloroform or 1,1,2-trichloroethene as the solvent.

The permeation rates were of the same order of magnitude for all solvents except for chlorobenzene (Table 6.2). However the mechanical strength of the membrane was greatly affected by the choice of solvent. Membranes prepared from chloroform solutions were very fragile and ruptured easily when tested. The strongest membranes were prepared with 1,1,2- trichloroethene and 1:1 mixtures of chloroform and 1,1,2-trichloroethene as the solvent.

Table 6.2 *Effect of solvent used in the preparation of PPO membranes*

Coupon	Solvent	CH_4 permeation (moles/ (m^2 s Pa))	CO_2 permeation (moles/ (m^2 s Pa))	CO_2/CH_4 permeation rate ratio
2-20C-6-18	chloroform	5.6×10^{-12}	5.6277×10^{-10}	100
2-20T-6-10	1,1,2-trichloroethene	5.6×10^{-12}	6.2933×10^{-10}	112
2-20CCT-6-7	30% 1,1,2-trichloroethene, 70% chloroform	4.286×10^{-11}	5.236×10^{-10}	12
2-20CT-6-6	50% 1,1,2-trichloroethene, 50% chloroform	5.6×10^{-12}	6.7866×10^{-10}	121
2-20CTT-6-1	70% 1,1,2-trichloroethene, 30% chloroform	5.6×10^{-12}	5.431×10^{-10}	97
2-20B-6-3L	chlorobenzene	1.6888×10^{-10}	7.7767×10^{-10}	4.6

This effect of the solvent on the mechanical strength of the membrane can be attributed to the interplay of the precipitation and crystallization rate of the polymer.

6.2.2. Effect of Casting Solution Concentration

As previously found by Wijmans et al. (1985) the porosity of the top layer of the membrane decreases with increasing PPO concentration. At 15% PPO by weight in chloroform, the membranes were very open and the pure gas permeation rate ratio for the CO_2-CH_4 separation was very low (Figures 6.3 and 6.4). The 15% PPO membranes were also more fragile. By blocking the larger pores by silicone rubber lamination of these 15% PPO membranes, the CO_2/CH_4 permeation rate ratio was improved. The errors on Figures 6.3 and 6.4 were calculated as in Section 6.1.3.

The concentration of polymer in the casting solution can be used as a factor to control the porosity of the membrane.

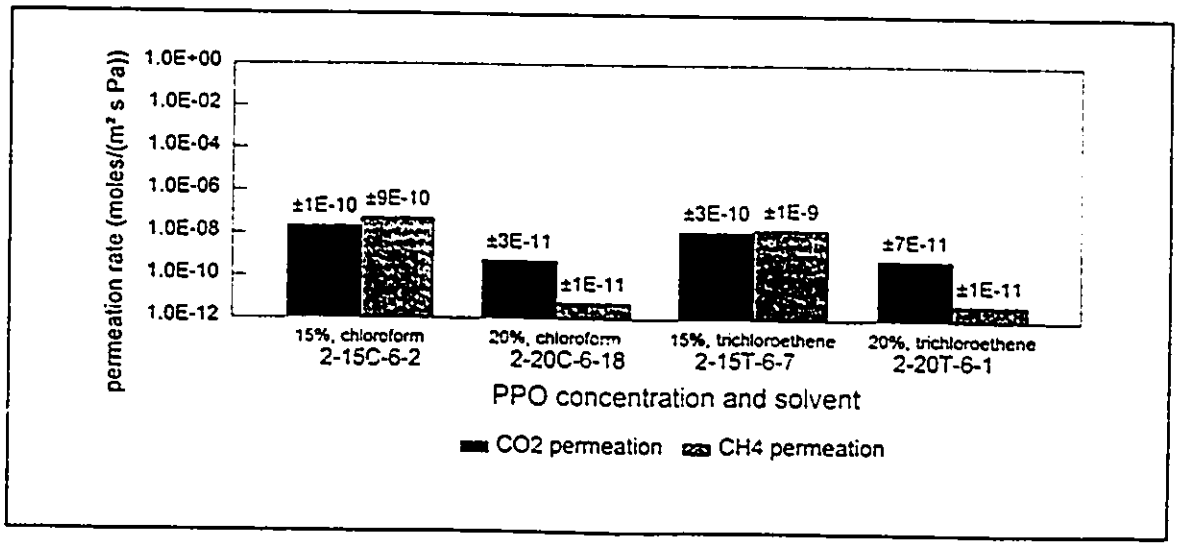

***Figure 6.3** Effect of polymer concentration on CO_2 and CH_4 permeation rates.*

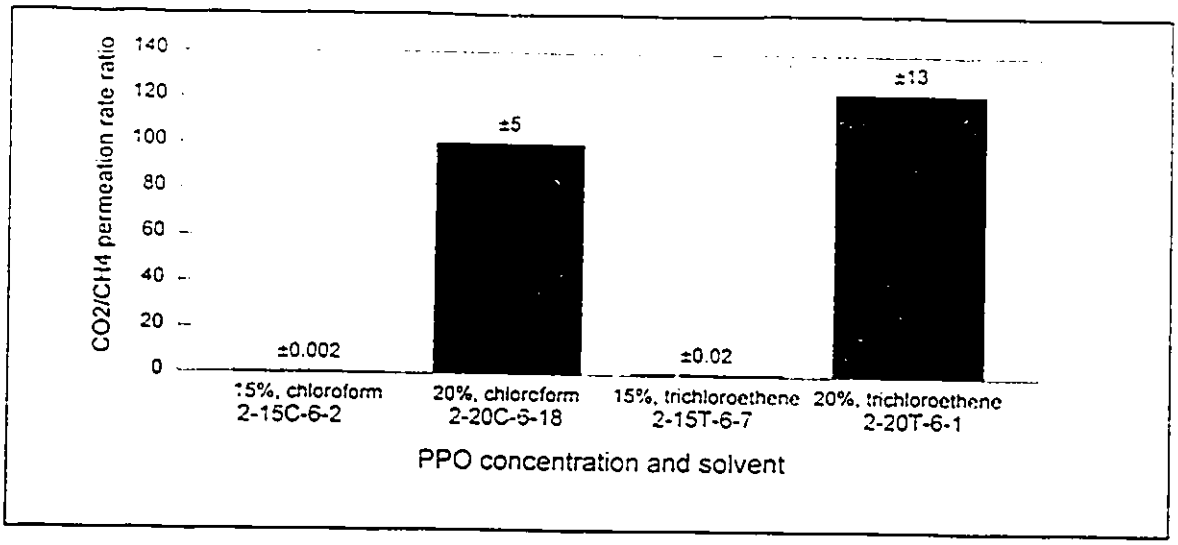

Figure 6.4 *Effect of polymer concentration on CO_2/CH_4 pure gas permeation rate ratio.*

6.2.3. Effect of Additive Concentration

The effect of different concentrations of 2-ethyl-1-hexanol additive on the permeation rate and separation of PPO membranes was studied. Membranes prepared from 20 wt% of PPO in 1,1,2-trichloroethene solutions with three different additive concentrations were tested and compared to membranes prepared from the same polymer and solvent, without the additive. The results are presented in Table 6.3.

There is a significant difference, in the performance of the membranes prepared with additive and without additive. A difference in the CO_2/CH_4 pure gas permeation rate ratio of 93.5 was obtained between the least selective membrane prepared without additive and the most selective membrane prepared

with additive. The presence of some additive significantly increases the permeation rate of both CO_2 and CH_4 but also lowers the pure gas permeation rate ratio. The presence of additive in the casting solution seems to increase the mechanical strength of the membranes. For the concentrations of additive tested, the permeation rates do not seem to depend on the concentration of additive but rather on the presence or absence of additive.

Table 6.3 *Effect of additive concentration on the performance of PPO membranes*

Coupon	Additive Concentration (wt% of total solvent)	CH_4 permeation (moles/(m^2 s Pa)) at 690 kPa	CO_2 permeation (moles/(m^2 s Pa)) at 690 kPa	CO_2/CH_4 permeation rate ratio
2-20T-6-1	0	$5.6\times10^{-12}\pm1\times10^{-11}$	$6.9\times10^{-10}\pm7\times10^{-11}$	123±12
2-20T-6-10	0	$5.6\times10^{-12}\pm1\times10^{-11}$	$6.3\times10^{-10}\pm4\times10^{-11}$	112±6
2-20T3A-6-1	12.5	$2.22\times10^{-10}\pm3\times10^{-12}$	$1.4\times10^{-9}\pm1\times10^{-10}$	6.2±0.5
2-20T3A-6-4	12.5	$5.1\times10^{-9}\pm1\times10^{-10}$	$6.5\times10^{-9}\pm4\times10^{-10}$	1.3±0.07
2-20T2A-6-1	14.3	$1.477\times10^{-9}\pm4\times10^{-12}$	$2.5\times10^{-9}\pm4\times10^{-10}$	1.7±0.3
2-20T2A-6-3	14.3	$7.7\times10^{-10}\pm2\times10^{-10}$	$2.1\times10^{-9}\pm5\times10^{-10}$	2.7±0.5
2-20TA-6-1	16.7	$1.03\times10^{-9}\pm1\times10^{-10}$	$2.9\times10^{-9}\pm2\times10^{-10}$	2.9±0.2
2-20TA-6-7	16.7	$1.13\times10^{-10}\pm2\times10^{-12}$	$2.0\times10^{-9}\pm2\times10^{-10}$	19±2

It is possible that the additive concentrations tested were too large to see the effect of the concentration of additive. The permeation rates for CO_2 and CH_4 may have reached a plateau at the additive concentration used.

As expected from the studies of Wijman et al. (1995) and Perego et al. (1991) the use of a non-solvent additive led to a more open pore structure and more permeable membranes.

The use of a non-solvent additive should permit a better control of the polymer coagulation rate during membrane preparation.

6.2.4. Effect of Chemical Modifications on PPO

Four different types of PPO polymer were tested: BHPP 820 (PPO) with an intrinsic viscosity of 0.4 dL/g, acylated PPO (ACYLATED) prepared from BHPP 820, 100% substitution on ring brominated PPO (PPOBr) prepared from BHPP 820, and high molecular weight PPO (HIGH MW) with intrinsic viscosity of 1.0 dL/g. Asymmetric membranes were prepared from 20 wt% polymer in chloroform for all membranes except HIGH MW, where 15 wt% of the polymer was used. The results are presented in Figures 6.5 and 6.6. The errors on Figure 6.5 and 6.6 were calculated as described in Section 6.1.3.

Both PPO and HIGH MW had very low CH_4 permeation rates and high CO_2/CH_4 pure gas permeation rate ratio. HIGH MW seemed to have more mechanical strength than PPO. It is also possible that a higher molecular

weight polymer has a lower gas resistance in the sublayer as found by Bauer et al. (1991).

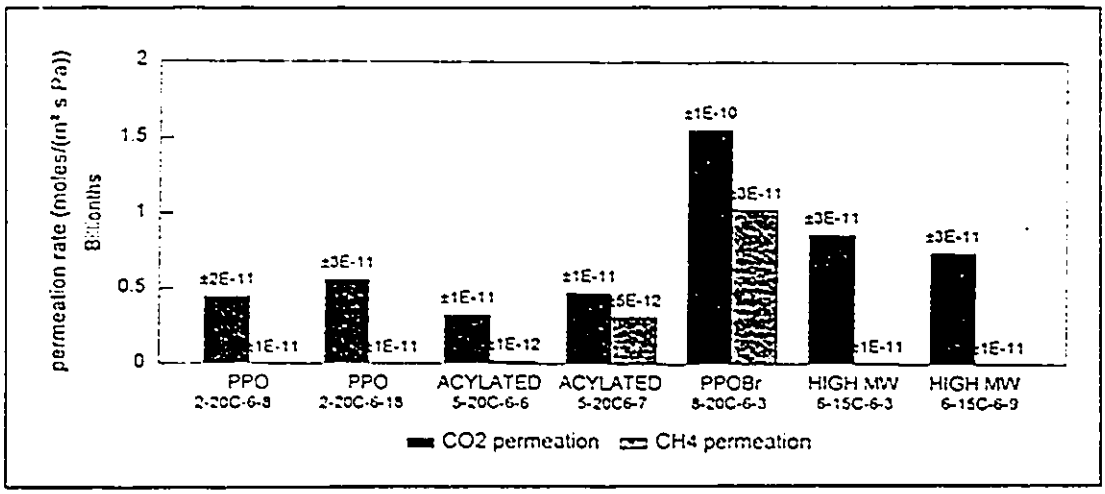

Figure 6.5 *Effect of chemical modifications on PPO on the CO_2 and CH_4 permeation rates at 690 kPa feed pressure.*

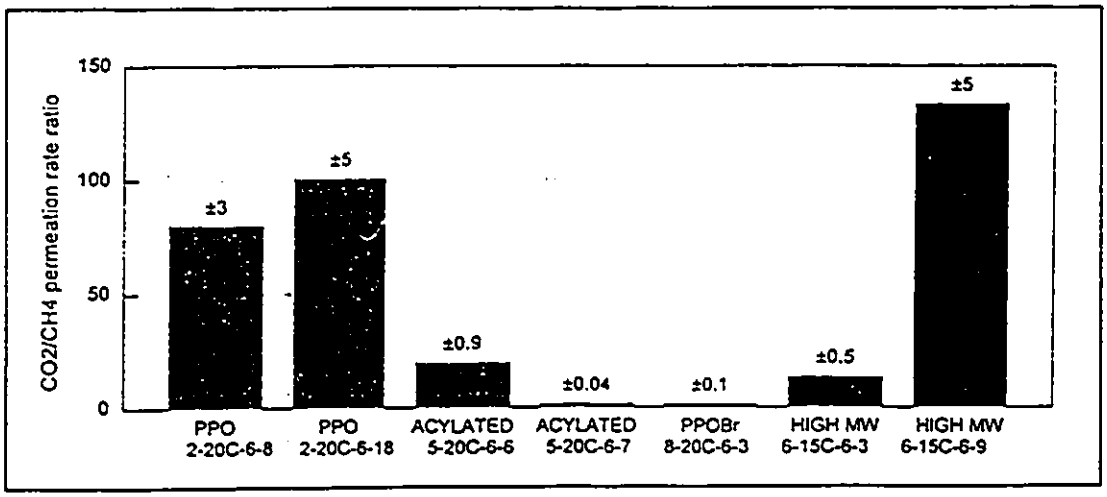

Figure 6.6 *Effect of chemical modifications on PPO on the CO2/CH4 pure gas permeation rate ratio at 690 kPa feed pressure.*

From research by Percec and Li (1988) the permeability and selectivity should increase with PPOBr. It is possible that the membranes prepared in this study were not defect free and the polymer used contained impurities from the bromination reaction. Also, it should be noted that Percec and Li (1988) had researched homogeneous membranes.

Since HIGH MW exhibited both the highest CO_2 permeation rate and pure gas permeation rate ratio, as well as mechanical strength, it was chosen for a thorough study using a fractional factorial design.

6.3. *Testing with Gas Mixtures*

Some membranes with high CO_2/CH_4 pure gas permeation rate ratios were tested with CO_2-CH_4 mixtures as the feed gas. The permeate was analyzed by gas chromatography. Separation factors of up to 22.4 were obtained (Table 6.4). The results also demonstrate that similar separation factors can be obtained with PPO and high molecular weight PPO.

The separation factors for the CH_4-CO_2 gas mixture are much lower than the pure gas permeation rate ratio obtained by testing the membranes with pure gases. This can be attributed to the plasticization effect of CO_2, resulting in a drop in selectivity.

Table 6.4 Separation of CO2-CH4 gas mixtures

Coupon	49.2% CO_2 in CH_4 mixture (690 kPa)		20.4% CO_2 in CH_4 mixture (690 kPa)	
	permeation rate (moles/(m^2 s Pa))	separation factor	permeation rate (moles/(m^2 s Pa))	separation factor
7-F0-6-1	$2.52\times10^{-09}\pm3\times10^{-10}$	10.4±1.4	$9.28\times10^{-10}\pm5\times10^{-11}$	7.7±2.3
7-F6-6-8	$3.25\times10^{-10}\pm2\times10^{-11}$	19.4±0.3	$1.89\times10^{-10}\pm4\times10^{-12}$	20.4±1.5
2-20C-6-19			$1.20\times10^{-10}\pm5\times10^{-11}$	22.4±0.9

6.4. *Testing at High Feed Pressures*

Some membrane coupons were tested with feed pressures of up to 1379 kPa (200 psig). As demonstrated in Figure 6.7, the permeation rate in moles/(m^2 s) increases with increasing pressure. However, the permeation rate ratio remains essentially the same (Figure 6.8).

Very few membrane coupons were strong enough mechanically to withstand testing at higher pressures. This may have been due in part to the design of the test cell which subjected the membrane to suction during the purging of the cell prior to testing as well as high pressures during the permeation tests.

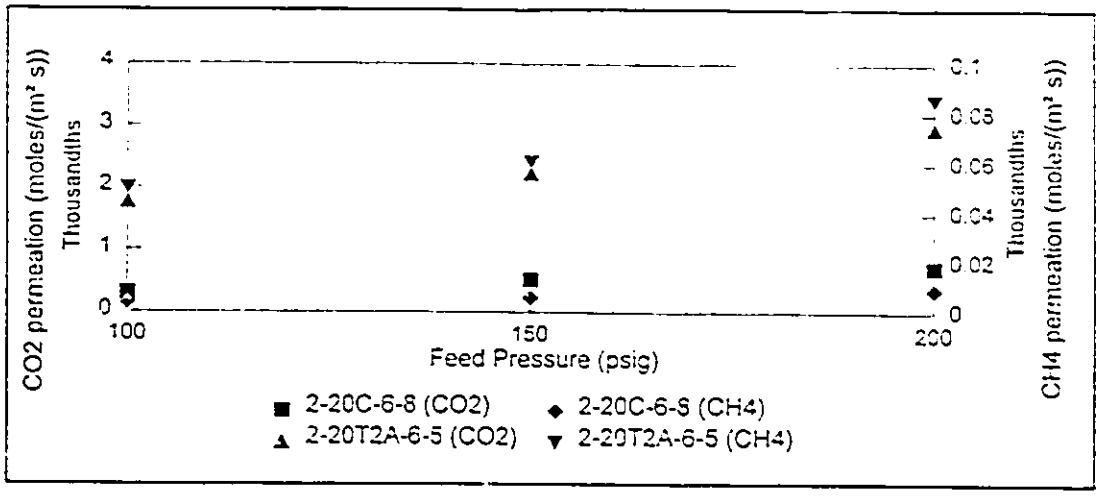

Figure 6.7 *Effect of feed pressure on CO_2 and CH_4 permeation rates.*

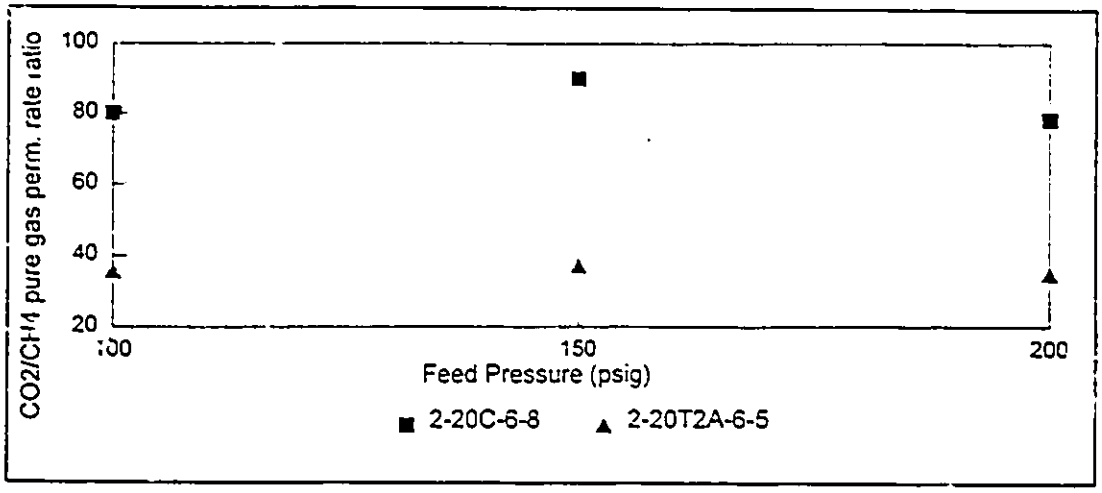

Figure 6.8 *Effect of feed pressure on CO_2/CH_4 pure gas permeation rate ratio.*

Unlike the coupons shown if Figures 6.7 and 6.8, most membrane coupons experienced a sharp increase in permeation rate and a pronounced decline in selectivity when tested at high pressures, indicating membrane damage.

6.5. Scanning Electron Microscope Observations

Scanning electron microscope (SEM) observations were performed on cross-sections of PPO membranes. These cross-sections were obtained by liquid nitrogen fractionation of a flat-sheet membrane.

The membranes are asymmetric. As observed in Figures 6.9 and 6.10, a thin dense skin layer (indicated by the arrow) is clearly observable on the surface of a very porous and much thicker sublayer. Because of the angle of the photograph part of the selective surface of the membrane can also be seen in Figure 6.10.

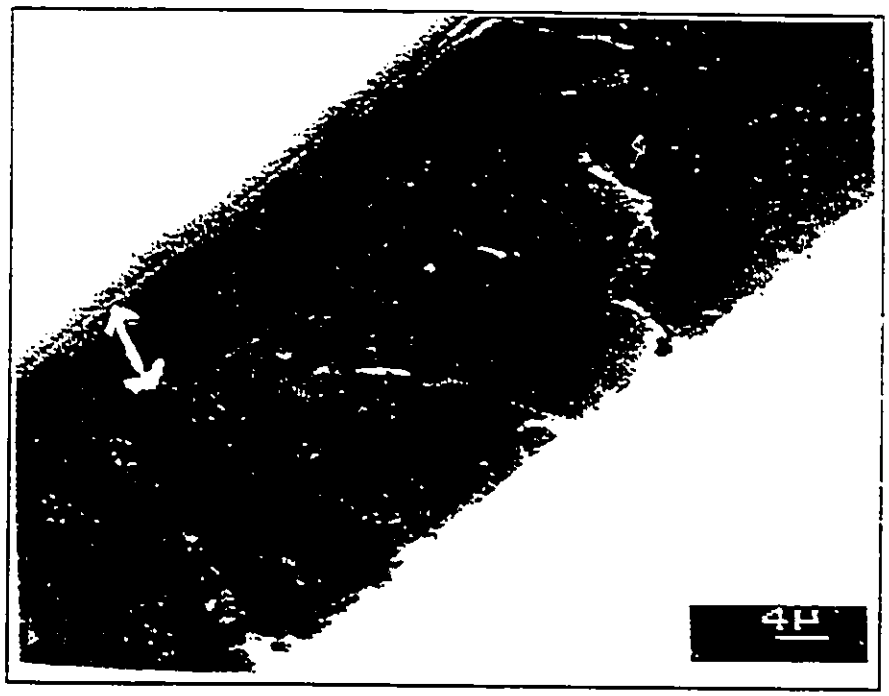

Figure 6.9 *Scanning electron micrograph of a cross-section of membrane 2-20C-6-17, the skin layer is indicated by the arrow.*

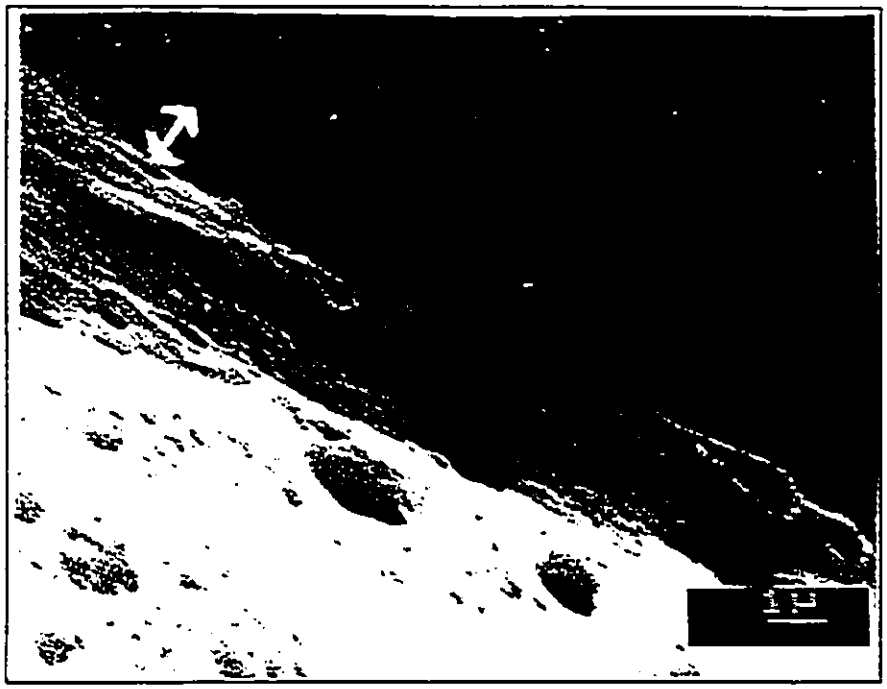

Figure 6.10 *Scanning electron micrograph of a cross-section of membrane 6-15C--6-5, the skin layer is indicated by the arrow.*

6.6. *Effect of Casting Conditions on Membrane Performance*

A 2^{4-1} fractional factorial experiment was used to determine the effect of several factors as shown in Table 6.5.

Table 6.5 *Casting conditions for fractional factorial design*

Factors	Levels	
	-1	+1
A Concentration of polymer (% by weight)	10	15
B Presence of additive	none	6:1 chloroform to 2-ethyl-1-hexanol, by weight (~14%)
C Evaporation time before gelation bath	0	1.5 minutes
D Temperature of casting solution	room temperature (~20 °C)	60 °C

The results of the 8 runs and casting conditions are presented in Table 6.6, where the number after the F in the coupon code is the number of the run.

Table 6.6 Results from fractional factorial design at 690 kPa feed pressure

Coupon Code	Polymer Concentration (wt%)	Additive	Evaporation time (min)	Temperature of casting solution (°C)	CH_4 permeation rate (moles/(m^2 s Pa))	CO_2 permeation rate (moles/(m^2 s Pa))	CO_2/CH_4 pure gas permeation rate ratio
7-F1-6-6	10	no	0	room	2.29×10^{-11}	2.80×10^{-9}	124.8
7-F1-6-7	10	no	0	room	$<5.6\times10^{-12}$	1.38×10^{-9}	>240
7-F2-6-2	15	no	0	60	3.40×10^{-10}	1.15×10^{-9}	3.38
7-F2-6-7	15	no	0	60	1.78×10^{-9}	2.16×10^{-9}	1.52
7-F3-6-1	10	yes	0	60	7.18×10^{-6}	4.33×10^{-6}	0.60
7-F3-6-11	10	yes	0	60	1.13×10^{-5}	5.39×10^{-6}	0.48
7-F4-6-3	15	yes	0	room	3.42×10^{-8}	7.98×10^{-8}	2.33
7-F4-6-7	15	yes	0	room	3.05×10^{-8}	7.64×10^{-8}	2.62
7-F4-6-8	15	yes	0	room	2.19×10^{-8}	5.23×10^{-8}	2.39
7-F5-6-4	10	no	1.5	60	3.12×10^{-11}	1.09×10^{-9}	34.8
7-F5-6-5	10	no	1.5	60	$<5.6\times10^{-12}$	1.22×10^{-9}	>210
7-F6-6-8	15	no	1.5	room	$<5.6\times10^{-12}$	9.88×10^{-10}	>170
7-F6-6-9	15	no	1.5	room	2.28×10^{-11}	9.82×10^{-10}	43.8
7-F7-6-2	10	yes	1.5	room	1.42×10^{-7}	1.98×10^{-7}	1.4
7-F8-6-6	15	yes	1.5	60	1.12×10^{-6}	7.60×10^{-6}	0.68
7-F8-6-9	15	yes	1.5	60	8.79×10^{-6}	6.33×10^{-6}	0.72

There was a large amount of variability between the coupons of any run. This is attributed to reproducibility problems in hand casting of the membranes and the presence of surface defects.

Membranes obtained from the set of conditions in run 5 and 6 (coupons 7-F5-6-4, 7-F5-6-5, 7-F6-6-8, 7-F6-6-9) had good performance with respect to the targeted values of permeation and separation. The CO_2 permeation rate was significantly lower than the target values of 3.37×10^{-8} moles/(m^2 s Pa) but the target CO_2/CH_4 pure gas permeation rate ratio of 50 was contained in the range of CO_2/CH_4 pure gas permeation rate ratio obtained for these membranes.

Of all the conditions giving membranes with a pure gas permeation rate ratio greater than 50, the membranes from run 1 had the highest CO_2 permeation rate.

The membranes formed under the conditions of runs 3 and 8 had very high permeabilities and were not selective, giving pure gas permeation rate ratio below 1.0.

Half-normal plots of the CO_2 permeation rate and CO_2/CH_4 pure gas permeation rate ratio were performed. The results of the ANOVA procedure and the SAS® outputs for the half-normal plots can be found in Appendix C.

From the half-normal plot of all the effects on the CO_2 permeation rate (Figure 6.11), it is difficult to determine which effects are significant since the effects do not fall on a straight line. The effect of factor *B* (additive concentration), seems to be significant. Half-normal plots for the CO_2 permeation rate with effect *B* removed (Figure 6.12) and effects *B*, *AC*, and *D* removed (Figure 6.13) confirm that all effects appear significant to some degree since a clear straight line through the origin is not obtained. Since the effects of factors *B* and *D* are very large, it is reasonable to assume that the alias of *AC*, the *BD* interaction is significant, while the *AC* effect could be of lesser importance in this confounded pair of 2-factor interactions.

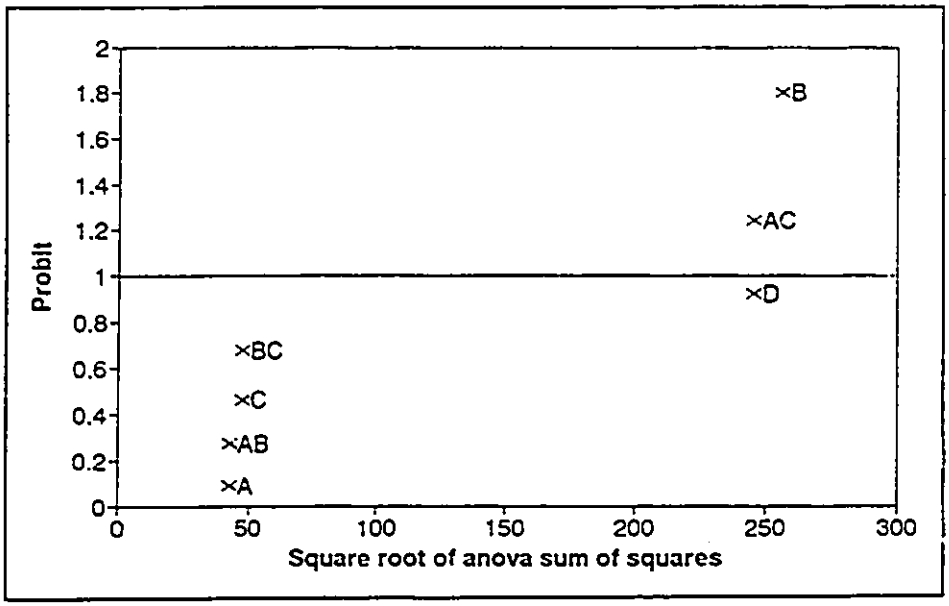

Figure 6.11 *Half-normal plot of the effects on CO_2 permeation rate.*

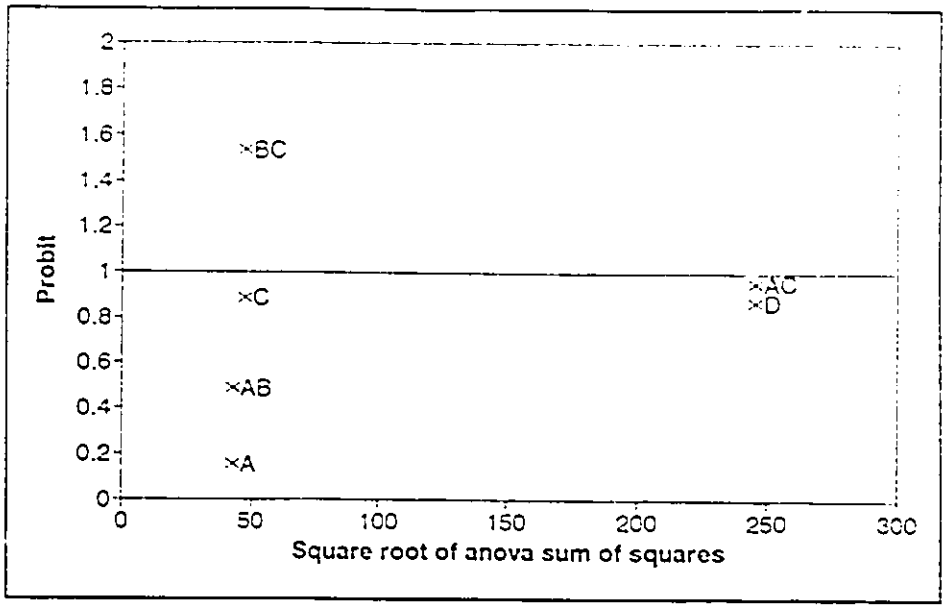

Figure 6.12 *Half-normal plot for the main effects on the CO_2 permeation rate, with B effect removed.*

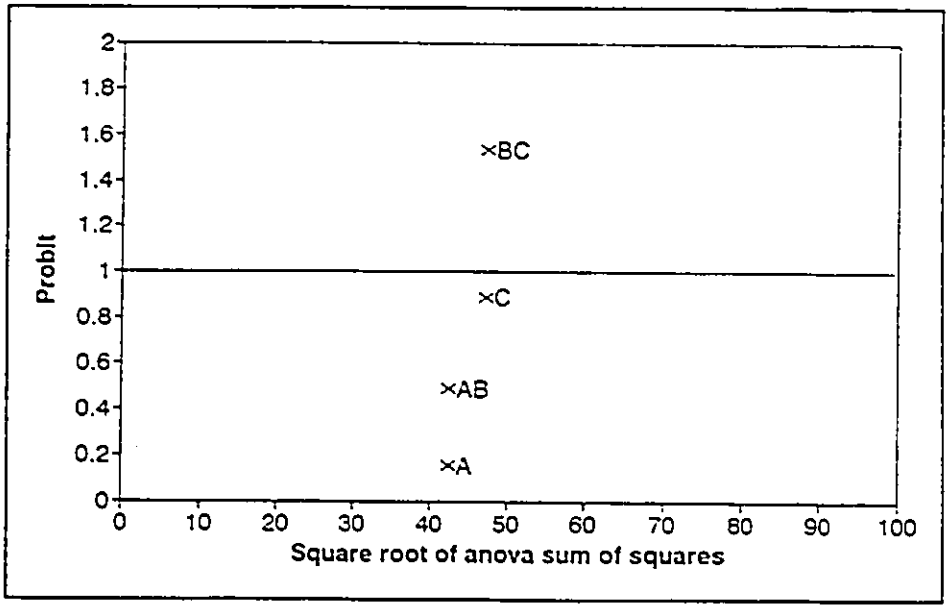

Figure 6.13 *Half-normal plot for the main effects on the CO2 permeation rate, without B, AC and D effects.*

It is not possible to estimate the variance of the CO_2 permeation rate from these plots.

The half-normal plot of all the effects on the CO_2/CH_4 pure gas permeation rate ratio (Figure 6.14) indicates that the factor *B*, additive concentration, seems to have a significant effect as well as the *AB* 2-factor interaction effect, since they do not fall on the straight line passing through the origin and the less important effects. From what is known of membrane making, it is expected that the combined effect of evaporation time before gelation (*C*) and the casting solution temperature (*D*), *CD* will be more significant than its alias *AB*, the combination of polymer concentration (*A*) and the additive

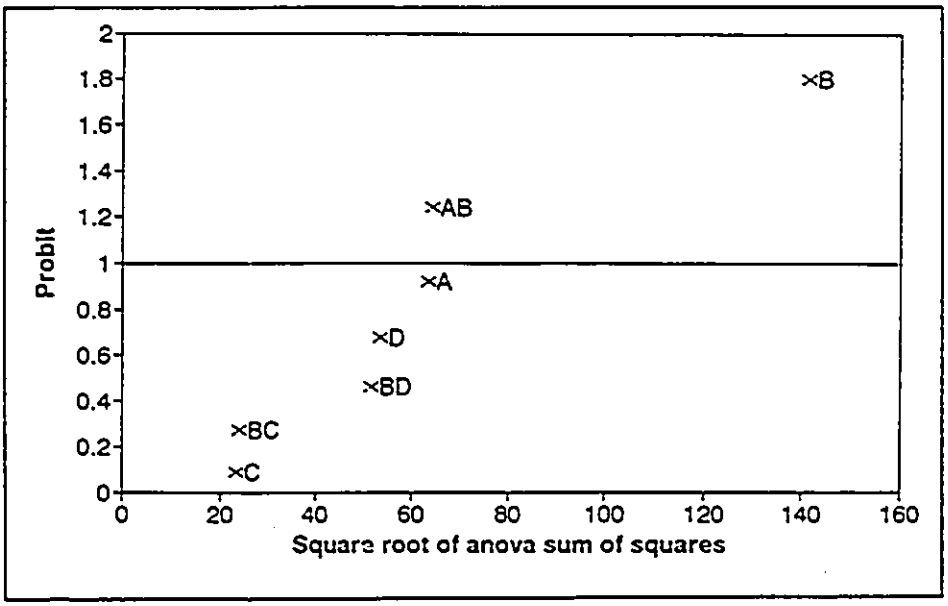

Figure 6.14 *Half-normal plot for CO_2/CH_4 pure gas permeation rate ratio.*

concentration (*B*).

A half-normal plot with these main effects removed (Figure 6.15) gives the expected straight line. The variance of the ratio is estimated at a probit value of 1, by linear regression.

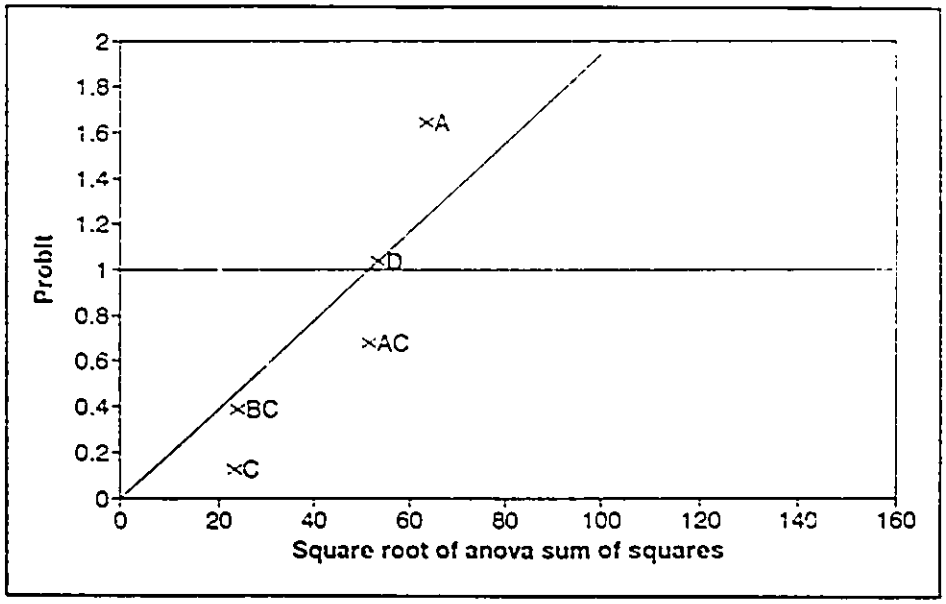

Figure 6.15 *Half-normal plot for the CO_2/CH_4 pure gas permeation rate ratio, with effects B and CD (=AB) removed.*

By backwards elimination from the most general model, the following equation was obtained for CO_2 permeation (moles/ (m^2 s Pa)):

$$CO_2Perm. = (15.1 + 2.5A + 15.1B + 2.8C + 14.5D + 14.6(BD + AC) + 2.5(CD + AB) + 2.8(BC + AD) \times 10^{-6} \quad \textit{Eq. 6-1}$$

where the factors *A*, *B*, *C*, and *D* are scaled from -1 to +1 as in Table 6.5. All the variables left in the model are significant at the 0.05 level. As expected form the half-normal plots of the CO_2 permeation rate, the effect of factors *B*, *D* and *BD* 2-factor interaction are significant as seen by the large absolute value of the parameters associated with these factors.

The residuals are plotted as a function of the predicted value of the CO_2 permeation rate (Appendix C). They appear randomly distributed about 0, but significant heteroscedasticity is present in the data. The variance of the observations is increasing with the magnitude of the predicted CO_2 permeation rate. This may be attributed to the linear extrapolation used to approximate the permeation rates of membranes with very high permeation rates such as in runs 3 and 8. This heteroscedasticity could not be removed by weighting since an estimate of the variance was not available. Model fitting of the data by Tukey biweight robust regression (Beaton and Tukey, 1974), in which observations with large residuals are given less weight and therefore are less influential on the regression, gave roughly the same values for the parameters as conventional linear regression.

An *F* test comparing the mean square of the model to the mean square of the error demonstrates the usefulness of the model for predicting the CO_2 pure gas permeation rate of the membranes since the probability that at least one of the parameters is different from zero is greater than 0.001. A coefficient of

determination, R^2, of 0.987 is obtained, demonstrating that most of the variability of the data is accounted for by the model.

Similarly, by backwards elimination, the following equation was obtained for the modeling of the CO_2/CH_4 permeation rate ratio:

$$Ratio = 49.1 - 20.5A - 47.8B - 21.1D + 20.4(BD + AC) + 20.8(CD + AB) \qquad Eq.\ 6\text{-}2$$

where the factors *A*, *B* and *D* are scaled between -1 and 1. All the variables left in the model are significant at the 0.25 level. The effect of factor *C* (evaporation time before gelation) was found to be negligible in the range of factors selected. The R^2 factor was 0.72, indicating that improvements to the model are possible, such as quadratic terms. It should also be noted that the between coupon variation is larger than any of the effects, due to the reproducibility problems of hand-casting the membranes.

As expected from the half-normal plot, the factor *B* is significant as demonstrated by the large absolute value of the parameter associated with it. A plot of the residuals (Appendix C) revealed heteroscedasticity of the observations, for the pure gas permeation rate ratios that were determined by linear extrapolation.

6.7. *Optimization*

Using the results obtained from the fractional factorial design, attempts were made to optimize the casting conditions in order to obtain the target values for CO_2 permeation rate and CO_2/CH_4 permeation rate ratio.

Since the intercept of the model for the CO_2/CH_4 pure gas permeation rate ratio was 49.1, very close to the target of 50, a test with the scaled conditions of A=0, B=0 and D=0 was attempted. The scaled value of factor C of -1 was chosen since it was not significant for the permeation rate ratio but there was less possible error in immersing the membranes in the gelation bath immediately after gelation than to have a timed solvent evaporation. This set of experimental conditions was identified as run F0. The uncoded variables for this set of conditions are:

A=0: 12.5 wt% high molecular weight PPO

B=0: 7 wt% 2-ethyl-1-hexanol additive in chloroform

C=-1: no evaporation of solvent before gelation

D=0: casting solution at 40 °C

A summary of the casting conditions and results are shown in Table 6.7.

Table 6.7 Results from the optimisation of the membrane casting conditions

Coupon Code	Polymer Concen-tration (wt%)	Additive (wt% of total solvent)	Evapora-tion time (min)	Tempe-rature of casting solution (°C)	CH_4 permea-tion rate (moles/(m^2 s Pa))	CO_2 permea-tion rate (moles/(m^2 s Pa))	CO_2/CH_4 pure gas permea-tion rate ratio
7-F0-6-1	12.5	7	0	40	5.73×10^{-11}	6.81×10^{-9}	119.0
7-F0-6-2	12.5	7	0	40	7.01×10^{-10}	1.19×10^{-8}	17.0
7-F0-6-13	12.5	7	0	40	3.26×10^{-10}	6.87×10^{-9}	21.1
7-OP1-6-4	12.5	8.75	0	23	4.08×10^{-10}	9.22×10^{-9}	19.2
7-OP1-6-5	12.5	8.75	0	23	1.11×10^{-9}	1.61×10^{-8}	14.4
7-OP2-6-1	10	9.8	0	27	7.97×10^{-7}	5.54×10^{-7}	0.7
7-OP2-6-4	10	9.8	0	27	6.17×10^{-7}	4.22×10^{-7}	0.7
7-OP2-6-5	10	9.8	0	27	9.45×10^{-7}	6.34×10^{-7}	0.7

The membranes obtained had good mechanical strength and were CO_2 selective. The range of the CO_2 /CH_4 permeation rate ratio obtained contains the expected value of 49 from the model but is not an improvement over the membranes from runs 5 and 6. However, the membranes obtained have a higher CO_2 permeation rate than the membranes from runs 5 and 6.

Contour plots of the modeled CO_2 permeation rate and CO_2/CH_4 permeation rate ratio were drawn in order to determine the casting conditions that would give a membrane which would have both the targeted CO_2

permeation rate of 3.37×10^{-8} moles/(m^2 s Pa) (2 mmoles/(m^2 min kPa)) and CO_2/CH_4 pure gas permeation rate ratio of 50 (Figures 6.16 and 6.17).

Two such points were identified by superimposing the contour plots of CO_2 permeation rate and CO_2/CH_4 permeation rate ratio and selecting the region that gave both the target permeation rate and permeation rate ratio. These runs were labeled OP1 and OP2. The conditions in uncoded variables were:

Set of optimum conditions 1 (OP1), corresponding to Figure 6.16 (❶):

A=0: 12.5 wt% high molecular weight PPO

B=0.25: 8.75 wt% 2-ethyl-1-hexanol additive in chloroform

C=-1: no evaporation of solvent before gelation

D=-0.85: casting solution at 23 °C

and set of optimum conditions 2 (OP2), corresponding to Figure 6.17 (❷):

A=-1: 10 wt% high molecular weight PPO

B=0.4: 9.8 wt% 2-ethyl-1-hexanol additive in chloroform

C=-1: no evaporation of solvent before gelation

D=-0.65: casting solution at 27 °C

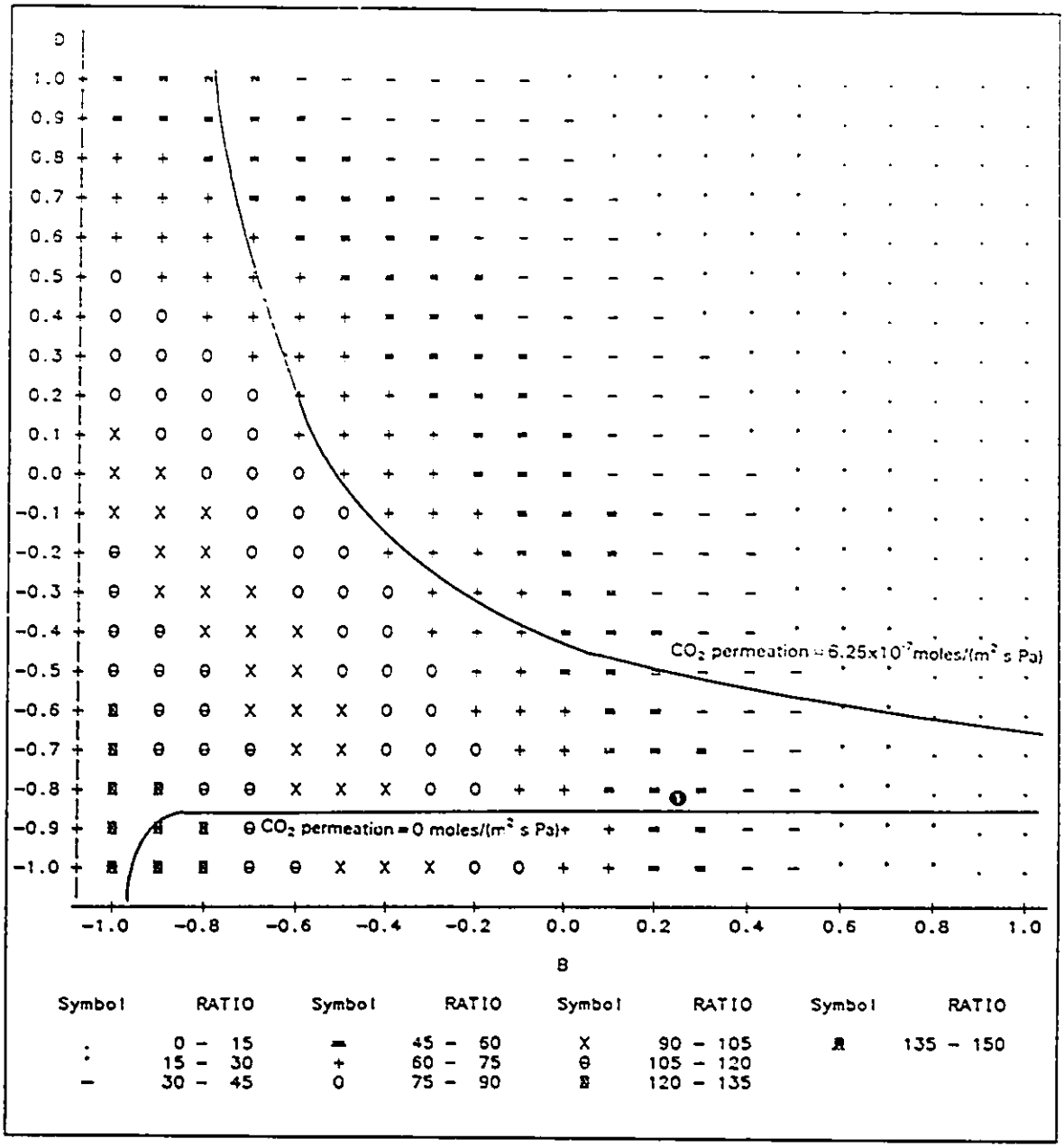

Figure 6.16 *Contour plot of the CO_2/CH_4 pure gas permeation rate ratio as a function of additive concentration (B) and casting solution temperature (D) with polymer concentration A=0 and evaporation time C=-1, with target CO_2 permeation rate region indicated and set of optimum casting conditions 1 identified* ❶.

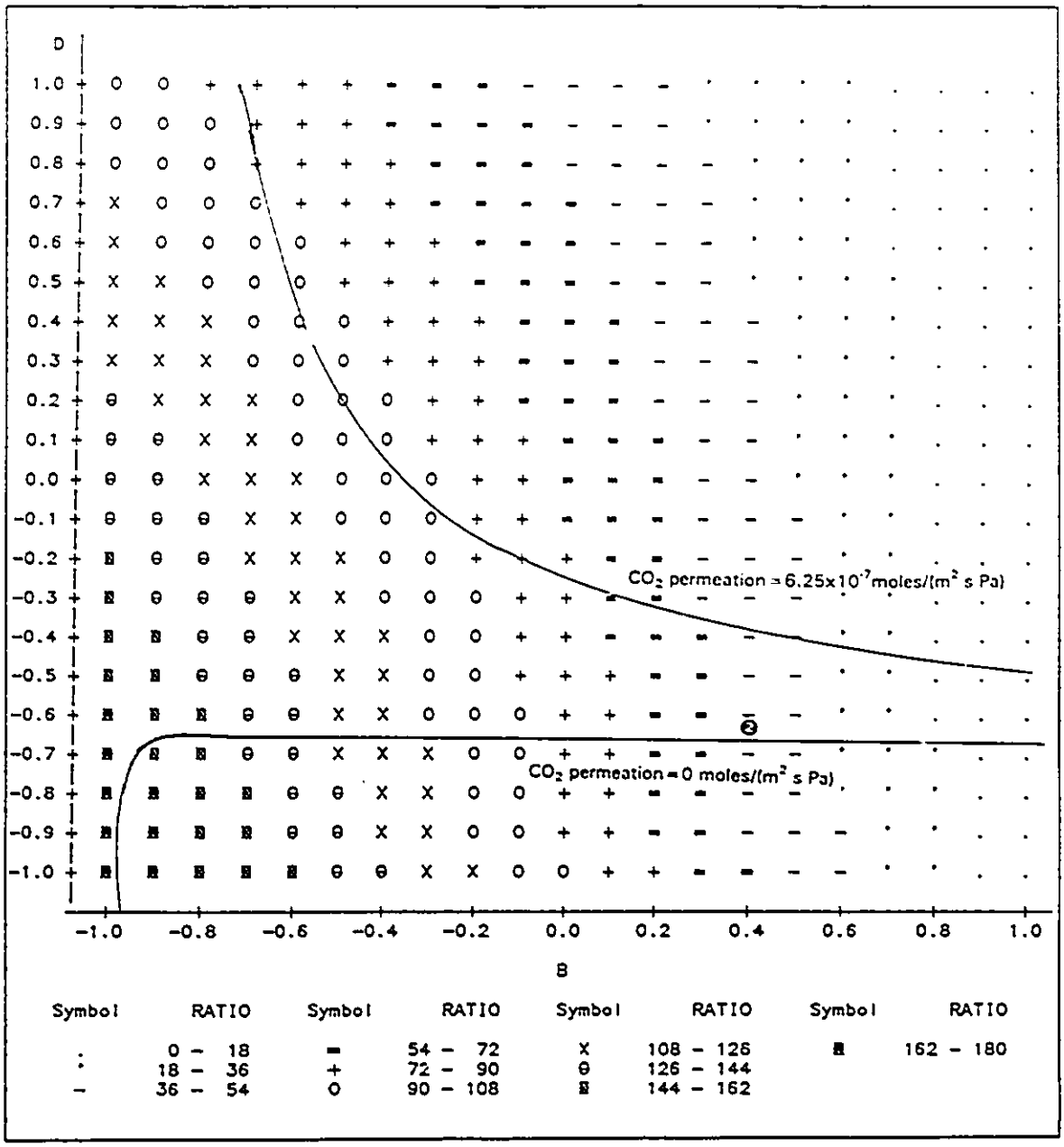

Figure 6.17 *Contour plot of the CO_2/CH_4 pure gas permeation rate ratio as a function of additive concentration (B) and casting solution temperature (D) with polymer concentration A=-1 and evaporation time C=-1, with target CO_2 permeation rate region indicated and set of optimum conditions 2 identified ❷.*

The results are presented in Table 6.7. The best result obtained so far is coupon 7-OP1-6-4 which had a CO_2 permeation rate of 9.22E-9 and a CO_2/CH_4 pure gas permeation rate ration of 19.2. The second set of conditions gave membranes that were very open and not selective.

These new data points were also used to improve the models for the CO_2 permeation rate and CO_2/CH_4 permeation rate ratio, by adding more data points and more degrees of freedom. It was also possible to verify the presence of quadratic terms, for example B^2. By backwards elimination from the most general model, the following equations were obtained for CO_2 permeation and CO_2/CH_4 pure gas permeation rate ratio.

$$CO_2 Perm. = (0.002 + 1.48B + 1.44D + 1.34BD + 1.49B^2) \times 10^{-6} moles/(m^2 sPa) \quad Eq.\ 6\text{-}3$$

$$Ratio = 44.8 - 51.7B + 25.5AB + 24.1BD \quad Eq.\ 6\text{-}4$$

where the factors A, B, and D are scaled from -1 to +1 as in Table 6.5. As expected from the factorial design analysis, factor B, the concentration of additive is very significant for both the CO_2 permeation rate and the selectivity of the membranes. The factor C, evaporation time before gelation, was not significant for the preparation of these high molecular weight PPO membranes, in the range studied. All the variables left in the model are significant at the 0.01 level for the CO_2 permeation rate and at the 0.1 level for the CO_2/CH_4 pure gas

permeation rate ratio. The outputs form the SAS® analysis can be found in Appendix B.

The residuals are plotted as a function of the predicted value of the CO_2 permeation rate and ratio (Appendix C). They appear randomly distributed about zero. As in the analysis of the factorial design, some heteroscedasticity is present in the data, due to the high error associated with runs 3 and 8 of the factorial design. There is no lack of fit in either models. Coefficients of determinations, R^2, of 0.929 and 0.575 are obtained for the CO_2 permeation rate and CO_2/CH_4 pure gas permeation rate ratio, respectively.

The models are valid only in the range of the variables presented in Table 6.5 . Improvements to the models could be made by increasing the number of coupons used for each of the runs and by doing replicates of the experiment.

7. Conclusions

Based on the research performed, it is possible to prepare asymmetric polyphenylene oxide (PPO) membranes with natural gas separation capabilities. Pure gas CO_2/CH_4 permeation rate ratios as high as 240 were achieved, with a CO_2 permeation rate of 1.38×10^{-9} moles/(m^2 s Pa) with the system used.

The asymmetricity of the membrane was confirmed by scanning electron microscopy and the CO_2-CH_4 separation capabilities of the membranes were demonstrated by pure gas permeation tests as well as permeation with gas mixtures.

With respect to membrane performance and mechanical strength, the following membrane preparation factors were found to be most significant: membrane wet casting thickness, solvent evaporation, polymer concentration, and additive concentration. The chemical modifications on the PPO polymer also had an effect on the gas separation capabilities of membranes prepared from the polymer. Acylation and bromination of the polymer decreased the selectivity of the membranes. High molecular weight PPO exhibited both the highest CO_2 permeation rate and CO_2/CH_4 pure gas permeation rate ratio, as well as good mechanical strength.

By using a fractional factorial design, it was possible to study the effect and interaction of polymer concentration, additive concentration, evaporation time before gelation and temperature of the casting solution on the performance of gas separation membranes. The CO_2 permeation rate of high molecular weight PPO was adequately modeled by a straight line, however, a linear model may not be appropriate for modeling the CO_2/CH_4 pure gas permeation rate ratio.

Using the models, it was possible to identify two sets of casting conditions that should have given the targeted CO_2 permeation rate of 3.37×10^{-8} moles/(m^2 s Pa) and CO_2/CH_4 pure gas permeation rate ratio of 50. When these membranes were prepared and tested, the target values were not attained but some improvements in membrane performance were achieved and a membrane coupon with CO_2 permeation rate of 9.22×10^{-9} moles/(m^2 s Pa) and CO_2/CH_4 pure gas permeation rate ratio of 19.2 was obtained.

8. Recommendations

Some recommendations concerning testing equipment and procedures can be formulated.

The testing apparatus should be modified to minimize the suction and pressure damage to the membrane coupons during purging of the cells and permeation testing. An apparatus to measure very small permeation rates, such as a constant volume system, should be used to test membranes with very small permeation rates.

The testing apparatus could also be modified to operate at the temperature the membrane will be subjected to when used for natural gas separation. Since permeability is temperature dependent, this will give a more accurate understanding of the usefulness of the membranes for such a separation. Also, testing with gas mixtures should be used instead of pure gas permeation to obtain a measure of the plasticization of the membrane when exposed to CO_2. Extended tests would give information on the time dependence of the separation factor.

The membrane casting should be performed using a machine capable of drawing the casting bar at a constant rate. This would reduce the coupon-to-coupon error associated with hand-casting of the membranes.

If a similar study of the effect of casting conditions is attempted, a full factorial design should be done. This may provide additional degrees of freedom and it may be possible to obtain an estimate of the variance, even if replicates are not done. Also, it may be useful to do a 3-level factorial design in order to obtain information on the quadratic effects of the factors tested.

9. References

Alger, M. S. M., "Polymer Science Dictionary", Elsevier Applied Science, London, (1989), p.338.

). W. Savage and A. Bisio, "Gas Treating with Chemical Solvents", J. \ ›ons, New York, (1983).

Bauer, C. J. M., J. Smid and J. Olijslager, "The resistance towards gas transport of the sublayer of asymmetric PPO hollow fiber membranes determined by plasma-etching", Journal of Membrane Science, **57**, 307-320 (1991).

Beaton, A. E. and J. W. Tukey, "The Fitting of Power Series, Meaning Polynomials, Illustrated on Band-Spectroscopic Data", Technometrics, **16**, 147-185 (1974).

Chern, R. T., "Repeat unit structure and gas transport properties of aromatic polymers", Separation Science and Technology, **25 (13-15)**, 1325-1338(1990).

Dietz, W. A., "Response Factors for Gas Chromatography Analyses", Journal of Gas Chromatography, **5**, 68 (1967).

Draper, N. R. and H. Smith, "Applied Regression Analysis", John Wiley & Sons, New York, (1981).

Franken, A. C. M. and A. G. Fane, "Environmental Management Using Membranes", in "CHEMECA '90, Australasian Chemical Engineering Conference", Univ. of Auckland School of Engineering, Auckland, NZ, (1990) pp. 754-761.

Fritzsche, A. K., R. E. Kesting and M. K. Murphy, "The Effect of Free Volume on Enhanced Transport Rates of Polysulfone Hollow Fiber Membranes Spun from Lewis Acid:Base Solvent Complexes", Journal of Membrane Science, **46**, 135-155 (1989).

Fu, H., L. Jia, and J. Xu, "Studies on the Sulfonation of Poly(phenylene oxide) (PPO) and Permeation Behaviour of Gases and Water Vapor Through Sulfonated PPO Membranes. I. Sulfonation of PPO and Characterization of the Products", Journal of Applied Polymer Science, **51**, 1399-1404 (1994).

Fu, H., L. Jia, and J. Xu, "Studies on the Sulfonation of Poly(phenylene oxide) (PPO) and Permeation Behaviour of Gases and Water Vapor through Sulfonated PPO Membranes. II. Permeation Behavior of Gases and Water Vapor Through Sulphonated PPO Membranes", Journal of Applied Polymer Science, **51**, 1405-1409 (1994).

Ghosal, K. and R. T. Chern, "Aryl-nitration of poly(phenylene oxide) and polysulfone. Structural characterization and gas permeability", Journal of Membrane Science, **72**, 91-97(1992).

Gurr, W. R., "An Operators Overview of Gas Membranes", Effective Industrial Membrane Processes-Benefits and Opportunities, (1991) pp.329-336.

Hay, A. S., "Discovery and commercialization of Noryl® Resins" in "High Performance Polymers: Their Origin and Development", R. B. Seymour and G. S. Kirshenbaum, Eds., Elsevier Science Publishing Co. Inc., (1986), pp. 209-213.

Henis, J. M. S. "Commercial and practical aspects of gas separation membranes" in "Polymeric Gas Separation Membranes", Paul, D.R. and Y.P. Yampol'skii, Eds., CRC Press, Boca Raton, FA, (1994), pp. 441-530.

Hines, W. W. and D. C. Montgomery, "Probability and Statistics in Engineering and Management Science", John Wiley & Sons, New York, (1980), 460-505.

Ho, W. S. W. and K. K. , "Overview" in "Membrane Handbook", W. S. W. Ho and K. K. Sirkar, Eds., Van Nostrand Reinhold, New York, NY, (1992).

Ikoku, Chi U. "Natural Gas Production Engineering", John Wiley & Sons, New York, (1984).

Ilinitch, O. M., G. L. Semin, M. V. Chertova and K. I. Zamaraev, "Novel polymeric membranes for separation of hydrocarbons" , Journal of Membrane Science, **66**, 1-8 (1992).

Kesting, R. E. and A. K. Fritzsche, "Polymeric Gas Separation Membranes", John Wiley & Sons, Inc., New York, (1993).

Koros, W. J. and I. Pinnau, "Membrane formation for gas separation processes" in "Polymeric Gas Separation Membranes", D. R. Paul and Y. P. Yampol'skii, Eds., CRC Press, Boca Raton, (1994), pp. 209-259.

Loeb, S. and S. Sourirajan, "Sea Water Demineralization by Means of an Osmotic Membrane", in Saline Water Conversion-II, American Chemical Society, Advances in Chemistry Series, **38**, 117-132, (1963).

Medici, M. "The Natural Gas Industry", Newnes-Butterworths, London, (1974).

Milliken, G. A. and D. E. Johnson, "Analysis of Messy Data", Van Nostrand Reinhold, New York, (1989).

Montgomery, D. C., "Design and Analysis of Experiments", John Wiley & Sons, New York, (1984).

Mulder, M., "Basic Principles of Membrane Technology", Kluwer Academic Publishers, Dordrecht, (1991).

Percec, S. and G. Li, "Chemical Modification of Poly(2,6-dimethyl-1,4-phenylene oxide) and Properties of the Resulting Polymers", in ACS Symposium Series, Washington, DC, **364**, 46-58 (1988).

Perego, G., A. Roggero, R. Sisto and C. Valentini, "Membranes for gas separations based on silylated polyphenylene oxide", Journal of Membrane Science, **55**, 325-331(1991).

Pesek, S. C. and W. J. Koros, "Aqueous quenched asymmetric polysulfone hollow fibers prepared by dry/wet phase separation", Journal of Membrane Science, **88**, 1-19 (1994).

Pixton, M. R. and D. R. Paul, "Relationships between structure and transport properties for polymers with aromatic backbones" in "Polymeric Gas Separation Membranes", Paul, D. R. and Y. P. Yampol'skii, Eds., CRC Press, Boca Raton, FA, (1994), pp. 83-149.

Raktoe, B. L., A. Hedayat, and W. T. Federer, "Factorial Designs", John Wiley & Sons, New York, (1981), pp. 144-152.

Reuvers, A. J., J. W. A. van den Berg, and C. A. Smolders, "Formation of membranes by means of immersion precipitation, Part I. A model to describe mass transfer during immersion precipitation", Journal of Membrane Science, **34**, 45-65 (1987).

Rezac, M. E., J. D. Le Roux, H. Chen, D. R. Paul and W. J. Koros, "Effect of Mild Solvent Post-Treatments on the Gas Transport Properties of Glassy Polymer Membranes", Journal of Membrane Science, **90**, 213-229 (1994).

Sanders, E. S., "Penetrant-induced plasticization and gas permeation in glassy polymers", Journal of Membrane Science, **37**, 63-80 (1988).

Sisto, R., C. Bonfanti, and C. Valentini, "Structure and gas permeability of alynylated poly(phenylene oxide)" in Journal of Membrane Science, **95**, 135-146 (1994).

Smid, J., J. H. M. Albers and A. P. M. Kusters, "The formation of asymmetric hollow fibre membranes for gas separations, using PPE of different intrinsic viscosities", Journal of Membrane Science, **64**, 121-128 (1991).

Spillman, R. W. "Economics of Gas Separation Membranes", Chemical Engineering Progress, **85**, no. 1, 41-62 (1989).

Stern, S. A. and S. S. Kulkarni, "Tests of a 'Free-Volume' Model of Gas Permeation through Polymer Membranes. I. Pure CO_2, CH_4, C_2H_4, and C_3H_8 in Polyethylene", Journal of Polymer Science: Polymer Physics Edition, **21**, 467-481 (1983).

Stern, S. A., "Polymers for gas separations: the next decade", Journal of Membrane Science, **94**, 1-65 (1994).

Stern, S. A., P. J. Gareis, T. F. Sinclair, and P. H. Mohr, "Performance of a Versatile Variable-Volume Permeability Cell. Comparison of Gas Permeability Measurements by the Variable-Volume and Variable-Pressure Methods", in Journal of Applied Polymer Science, **7**, 2035-2051 (1963).

Stookey, D. J., T. E. Graham and W. M. Pope, "Natural Gas Processing with PRISM® Separators", in "Acid and Sour Gas Treating Processes", Gulf Publishing Company, Houston, TS, (1985).

Story, B. J. and W. J. Koros, "Sorption and transport of CO_2 and CH_4 in chemically modified poly(phenylene oxide), Journal of Membrane Science, **67**, 191-210 (1992).

Street, A. P. and D. J. Street, "Combinatorics of Experimental Design", Clarendon Press, Oxford, (1987), 193-236.

Sundararajan, P. R., "Poly(1,4-Phenylenes): Steric Factor Redefined", Polymeric Materials Science and Engineering, American Chemical Society, **63**, 392-396 (1990).

Tsujita, Y., H. Hachisuka, T. Imai, A. Takizawa and T. Kinoshita, "Solubility and permeability of quenched poly(2,6-dimethyl phenyleneoxide) with various microvoids", Journal of Membrane Science, **60**, 103-111 (1991).

Volkov, V. V., "Free Volume Structure and Transport Properties of Glassy Polymers-Materials for Separating Membranes", Polymer Journal, **23**, 457-466 (1991).

Weber, W. F. and W. Bowman, "Membranes Replacing Other Separation Technologies", Chemical Engineering Progress, **86**, 23-28, (1986).

Wijmans, J. G., H. J. J. Rutten and C. A. Smolders, "Phase separation phenomena in solutions of poly(2,6-dimethyl-1,4-phenylenoxide) in mixtures of trichloroethylene, 1-octanol, and methanol: Relationship to membrane formation", Journal of Polymer Science: Polymer Physics Edition, **23**, 1941-1955 (1985).

Zolandz, R. R. and G. K. Fleming, "Gas Permeation" in "Membrane Handbook" , W. S. W. Ho and K. K. Sirkar, Eds., Van Nostrand Reinhold, New York (1992), pp.17-101.

Appendix A

Permeation data

Extrapolation for permeation of membranes 7-F3-6-* and 7-F8-6-*

Data from gas mixture tests

Assymetric 20% PPO in chloroform membranes (2-20C-)

filtered solutions

results at STP

coupon	date cast	He perm. moles (m2 s Pa) 60 psi	H2 perm. moles (m2 s Pa) 100 psi	CH4 perm. moles (m2 s Pa) 100 psi	CO2 perm. moles (m2 s Pa) 100 psi	N2 perm. moles (m2 s Pa) 100 psi	H2 perm. moles (m2 s Pa) 150 psi	CH4 perm. moles (m2 s Pa) 150 psi	CO2 perm. moles (m2 s Pa) 150 psi	N2 perm. moles (m2 s Pa) 150 psi	H2 perm. moles (m2 s Pa) 200 psi	CH4 perm. moles (m2 s Pa) 200 psi	CO2 perm moles (m2 s Pa) 200 psi	N2 perm moles (m2 s Pa) 200 psi	20 4%CO2 in CH4 120psi moles (m2 s Pa)	48 2% CO2 in CH4 120 psig moles (m2 s Pa)
6-1	3/8/93	* 2.2305E-07	ruptured		6.1588E-08											
6-2	3/8/93	* 2.6996E-07				ruptured										
6-3	3/8/93		4.86285E-09	2.5694E-09	2.4287E-09			2.582E-09	2.677E-09							
6-3 lam.			2.28392E-10	5.600E-12	4.9485E-10	5.600E-12										
6-4	3/8/93		* 3.9599E-10	ruptured	6.955E-10	1.6627E-11										
6-5	3/8/93		ruptured			* 1.0982E-08										
6-6	3/8/93		ruptured													
6-7	3/31/93		ruptured													
6-8	3/31/93		1.71833E-10	5.600E-12	4.4871E-10	5.600E-12	2.393E-10	5.600E-12	5.033E-10		2.604E-10	6.731E-12	5.272E-10			
6-9	3/31/93			ruptured	6.4997E-10											
6-10	3/31/93		ruptured	5.600E-12	6.2293E-08											
6-11	3/31/93		ruptured													
6-12	4/6/93		* 2.5992E-07			ruptured										
6-13	4/6/93	not tested	did not gel	evenly												
6-14	4/6/93		5.90013E-10	5.600E-12	9.7067E-10			5.634E-09	ruptured							
6-15	3/14/94															
6-16	3/14/94		ruptured													
6-17	3/14/94															
6-18	5/24/94			5.6E-12	5.6277E-10										3.4446E-10	5.2465E-10
6-19	5/24/94			8.6813E-12	5.5127E-10										1.1997E-10	2.4433E-09
6-20	5/24/94	ruptured														
6-21	5/24/94			5.6E-12	5.9095E-10										2.6894E-10	3.9526E-10
6-22	5/24/94			1.3507E-10	1.56E-09											
6-23	5/24/94			too high												

1) * not at steady state, usually rupturing

2) when permeation rate was non-detectable, it was estimated at 5.6E-12 moles/(m2 s Pa)

Assymetric 20% PPO in chloroform membranes (2-20C-)

filtered solutions

pure gas permeation rate ratio

coupon	date cast	H2/N2 100 psi	H2/CH4 100 psi	H2/CO2 100 psi	CO2/CH4 100 psi	H2/CH4 150 psi	H2/CO2 150 psi	CO2/CH4 150 psi	H2/CH4 200 psi	H2/CO2 200 psi	CO2/CH4 200 psi
6-1	3/8/93	ruptured									
6-2	3/8/93	ruptured									
6-3	3/8/93		1.89	2.00	0.94			1.04			
6-3 lam.		very large	very large	0.46	very large						
6-4	3/8/93	23.5		0.57							
6-5	3/8/93	ruptured									
6-6	3/8/93	ruptured									
6-7	3/31/93	ruptured									
6-8	3/31/93	very large	very large	0.38	very large	very large	0.48	very large	41.67	0.53	78.33
6-9	3/31/93										
6-10	3/31/93	ruptured									
6-11	3/31/93	ruptured									
6-12	4/6/93	ruptured									
6-13	4/6/93	not tested									
6-14	4/6/93		very large	0.61	very large			ruptured			
6-15	3/14/94										
6-16	3/14/94										
6-17	3/14/94										
6-18	5/24/94										
6-19	5/24/94				66.73						
6-20	5/24/94										
6-21	5/24/94										
6-22	5/24/94				11.56						
6-23	5/24/94										

Assymetric 15% PPO in chloroform membranes (2-15C-)
filtered solutions

results at STP

coupon	date cast	H2 perm. moles (m2 s Pa) 100 psi	CH4 perm. moles (m2 s Pa) 100 psi	CO2 perm. moles (m2 s Pa) 100 psi	N2 perm. moles (m2 s Pa) 100 psi	H2 perm. moles (m2 s Pa) 150 psi	CH4 perm. moles (m2 s Pa) 150 psi	CO2 perm. moles (m2 s Pa) 150 psi	N2 perm. moles (m2 s Pa) 150 psi	H2 perm. moles (m2 s Pa) 200 psi	CH4 perm moles (m2 s Pa) 200 psi	CO2 perm moles (m2 s Pa) 200 psi	N2 perm moles (m2 s Pa) 200 psi
6-1	4/15/93		* 1.465E-09	8.460E-10									
6-1, lam.		4.137E-10	5.600E-12	7.139E-10	5.600E-12		1.066E-11	7.779E-10	5.600E-12	6.990E-10	3.142E-11	9.022E-10	7.413E-11
6-2	4/15/93	8.696E-08	4.990E-08	2.210E-08	1.543E-07	rupturing							
6-3, lam.	4/15/93	no flow											
6-4, lam.	4/15/93	2.993E-10 3.613E-10	5.600E-12 < 2.244E-12	6.035E-10 6.599E-10	1.784E-11	4.210E-10	2.939E-10	7.007E-10	1.428E-10	6.783E-10	ruptured		
6-5	4/15/93		2.154E-08	1.256E-08	ruptured								
6-6	4/15/93	ruptured											
6-7	6/6/94	ruptured											
6-8	6/6/94	no resistance											
6-9	6/6/94												
6-10	6/6/94												
6-11	6/6/94												
6-12	6/6/94												
8-1	4/15/93												
8-2	4/15/93												

* not at steady-state, usually rupturing
when permeation was non-detectable, it was estimated at 5.6E-12 moles/(m2 s Pa)

Assymetric 15% PPO in chloroform membranes (2-15C-)
filtered solutions

permeation rate ratio

coupon	date cast	H2/CH4 100 psi	H2/CO2 100 psi	CO2/CH4 100 psi	H2/CH4 150 psi	H2/CO2 150 psi	CO2/CH4 150 psi	H2/CH4 200 psi	H2/CO2 200 psi	CO2/CH4 200psi
thick. 6 mil										
6-1	4/15/93			0.58						
6-1, lam.		very large	0.58	very large			73.0	22.2	0.77	28.7
6-2	4/15/93	1.78	4.03	0.44						
6-3, lam.	4/15/93	no flow								
6-4, lam.	4/15/93	very large >161.05	0.50 0.55	very large >294.2	1.43	0.60	2.38			
6-5	4/15/93			0.58						
6-6	4/15/93									
6-7	6/6/94									
6-8	6/6/94									
6-9	6/6/94									
6-10	6/6/94									
6-11	6/6/94									
6-12	6/6/94									
8-1	4/15/93									
8-2	4/15/93									
2	15/4/93									

* not at steady-state, usually rupturing

Assymetric 20% PPO in trichloroethylene membranes (2-20T-)
filtered solutions

results at STP

time in oven at 60C before MeOH bath	coupon	date cast	He perm. moles (m2 s Pa) 60 psi	CO2 perm. moles (m2 s Pa) 60 psi	N2 perm. moles (m2 s Pa) 60 psi	H2 perm. moles (m2 s Pa) 100 psi	CH4 perm. moles (m2 s Pa) 100 psi	CO2 perm. moles (m2 s Pa) 100 psi	N2 perm. moles (m2 s Pa) 100 psi	H2 perm. moles (m2 s Pa) 150 psi	CH4 perm moles (m2 s Pa) 150 psi	CO2 perm. moles (m2 s Pa) 150 psi	N2 perm. moles (m2 s Pa) 150 psi	CH4 perm moles (m2 s Pa) 200 psi	CO2 perm moles (m2 s Pa) 200 psi
(minutes)															
0	6-1	03/02/93	5.6000E-12 3.0951E-10		5.6000E-12 5.6000E-12	3.1983E-10	0.0000E+00	6.9124E-10		3.9617E-10	2.3385E-11	6.1489E-10			
3	6-2	03/02/93	* 1.8285E-7	1.5574E-08	7.9534E-09		ruptured								
3	6-3	03/02/93	2.7122E-10		5.6000E-12		ruptured	1.6853E-08							
	6-4, lam.	03/02/93	5.6000E-12		5.6000E-12										
1	6-4		* 3.9561E-7			2.4368E-07	5.0368E-08	ruptured	* 7.369E-08						
1	6-5	03/02/93				* 8.5143E-08	ruptured		5.6000E-12						
10	6-6	03/02/93				6.1698E-10	3.5448E-09	1.4808E-09		Knudsen flo					
	6-6, lam.					6.3942E-10	0.0000E+00	7.8525E-10							
10	6-7	03/02/93				* 1.2227E-09	ruptured								
0	6-8	03/15/93					ruptured								
0	6-9	03/15/93				2.5352E-08	2.0181E-07	6.3936E-08	rupturing						
0	6-10	03/15/93				2.9610E-10 3.1873E-10	5.6000E-12	6.2933E-10	5.6000E-12	* 3.2906E-10 3.5765E-10	0.0000E+00	5.3648E-10	5.0897E-11	2.5782E-12	* 4.8797E-10
0	6-11	03/15/93	not tested	had dust											
0	6-12	04/23/93				ruptured									
0	6-13	04/23/93				8.0472E-10	7.6345E-11	1.0523E-09	* 1.3402E-08	* 8.534E-10	* 8.527E-08				
0	6-14	04/23/93				ruptured									
0	6-15	04/23/93					5.6000E-12	8.1902E-10	* 6.3942E-11						
0	6-16	04/23/93				*8.4599E-10	8.5552E-09	rupturing							
0	6-17	04/23/93							* 1.2598E-08	ruptured					
0	6-18	04/23/93													
0	6-19	04/23/93				ruptured		1.0657E-09							
0	6-20	04/23/93				had hole									
0, EtOH bath	6-21	06/18/93													
0, EtOH bath	6-22	06/18/93													
0	6-1	03/15/93				3.0288E-10	ruptured								
0	6-2	03/15/93													

* not at steady state, usually rupturing
when permeation rate was non-detectable, it was estimated at 5.6E-12 moles/(m2 s Pa)

Assymetric 20% PPO in trichloroethylene membranes (2-20T-)
filtered solutions

pure gas permeation rate ratio

time in oven at 60C before MeOH bath	coupon	date cast	He/N2 50 psi	He/CO2 50 psi	H2/CH4 100 psi	H2/CO2 100 psi	H2/N2 100 psi	CO2/CH4 100 psi	H2/CH4 150 psi	H2/CO2 150 psi	CO2/CH4 150 psi	H2/CH4 200 psi	H2/CO2 200 psi	CO2/CH4 200 psi
0	6-1	03/02/93	none very large		very large	0 46		very large	16 94	0 64	26 29			
3	6-2	03/02/93	13 80	11.74	ruptured									
3	6-3	03/02/93	very large		ruptured									
	6-4, lam.	03/02/93	none	none										
1	6-4				4 84	ruptured	3 31	ruptured						
1	6-5	03/02/93					very large							
10	6-6	03/02/93			0.17	0.42		0 42	Knudsen Flow					
	6-6, lam.				very large	0 81		very large						
10	6-7	03/02/93	ruptured											
0	6-8	03/15/93	ruptured											
0	6-9	03/15/93			0.13	0 40		0 32	rupturing					
0	6-10	03/15/93			very large	0 49	very large	very large	very large	0 67	very large			* 174
0	6-11	03/15/93	not tested											
0	6-12	04/23/93			ruptured									
0	6-13	04/23/93			10 54	0 76	0 06	13 78						
0	6-14	04/23/93			ruptured									
0	6-15	04/23/93						very large						
0	6-16	04/23/93			0 09	rupturing								
0	6-17	04/23/93							ruptured					
0	6-18	04/23/93												
0	6-19	04/23/93			ruptured									
0	6-20	04/23/93	not tested	had hole										
0, EtOH bath	6-21	06/18/93												
0, EtOH bath	6-22	06/18/93												
0	6-1	03/15/93			ruptured									
0	6-2	03/15/93												

Assymetric 15% PPO in trichloroethene membranes (2-15T-)
filtered solutions

results at STP

coupon	date cast	H2 perm. moles (m2 s Pa) 100 psi	CH4 perm. moles (m2 s Pa) 100 psi	CO2 perm. moles (m2 s Pa) 100 psi	N2 perm. moles (m2 s Pa) 100 psi	H2 perm. moles (m2 s Pa) 150 psi	CH4 perm. moles (m2 s Pa) 150 psi	CO2 perm. moles (m2 s Pa) 150 psi	N2 perm. moles (m2 s Pa) 150 psi	H2 perm. moles (m2 s Pa) 200 psi	CH4 perm. moles (m2 s Pa) 200 psi	CO2 perm. moles (m2 s Pa) 200 psi	N2 perm moles (m2 s Pa) 200 psi
6-1, lam.	4/28/93	1.536E-10	5.600E-12	5.814E-10	ruptured								
6-2, lam.	4/28/93	2.655E-10	< 1.12E-12	6.475E-10	5.600E-12								
6-3	4/28/93	5.478E-10	ruptured										
6-4	4/28/93												
6-5	4/28/93												
6-6	4/28/93	* 1.38E-8	5.163E-09										
6-7	4/28/93	4.351E-08	1.762E-08	1.427E-08									
6-8, lam.	4/28/93	2.426E-10	0.000E+00	6.035E-10	1.245E-11	3.732E-10	0.000E+00	6.705E-10	3.515E-13	4.510E-10	2.131E-11	7.538E-10	2.990E-11
6-9	5/19/93												
6-10	5/19/93												
6-11	5/19/93												
6-12	5/19/93												
6-13	5/19/93												
6-14	5/19/93												
6-1	5/19/93												

* not at steady-state, usually rupturing

when permeation was non-detectable, it was estimated at 5.6E-12 moles/(m2 s Pa)

Assymetric 15% PPO in trichloroethene membranes (2-15T-)
filtered solutions

pure gas permeation rate ratio

coupon	date cast	H2/CH4 100 psi	H2/CO2 100 psi	CO2/CH4 100 psi	H2/CH4 150 psi	H2/CO2 150 psi	CO2/CH4 150 psi	H2/CH4 200 psi	H2/CO2 200 psi	CO2/CH4 200 psi
6-1, lam.	4/28/93	very large	0.26	very large						
6-2, lam.	4/28/93	279.00	0.41	680.4						
6-3	4/28/93									
6-4	4/28/93									
6-5	4/28/93									
6-6	4/28/93	2.66								
6-7	4/28/93	2.47	3.05	0.81						
6-8, lam.	4/28/93	very large	0.40	very large	very large	0.56	very large	21.16	0.60	35.37
6-9	5/19/93									
6-10	5/19/93									
6-11	5/19/93									
6-12	5/19/93									
6-13	5/19/93									
6-14	5/19/93									
8-1	5/19/93									

Assymetric 20% PPO in (1:1 trichloroethylene:chloroform) membranes (2-20CT-)

filtered solutions

results at STP

coupon	date cast	H2 perm. moles (m2 s Pa) 100 psi	CH4 perm. moles (m2 s Pa) 100 psi	CO2 perm. moles (m2 s Pa) 100 psi	N2 perm. moles (m2 s Pa) 100 psi	H2 perm. moles (m2 s Pa) 150 psi	CH4 perm. moles (m2 s Pa) 150 psi	CO2 perm. moles (m2 s Pa) 150 psi	N2 perm. moles (m2 s Pa) 150 psi	H2 perm. moles (m2 s Pa) 200 psi	CH4 perm. moles (m2 s Pa) 200 psi	CO2 perm. moles (m2 s Pa) 200 psi	N2 perm. moles (m2 s Pa) 200 psi
6-1	3/17/93	ruptured											
6-2	3/17/93	ruptured											
6-3	3/18/93	ruptured											
6-4	3/18/93	9.984E-10	3.253E-10	2.962E-09	rupturing								
6-5	3/18/93	2.690E-08	1.662E-07	7.393E-08									
6-5, lam.		0.000E+00 *d 1.784E-08	1.582E-09	5.755E-09	1.739E-09								
6-6	3/18/93	3.580E-10 4.539E-10	5.600E-12	6.789E-10		1.582E-10 *d 8.975E-10	5.600E-12	5.805E-10	1.639E-09		* 6.0221E-09	7.547E-10	3.334E-08
6-7	4/19/93		5.600E-12	1.627E-00	6.006E+03	ruptured							
6-8	4/19/93	* 4.187E-08	5.600E-12	6.090E-09	ruptured								
6-9	4/19/93		3.074E-08	flow very high	most likely	hole							
6-10	4/19/93	4.420E-10	9.638E-11	6.521E-10	9.356E-11	6.716E-10	1.221E-10	6.342E-10	* 2.161E-10	* 4.330E-09	1.209E-09	7.017E-10	* 3.629E-09
6-11	4/19/93	ruptured											
8-1	3/17/93	3.119E-10	5.600E-12	7.617E-10	5.600E-12								
8-2	3/18/93	ruptured											
8-3	3/18/93	ruptured											
8-4	4/6/93	not tested	uneven	surface									
8-5	4/6/93	not tested											
8-6	4/19/93	1.761E-10	1.608E-10	6.661E-09	ruptured								
8-7	4/19/93												
8-8	4/19/93												

* not at steady state, usually rupturing

when permeation rate was non-detectable, it was estimated at 5.6E-12 moles/(m2 s Pa)

Assymetric 20% PPO in (1:1 trichloroethylene:chloroform) membranes (2-20CT-)

filtered solutions

pure gas permeation rate ratio

coupon	date cast	H2/CH4 100 psi	H2/CO2 100 psi	CO2/CH4 100 psi	H2/CH4 150 psi	H2/CO2 150 psi	CO2/CH4 150 psi	H2/CH4 200 psi	H2/CO2 200 psi	CO2/CH4 200 psi
6-1	3/17/93	ruptured								
6-2	3/17/93	ruptured								
6-3	3/18/93	ruptured								
6-4	3/18/93	3 07	0 34	9 10	was rupturing					
6-5	3/18/93	0.16	0 36	0 44	Knudsen flow					
6-5, lam.		11.28	3 10	3 64						
6-6	3/18/93	very large	0 67	very large	very large	0 27	very large	rupturing		
6-7	4/19/93		rupturing	very large						
6-8	4/19/93	ruptured		very large						
6-9	4/19/93	has hole								
6-10	4/19/93	4 49	0 68	6 63	5 50	1 06	5 19	rupturing		
6-11	4/19/93	ruptured								
8-1	3/17/93	very large	0 41	very large						
8-2	3/18/93	ruptured								
8-3	3/18/93	ruptured								
8-4	4/6/93	not tested								
8-5	4/6/93	ruptured								
8-6	4/19/93	ruptured	0 03							
8-7	4/19/93									
8-8	4/19/93									

Assymetric 20% PPO in (30% trichloroethene, 70% chloroform) membranes (2-20CCT-)
filetered solutions

results at STP

coupon	date cast	H2 perm. moles (m2 s Pa) 100 psi	CH4 perm. moles (m2 s Pa) 100 psi	CO2 perm. moles (m2 s Pa) 100 psi	N2 perm. moles (m2 s Pa) 100 psi	H2 perm. moles (m2 s Pa) 150 psi	CH4 perm. moles (m2 s Pa) 150 psi	CO2 perm. moles (m2 s Pa) 150 psi	N2 perm. moles (m2 s Pa) 150 psi
6-1	6/8/93	no resistance							
6-1, lam.		* 1.100E-08	1.03496E-08	* 1.273E-08	2.084E-08	rupturing			
6-2	6/8/93	no resistance							
6-2, lam.		4.361E-10	5.600E-12	8.02E-10	1.754E-11	4.091E-10			
6-3	6/8/93	3.742E-08	rupturing						
6-4	6/8/93	5.87E-08	3.13E-08	1.37E-08	ruptured				
6-5	6/8/93	no resistance							
6-6	6/8/93	* 7.40e-10	ruptured						
6-7	6/8/93	3.391E-10	4.286E-11	5.236E-10	3.333E-10	* 5.949E-09	rupturing		

* not at steady-state, usually rupturing
when permeation was non-detectable, it was estimated at 5.6E-12 moles/(m2 s Pa)

Assymetric 20% PPO in (30% trichloroethene, 70% chloroform) membranes (2-20CCT-)
filetered solutions

pure gas permeation rate ratio

coupon	date cast	H2/CH4 100 psi	H2/CO2 100 psi	CO2/CH4 100 psi	H2/CH4 150 psi	H2/CO2 150 psi	CO2/CH4 150 psi	H2/CH4 200 psi	H2/CO2 200 psi	CO2/CH4 200 psi
6-1	6/8/93	no resistanc								
6-1, lam.		1.07	0.87	1.23	0.53	rupturing				
6-2	6/8/93	no resistanc								
6-2, lam.		very large	0.54	very large						
6-3	6/8/93	rupturing								
6-4	6/8/93	1.88	4.27	0.44						
6-5	6/8/93	no resistanc								
6-6	6/8/93	ruptured								
6-7	6/8/93	7.93	0.65	12.23						

Assymetric 20% PPO in (70% trichloroethene, 30% chloroform),membranes (2-20CTT-)
filtered solutions

results at STP

coupon	date cast	H2 perm. moles (m2 s Pa) 100 psi	CH4 perm. moles (m2 s Pa) 100 psi	CO2 perm. moles (m2 s Pa) 100 psi	N2 perm. moles (m2 s Pa) 100 psi	H2 perm. moles (m2 s Pa) 150 psi	CH4 perm. moles (m2 s Pa) 150 psi	CO2 perm. moles (m2 s Pa) 150 psi	N2 perm. moles (m2 s Pa) 150 psi
6-1	4/28/93	3.2292E-10	5.6000E-12	5.4267E-10	1.8569E-11	4.0810E-09	2.1360E-09	1.3830E-09	7.6590E-09
6-2	4/28/93	ruptured							
6-3	4/28/93	* 5.577E-10	3.4925E-10	* 6.471E-10	* 3.828E-09	rupturing			
6-4	4/28/93	2.3201E-08	had hole						
6-5	4/28/93	2.6931E-10	ruptured						
6-6	4/28/93		4.3604E-09	3.0232E-09	* 9.0517E-09				
6-7	4/28/93								
6-8	4/28/93								
6-9	5/19/93	9.4230E-10	5.6313E-10	9.6137E-10	8.4807E-10				
6-10	5/19/93								
6-11	5/19/93								
6-12	5/19/93								
6-13	5/19/93								
6-14	5/19/93								
8-1	5/19/93								

* not at steady-state, usually rupturing
when permeation was non-detectable, it was estimated at 5.6E-12 moles/(m2 s Pa)

Assymetric 20% PPO in (70% trichloroethene, 30% chloroform),membranes (2-20CTT-)
filtered solutions

pure gas permeation rate ratio

coupon	date cast	H2/CH4 100 psi	H2/CO2 100 psi	CO2/CH4 100 psi	H2/CH4 150 psi	H2/CO2 150 psi	CO2/CH4 150 psi	H2/CH4 200 psi	H2/CO2 200 psi	CO2/CH4 200 psi
6-1	4/28/93	very large	0.60	very large	1.91	2.94	0.65	rupturing		
6-2	4/28/93	ruptured								
6-3	4/28/93	1.60	0.86	1.85	rupturing					
6-4	4/28/93	had hole								
6-5	4/28/93	ruptured								
6-6	4/28/93			0.69						
6-7	4/28/93									
6-8	4/28/93									
6-9	5/19/93	1.67	0.98	1.71						
6-10	5/19/93									
6-11	5/19/93									
6-12	5/19/93									
6-13	5/19/93									
6-14	5/19/93									
8-1	5/19/93									

Assymetric 20% PPO in (5:1 trichloroethene:2-ethyl-1-hexanol additive) membranes (2-20TA)
filtered solutions

results at STP

coupon	date cast	H2 perm. moles (m2 s Pa) 100 psi	CH4 perm. moles (m2 s Pa) 100 psi	CO2 perm. moles (m2 s Pa) 100 psi	N2 perm. moles (m2 s Pa) 100 psi	H2 perm. moles (m2 s Pa) 150 psi	CH4 perm. moles (m2 s Pa) 150 psi	CO2 perm. moles (m2 s Pa) 150 psi	N2 perm. moles (m2 s Pa) 150 psi	H2 perm. moles (m2 s Pa) 200 psi	CH4 perm. moles (m2 s Pa) 200 psi	CO2 perm. moles (m2 s Pa) 200 psi	N2 perm. moles (m2 s Pa) 200 psi
6-1	06/16/93	4.651E-09	1.030E-09	2.949E-09	9.661E-10	ruptured							
6-2, lam.	06/16/93	9.745E-10	5.189E-11	1.334E-09	9.176E-11	1.395E-09	6.483E-11	1.641E-09	7.379E-11	1.617E-09	6.076E-11	1.675E-09	6.732E-11
6-3	06/16/93	6.616E-09	3.056E-09	6.880E-09	ruptured								
6-4	06/16/93												
6-5	06/16/93	1.342E-09 1.396E-09	6.451E-11	2.287E-09	2.664E-08 rupturing								
6-6	06/16/93	1.603E-09	1.791E-11	2.075E-09	5.298E-11	2.015E-09	0.000E+00 1.014E-07	4.603E-08 4.865E-08	1.428E-07	ruptured			
6-7	06/16/93	2.037E-09	1.129E-10	2.091E-09	1.306E-10	2.398E-09	3.477E-09						

* not at steady state, usually rupturing

when permeation was non-detectable it was estimated at 5.6E-12 moles/(m2 s Pa)

Assymetric 20% PPO in (5:1 trichloroethene:2-ethyl-1-hexanol additive) membranes (2-20TA)
filtered solutions

permeation rate ratio

coupon	date cast	H2/CH4 100 psi	H2/CO2 100 psi	CO2/CH4 100 psi	H2/CH4 150 psi	H2/CO2 150 psi	CO2/CH4 150 psi	H2/CH4 200 psi	H2/CO2 200 psi	CO2/CH4 200 psi
6-1	06/16/93	4.52	1.58	2.86						
6-2, lam.	06/16/93	18.90	0.73	25.86	21.51	0.85	25.30	23.18	0.97	24.01
6-3	06/16/93	2.16	0.96	2.25						
6-4	06/16/93									
6-5	06/16/93	16.20 averaged	0.60 averaged	27.06 rupturing						
6-6	06/16/93	89.38	0.77	115.56	very large	0.04	very large ruptured			
6-7	06/16/93	18.05	0.97	18.53	0.69	rupturing				

Assymetric 20% PPO in (6:1 trichloroethene:2-ethyl-1-hexanol additive) membranes (2-20T2A-)
filtered solutions

results at STP

coupon	date cast	H2 perm. moles (m2 s Pa) 100 psi	CH4 perm. moles (m2 s Pa) 100 psi	CO2 perm moles (m2 s Pa) 100 psi	N2 perm. moles (m2 s Pa) 100 psi	O2 perm. moles (m2 s Pa) 100 psi	H2 perm. moles (m2 s Pa) 150 psi	CH4 perm. moles (m2 s Pa) 150 psi	CO2 perm. moles (m2 s Pa) 150 psi	N2 perm. moles (m2 s Pa) 150 psi	H2 perm. moles (m2 s Pa) 200 psi	CH4 perm. moles (m2 s Pa) 200 psi	CO2 perm. moles (m2 s Pa) 200 psi	N2 perm. moles (m2 s Pa) 200 psi
6-1	08/24/93	3.59E-09	1.48E-09	2.5E-09	1.06E-09	1.42E-09	6.08E-09	1.76E-09	2.95E-09	1.32E-09	7.21E-09	1.89E-09	3.28E-09	1.55E-09
6-2, lam.	08/24/93	8.92E-10	1.82E-11	1.8E-09	ruptured									
6-3	08/24/93	1.08E-09	7.67E-10	2.1E-09	5.46E-10	3.75E-09	1.06E-08	ruptured						
6-4	08/24/93													
6-5	08/24/93	2.74E-09 2.59E-09	7.18E-11	2.6E-09	1.03E-10 rupturing	6.23E-10	3.13E-09	7.68E-11 5.85E-11	2.17E-09	7.38E-11	2.66E-09	6.20E-11	2.17E-09	9.66E-11
6-6	08/24/93	1.26E-07	1.20E-07	5.6E-08	8.72E-08									
6-7	08/24/93													
6-8	08/24/93													
6-9	08/24/93													

* not at steady state, usually rupturing
when permeation was non-detectable, it was estimated at 5.6E-12 mols/(m2 s Pa)

Assymetric 20% PPO in (6:1 trichloroethene:2-ethyl-1-hexanol additive) membranes (2-2072A-)
filtered solutions

pure gas permeation rate ratio

coupon	date cast	H2/CH4 100 psi	H2/CO2 100 psi	CO2/CH4 100 psi	O2/N2 100 psi	H2/CH4 150 psi	H2/CO2 150 psi	CO2/CH4 150 psi	H2/CH4 200 psi	H2/CO2 200 psi	CO2/CH4 200 psi
6-1	06/24/93	2.43	1.43	1.71	1.34	3.46	2.06	1.68	3.83	2.20	1.74
6-2, lam.	06/24/93	45.13	0.47	96.79	ruptured	high due to	rupture				
6-3	06/24/93	1.41	0.51	2.74	6.84						
6-4	06/24/93										
6-5	06/24/93	37.15 averaged	1.04 averaged	35.76	6.03	40.75	1.44	37.14	42.83	1.23	34.93
6-6	06/24/93	1.05	2.19	0.48	removed						
6-7	06/24/93	ruptured									
6-8	06/24/93										
6-9	06/24/93	ruptured									

Assymetric 20% PPO in (7:1 trichloroethene:2-ethyl-1-hexanol additive) membranes (2-20T3A-)
filtered solutions

results at STP

coupon	date cast	H2 perm. moles (m2 s Pa) 100 psi	CH4 perm. moles (m2 s Pa) 100 psi	CO2 perm. moles (m2 s Pa) 100 psi	N2 perm. moles (m2 s Pa) 100 psi	O2 perm. moles (m2 s Pa) 100 psi	H2 perm. moles (m2 s Pa) 150 psi	CH4 perm. moles (m2 s Pa) 150 psi	CO2 perm. moles (m2 s Pa) 150 psi	N2 perm. moles (m2 s Pa) 150 psi
6-1			2.2209E-10	1.3762E-09	2.2497E-10	5 0152E-10				
6-2			9.2141E-08	8.4165E-08		6.0926E-08				
6-3										
6-4			5.126E-09	6.546E-09	4.511E-09					

*** not at steady state, usually rupturing**
when permeation was non-detectable, it was estimated at 5.6E-12 mols/(m2 s Pa)

Assymetric 20% PPO in (7:1 trichloroethene:2-ethyl-1-hexanol additive) membranes (2-20T3A-)
filtered solutions

pure gas permeation rate ratio

coupon	date cast	H2/CH4 100 psi	H2/CO2 100 psi	CO2/CH4 100 psi	O2/N2 100 psi	H2/CH4 150 psi	H2/CO2 150 psi	CO2/CH4 150 psi
6-1				6.20	2.23			
6-2				0.91				
6-3								
6-4				1.28				

Assymetric 20% PPO in chlorobenzene membranes (2-20B-)

filtered solutions

results at STP

coupon	date cast	H2 perm. moles (m2 s Pa) 100 psi	N2 perm. moles (m2 s Pa) 100 psi	CH4 perm. moles (m2 s Pa) 100 psi	CO2 perm. moles (m2 s Pa) 100 psi	H2 perm. moles (m2 s Pa) 150 psi	CO2 perm. moles (m2 s Pa) 150 psi	CH4 perm. moles (m2 s Pa) 150 psi	N2 perm. moles (m2 s Pa) 150 psi
6-1	03/31/93	not tested	had cracks						
6-2	03/31/93	not tested	had cracks						
6-3, lam.	04/01/93	2.9413E-10		1.689E-10	7.777E-10	1.0537E-08	1.2977E-09	3.9933E-10 5.0339E-09	3.6279E-10
6-4	04/01/93	ruptured							
8-1, lam.	03/31/93	3.5873E-10		2.242E-11	6.502E-10	4.0357E-10			ruptured
8-2	03/31/93								
8-3	03/31/93								
8-4	03/31/93	ruptured			5.135E-10				
8-5	04/01/93								
8-6	04/01/93	not tested,	has a hole						

* not at steady state, usully rupturing

when permeation rate was non-detectable, it was estimated at 5.6E-12 moles/(m2 s Pa)

Assymetric 20% PPO in chlorobenzene membranes (2-20B-)

filtered solutions

pure gas permeation rate ratio

coupon	date cast	H2/N2 100 psi	H2/CH4 100 psi	H2/CO2 100 psi	CO2/CH4 100 psi	H2/CH4 150 psi	H2/CO2 150 psi	CO2/CH4 150 psi
6-1	03/31/93	not tested						
6-2	03/31/93	not tested						
6-3, lam.	04/01/93		very large	0.38	very large	2.09	8.10	3.25
6-4	04/01/93							
8-1, lam.	03/31/93		16	0.55	29			
8-2	03/31/93							
8-3	03/31/93							
8-4	03/31/93							
8-5	04/01/93							
8-6	04/01/93	not tested						

Assymetric 20% MPPO (acylated PPO) in chloroform membranes (5-20C-)
filtered solutions

results at STP

coupon	date cast	H2 perm. moles (m2 s Pa) 100 psi	CH4 perm. moles (m2 s Pa) 100 psi	CO2 perm. moles (m2 s Pa) 100 psi	N2 perm. moles (m2 s Pa) 100 psi	H2 perm. moles (m2 s Pa) 150 psi	CH4 perm. moles (m2 s Pa) 150 psi	CO2 perm. moles (m2 s Pa) 150 psi	N2 perm. moles (m2 s Pa) 150 psi	H2 perm. moles (m2 s Pa) 200 psi	CH4 perm. moles (m2 s Pa) 200 psi	CO2 perm. moles (m2 s Pa) 200 psi	N2 perm. moles (m2 s Pa) 200 psi
6-1	06/29/93		3.2082E-10	4.6591E-10	2.3813E-10	5.0753E-10	4.148E-10	5.435E-10	3.700E-10	8.016E-10	5.292E-10	6.642E-10	4.688E-10
6-2	06/29/93	1.3406E-09	7.8578E-10	4.2748E-10	1.0195E-09	* 3.0968E-09	6.495E-09	* 3.3405E-1	2.046E-09				
6-3	06/29/93	* 5.719E-09	* 5.584E-09	not selective									
6-4	06/29/93	* 1.251E-08	6.0646E-09	1.2275E-09	4.9360E-09	Knudsen							
6-5	06/29/93	no resistance											
6-6	06/29/93	9.701E-11	1.6270E-11	3.2589E-10	3.6070E-12	* 7.442E-09	5.510E-09	1.662E-09	6.152E-09	ruptured			
6-7	06/29/93	1.254E-10	1.1060E-10	4.7466E-10	ruptured								
6-8	06/29/93	* 7.5947E-10	* 7.7654E-10	not selective									
6-8, lam.		9.1907E-11	1.1204E-11	2.4269E-10	7.234E-12	1.4481E-10	3.146E-11	2.97/E-10	2.389E-11	1.05E-10	5.231E-11	3.284E-10	1.172E-09
6-9	06/29/93	no resistance											

* not at steady state, usually rupturing
when permeation rate was non-detectable, it was estimated at 5.6E-12 moles/(m2 s Pa)

Assymetric 20% MPPO (acylated PPO) in chloroform membranes (5-20C-)
filtered solutions

pure gas permeation rate ratio

coupon	date cast	H2/CH4 100 psi	H2/CO2 100 psi	CO2/CH4 100 psi	H2/CH4 150 psi	H2/CO2 150 psi	CO2/CH4 150 psi	H2/CH4 200 psi	H2/CO2 200 psi	CO2/CH4 200 psi
6-1	06/29/93			1.45	1.22	0.93	1.31	1.51	1.21	1.26
6-2	06/29/93	1.71	3.14	0.54	0.48	9.26	0.05	Knudsen flow		
6-3	06/29/93									
6-4	06/29/93	2.06	6.80	0.30						
6-5	06/29/93									
6-6	06/29/93	6.00	0.30	20.15	1.35	4.48	0.30	ruptured		
6-7	06/29/93									
6-8										
6-8, fam.	06/29/93	6.08	0.38	21.25	3.16	0.33	9.46	2.01	0.32	6.28
6-9	06/29/93									

Assymetric 15% high molecular weight PPO (HPPO) in chloroform (6-15C-)
filtered solutions

results at STP

coupon	date cast	H2 perm. moles (m2 s Pa) 100 psi	CH4 perm. moles (m2 s Pa) 100 psi	CO2 perm. moles (m2 s Pa) 100 psi	N2 perm. moles (m2 s Pa) 100 psi	O2 perm. moles (m2 s Pa) 100 psi	H2 perm. moles (m2 s Pa) 150 psi	CH4 perm. moles (m2 s Pa) 150 psi	CO2 perm. moles (m2 s Pa) 150 psi	N2 perm. moles (m2 s Pa) 150 psi	H2 perm. moles (m2 s Pa) 200 psi	CH4 perm. moles (m2 s Pa) 200 psi	CO2 perm. moles (m2 s Pa) 200 psi	N2 perm. moles (m2 s Pa) 200 psi
6-1	09/13/93	8.16E-10	1.34E-09	2.70E-09	* 4.7722E-0	4.96E-09	ruptured							
6-2	09/13/93	3.80E-10	5.60E-12	3.24E-09	ruptured									
6-3	09/13/93	5.03E-10	7.61E-12	8.64E-10	8.556E-13	1.92E-10	ruptured							
6-4	09/13/93	* 2.07E-09	1.19E-09	1.74E-09	1.625E-09	1.91E-09	removed							
6-5	09/13/93													
6-6	09/13/93													
6-7	09/13/93													
6-8	09/13/93	8.21E-10	1.94E-10	1.72E-09	2.73E-10	4.69E-10	removed							
6-9	09/13/93	5.71E-10	1.78E-12	7.46E-10	1.008E-10	2.45E-10	1.34E-09	8.36E-10	1.68E-09	4.94E-10	2.88E-09	1.07E-09	2.18E-09	8.35E-10
6-10	09/13/93	* 1.637E-0	1.17E-08	6.10E-09	Knudsen flo									

* not at steady state, usually rupturing
when permeation was non-detectable, it was estimated at 5.6E-12 moles/(m2 s Pa)

Asaymetric 15% high molecular weight PPO (HPPO) in chloroform (6-15C-)
filtered solutions

pure gas permeation rate ratio

coupon	date cast	H2/CH4 100 psi	H2/CO2 100 psi	CO2/CH4 100 psi	O2/N2 100 psi	H2/CH4 150 psi	H2/CO2 150 psi	CO2/CH4 150 psi	H2/CH4 200 psi	H2/CO2 200 psi	CO2/CH4 200 psi
6-1	09/13/93	0.83	0.30	2.07	1.04	ruptured					
6-2	09/13/93	very large			ruptured						
6-3	09/13/93	66.13	0.58	113.45	224.33	high due to	rupture				
6-4	09/13/93	1.73	1.19	1.46	1.17	removed					
6-5	09/13/93										
6-6	09/13/93										
6-7	09/13/93										
6-8	09/13/93	4.23	0.48	8.87	1.72	removed					
6-9	09/13/93	321.37	0.76	420.14	2.43	1.60	0.79	2.01	2.70	1.32	2.05
6-10	09/13/93	Knudsen flow									

Assymetric 20% BrPPO (brominated PPO, 100% substitution on ring) in chloroform (8-20C-)
filtered solutions

results at STP

coupon	date cast	H2 perm. moles (m2 s Pa) 100 psi	CH4 perm. moles (m2 s Pa) 100 psi	CO2 perm. moles (m2 s Pa) 100 psi	N2 perm. moles (m2 s Pa) 100 psi	O2 perm. moles (m2 s Pa) 100 psi	H2 perm. moles (m2 s Pa) 150 psi	CH4 perm. moles (m2 s Pa) 150 psi	CO2 perm. moles (m2 s Pa) 150 psi	N2 perm. moles (m2 s Pa) 150 psi	H2 perm. moles (m2 s Pa) 200 psi	CH4 perm moles (m2 s Pa) 200 psi
6-1	10/13/93											
6-2	10/13/93	ruptured										
6-3	10/13/93	2.3258E-09 2.588E-09	1.0283E-09	1.5600E-09	1.0182E-09 1.0383E-09	1.1259E-09	3.1169E-09	1.3288E-09	1.6340E-09	1.01895E-09 1.1762E-09	4.7742E-09	1.6640E-09
6-4	10/13/93	6.327E-10	1.5524E-11	9.7903E-10	8.0584E-10 2.867882E-09	2.24295E-09	2.00806E-08	1.235517E-10	9.523432E-10	9.6467E-10 * 6.326E-09		
6-5	10/13/93	ruptured										
6-6	06/14/94		ruptured									
6-7	06/14/94	5.4372E-08	2.15E-08	ruptured								
6-8	06/14/94	7.3481E-08	3.59E-08	ruptured								
6-9	06/15/94		5.6E-12	ruptured								
6-10	06/15/94	4.0623E-08										
6-11	06/15/94		1.1833E-08	ruptured								

* not at steady state, usually rupturing

when permeation was non-detectable, it was estimated at 5.5E-12 moles/(m2 s Pa)

Assymetric 20% BrPPO (brominated PPO, 100% substitution on ring) in chloroform (6-20C-)
filtered solutions

pure gas permeation rate ratio

coupon	date cast	H2/CH4 100 psi	H2/CO2 100 psi	CO2/CH4 100 psi	H2/CH4 150 psi	H2/CO2 150 psi	CO2/CH4 150 psi	H2/CH4 200 psi	H2/CO2 200 psi	CO2/CH4 200 psi
6-1	10/13/93									
6-2	10/13/93									
6-3	10/13/93	2.52	1.66	1.51	2.35	1.91	1.23	2.87		
6-4	10/13/93	40.87	0.65	63.31	162.60	21.09	7.71			
6-5	10/13/93									
6-6	06/14/94									
6-7	06/14/94	2.53	3.18	0.80						
6-8	06/14/94	2.04								
6-9	06/15/94									
6-10	06/15/94									
6-11	06/15/94									

Assymetric, HIPPO membranes from fractionnal factorial design (7-Plate#-)
filtered solutions

results at STP

coupon	date cast	H2 perm. moles (m2 s Pa) 100 psi	CH4 perm. moles (m2 s Pa) 100 psi	CO2 perm. moles (m2 s Pa) 100 psi	N2 perm. moles (m2 s Pa) 100 psi	O2 perm. moles (m2 s Pa) 100 psi	CH4 repeat moles (m2 s Pa) 100 psi	49.2% CO2 in CH4 moles (m2 s Pa)	20.4% CO2 in CH4 moles (m2 s Pa)
F1-6-1	01/26/94	4.993GE-06	2.0317E-09	1.3774E-06			2.384E-06		
F1-6-2	01/26/94	1.7649E-09	1.8465E-09	2.5742E-09	6.3061E-09	6.768961E-09	ruptured		
F1-6-3	01/26/94								
F1-6-4	01/26/94								
F1-6-5	01/26/94		1.5033E-10	2.0030E-09					
F1-6-6	01/26/94	1.6812E-09	2.1068E-11	2.574E-09	7.6032E-11	8.573E-10		7.403E-10	4.13222E-10
F1-6-7	01/26/94	5.155E-10	5.6000E-12	1.1700E-09	5.6000E-12	2.0926E-10			
F1-6-8	01/26/94	1.7243E-06	2.41E-06						
F1-6-9	01/26/94	2.5872E-09	1.33E-09	1.899E-09	1.273E-09	1.4009E-09			
F2-6-1	02/01/94	9.7885E-06	4.3094E-06	1.65406E-06	2.8554E-06	3.06781E-06			
F2-6-2	02/01/94	1.1797E-09	3.4033E-10	1.15028E-09	3.2129E-10	5.33063E-10			
F2-6-3	02/01/94								
F2-6-4	02/01/94	1.3996E-07	5.07565E-06	5.9968E-06	7.3781E-06	6.496E-06			
F2-6-5	02/01/94	1.522589E-06	7.5366E-09	1.14315E-06	1.43074E-06	2.35946E-06			
F2-6-6	02/01/94	3.204122E-06	1.421851E-06	9.371356E-09	Knudsen				
F2-6-7	02/01/94	2.79566E-09	1.64116E-09	1.9696E-09	1.372573E-09	1.53658E-09			
F3-6-1	01/18/94		7.182797E-06	4.329535E-06					
F3-6-2	01/18/94								
F3-6-3	01/18/94	no resistance							
F3-6-4	01/18/94								
F3-6-5	01/18/94		1.419941E-05	9.554684E-06					
F3-6-6	01/18/94	no resistance							
F3-6-7	01/18/94	no resistance							
F3-6-8	03/21/94								
F3-6-9	03/21/94								
F3-6-10	03/21/94		4.6766E-05	2.721247E-05					
F3-6-11	03/21/94		1.131583E-05	5.386669E-06					
F4-6-1	02/24/94	7.878E-06	5.8424E-09	3.486E-06	5.01336E-09	1.21056E-06			
F4-6-2	02/24/94		2.2663E-06 9.81276E-06	9.715E-06	6.97344E-06	7.74253E-06	9.501E-06		
F4-6-3	02/24/94	1.9881E-07	3.4227E-06	7.98E-06	2.50672-06	3.83005E-09			
F4-6-4	02/24/94								
F4-6-5	02/24/94	3.638379E-07	1.167484E-07 1.073979E-07	1.286245E-07	8.567229E-06	8.644427E-06			
F4-6-6	02/24/94	5.019197E-07	1.732448E-07	1.696346E-07	1.245934E-07				
F4-6-7	02/24/94	1.8584E-07	3.0518E-06 2.9193E-06	7.837E-06	2.4b2E-06	3.648E-06			
F4-6-8	02/24/94	1.363E-07	2.18696E-06	5.2258E-06	1.642E-06	2.5109E-06	2.28663E-06		

Asesymetric, HPPO membranes from fractionnal factorial design (7-Fleet#-)
filtered solutions

results at STP

coupon	date cast	H2 perm. moles (m2 s Pa) 100 psi	CH4 perm. moles (m2 s Pa) 100 psi	CO2 perm. moles (m2 s Pa) 100 psi	N2 perm. moles (m2 s Pa) 100 psi	O2 perm. moles (m2 s Pa) 100 psi	CH4 repeat moles (m2 s Pa) 100 psi	49.2% CO2 in CH4 moles (m2 s Pa)	20.4% CO2 in CH4 moles (m2 s Pa)
F5-6-1	01/24/94								
F5-6-2	01/24/94								
F5-6-3	01/24/94	2.5336E-09	7.0513E-10	1.966E-09	6.3264E-10	6.8364E-10			
F5-6-4	01/24/94	6.277E-10	3.1216E-11	1.0922E-09	5.6667E-11	2.64341E-10			
F5-6-5	01/24/94	4.6431E-10	5.6E-12	1.033E-09	5.6E-12	1.8764E-10			
F5-6-6	01/24/94	1.52673E-07	6.234931E-08	1.840664E-07	3.596423E-07	3.8217025E-07	ruptured		
F6-6-1	01/06/94								
F6-6-2	01/06/94	1.706999E-06	rupturing						
F6-6-3	01/06/94								
F6-6-4	01/06/94		2.7254E-06	1.0535E-06					
F6-6-5	01/06/94								
F6-6-6	01/06/94	ruptured							
F6-6-7	01/06/94		4.2714E-09	9.9726E-09					
F6-6-8	01/06/94	4.0714E-10	1.8678E-12	8.3839E-10	5.6E-12	1.8656E-10	1.7297E-10	4.6066E-10	1.5978E-10
F6-6-9	01/06/94	5.3102E-10	2.28E-11	9.823E-10	5.0668E-11	2.45E-10			
F7-6-1	03/21/94	hole	1.5711E-06	9.3339E-07					
F7-6-2	03/21/94	3.977E-07	1.305E-07	1.824E-07	1.0512E-07	1.1753E-07			
F7-6-3	03/21/94	2.3119E-06	1.0185E-06 1.0122E-06	8.47E-07 7.1654E-07	6.6614E-07	7.187E-07			
F7-6-4	02/22/94								
F7-6-5	02/22/94	no resistance							
F7-6-6	02/22/94	no resistance							
F7-6-7	02/22/94	no resistance							
F7-6-8	02/22/94	no resistance							
F7-6-9	02/22/94	no resistance							
F7-6-10	02/22/94	no resistance							
F8-6-1	01/14/94								
F8-6-2	01/14/94								
F8-6-3	01/14/94								
F8-6-4	01/14/94								
F8-6-5	01/14/94								
F8-6-6	05/05/94		1.121119E-06	7.612587E-06					
F8-6-7	05/05/94	no resistance							
F8-6-8	05/05/94	no resistance							
F8-6-9	05/05/94		8.796805E-06	6.330217E-06					
F8-6-10	05/06/94	no resistance							
F8-6-11	05/06/94	no resistance							
F8-6-12	05/06/94	ruptured							

* not at steady state, usually rupturing

when permeation rate was non-detectable, it was estimated at 5.6e-12 moles/m2 s Pa

Assymetric, HPPO membranes from fractionnal factorial design (7-Ftest#-)
filtered solutions

pure gas permeation rate ratio

coupon	date cast	H2/CH4 100 psi	H2/CO2 100 psi	CO2/CH4 100 psi	O2/N2 100 psi
F1-6-1	01/26/94	24.57	3.63	6.78	
F1-6-2	01/26/94	0.96	0.08	12.22	1.07
F1-6-3	01/26/94				
F1-6-4	01/26/94				
F1-6-5	01/26/94			13.33	
F1-6-6	01/26/94	81.50	0.65	124.75	7.92
F1-6-7	01/26/94	very large	0.44	very large	very large
F1-6-8	01/26/94			1.40	
F1-6-9	01/26/94	1.95	1.36	1.43	1.10
F2-6-1	02/01/94	2.27	5.92	0.38	1.07
F2-6-2	02/01/94	3.47	1.03	3.38	1.65
F2-6-3	02/01/94				
F2-6-4	02/01/94	2.76	2.33	1.18	0.88
F2-6-5	02/01/94	2.02	1.33	1.52	1.65
F2-6-6	02/01/94	2.25	3.42	0.66	
F2-6-7	02/01/94	1.70	1.40	1.21	1.12
F3-6-1	01/18/94	very open		0.60	
F3-6-2	01/18/94				
F3-6-3	01/18/94	very open			
F3-6-4	01/18/94				
F3-6-5	01/18/94			0.67	
F3-6-6	01/18/94	very open			
F3-6-7	01/18/94	very open			
F3-6-8	03/21/94	very open			
F3-6-9	03/21/94	very open			
F3-6-10	03/21/94			0.58	
F3-6-11	03/21/94			0.48	
F4-6-1	02/24/94	13.48	2.26	5.97	2.41
F4-6-2	02/24/94			4.29	
F4-6-3	02/24/94	5.81	2.49	2.33	1.53
F4-6-4	02/24/94				
F4-6-5	02/24/94	3.39	2.87	1.18	1.01
F4-6-6	02/24/94	2.90	2.96	0.98	
F4-6-7	02/24/94	6.37	2.43	2.62	1.48
F4-6-8	02/24/94	6.32	2.65	2.39	1.53

Assymetric, HPPO membranes from fractionnal factorial design (7-Ftest#-)
filtered solutions

pure gas permeation rate ratio

coupon	date cast	H2/CH4 100 psi	H2/CO2 100 psi	CO2/CH4 100 psi	O2/N2 100 psi
F5-6-1	01/24/94				
F5-6-2	01/24/94				
F5-6-3	01/24/94	3.59	1.29	2.79	1.40
F5-6-4	01/24/94	20.00	0.57	34.79	4.83
F5-6-5	01/24/94		0.45		
F5-6-6	01/24/94	2.45	0.83	2.95	1.06
F6-6-1	01/06/94				
F6-6-2	01/06/94				
F6-6-3	01/06/94				
F6-6-4	01/06/94			0.39	
F6-6-5	01/06/94				
F6-6-6	01/06/94				
F6-6-7	01/06/94			2.33	
F6-6-8	01/06/94	214.00	0.49	440.50	
F6-6-9	01/06/94	23.65	0.54	43.80	4.84
F7-6-1	03/21/94	hole		0.59	
F7-6-2	03/21/94	3.05	2.18	1.40	1.12
F7-6-3	03/21/94	2.27	3.57	0.64 0.70	1.08
F7-6-4	05/17/94				
F7-6-5	05/17/94	no resistance			
F7-6-6	05/17/94	no resistance			
F7-6-7	05/17/94	no resistance			
F7-6-8	05/22/94	no resistance			
F7-6-9	05/22/94	no resistance			
F7-6-10	05/22/94	no resistance			
F8-6-1	02/14/94				
F8-6-2	02/14/94				
F8-6-3	02/14/94				
F8-6-4	02/14/94				
F8-6-5	02/14/94				
F8-6-6	05/05/94			0.68	
F8-6-7	05/05/94				
F8-6-8	05/05/94				
F8-6-9	05/05/94			0.72	
F8-6-10	05/06/94				
F8-6-11	05/06/94				
F8-6-12	05/06/94				

Assymetric, High MW PPO membranes from fractionnal factorial design optimization (7-)
filtered solutions

results at STP

coupon	date cast	H2 perm. moles (m2 s Pa) 100 psi	CH4 perm. moles (m2 s Pa) 100 psi	CO2 perm. moles (m2 s Pa) 100 psi	N2 perm. moles (m2 s Pa) 100 psi	O2 perm. moles (m2 s Pa) 100 psi	CH4 repeat moles (m2 s Pa) 100 psi	49.2% CO2 in CH4 moles (m2 s Pa)	20.4% CO2 in CH4 moles (m2 s Pa)
12.5% HPPO in (7% additive, 93% CHCl3), at 40 C, no evap									
F0-6-1	07/20/94		5.7254E-11	6.8140E-09	1.0502E-10		2.2244E-10	2.5192E-09	9.2755E-10
F0-6-2	07/20/94		7.0110E-10	1.1907E-08					
F0-6-3	07/20/94		4.2100E-09	7.7056E-09	7.1170E-10				
F0-6-4	07/20/94		3.4675E-09	8.2648E-09	ruptured				
F0-6-5	07/20/94		4.3000E-10	5.0839E-09	1.6332E-10			1.9209E-09	
F0-6-6	07/20/94		4.3658E-08	3.3298E-08					
F0-6-7	07/20/94		1.8671E-10	4.3535E-09				1.532E-09	8.4685E-10
F0-6-8	08/08/94		6.1778E-09	1.1580E-08			5.0710E-06	7.8896E-09	7.347E-09
F0-6-9	08/08/94								
F0-6-10	08/08/94		5.3773E-09	2.3296E-08					
F0-6-11	08/08/94								
F0-6-12	08/08/94								
F0-6-13	08/08/94		3.2553E-10	6.8715E-09	4.1408E-10			2.8866E-09	1.0551E-09
F0-6-14	08/08/94								
F0-6-15	08/08/94		2.6842E-09	1.3736E-08			1.0230E-08		
12.5 % HPPO, 8.75% additive in CHCl3, at 23 C, no evaporation									
OP1-6-1	08/16/94		6.608E-09	2.1368E-08	3.97E-08				
OP1-6-2	08/16/94								
OP1-6-3	08/16/94								
OP1-6-4	08/16/94		4.8032E-10	9.2247E-09					
OP1-6-5	08/16/94		1.1137E-09	1.6053E-08	1.276E-09				
10% HPPO, 9.5% additive in CHCl3, no evap.									
OP2-6-1	08/18/94	2.053E-06	7.9689E-07	5.54E-07					
OP2-62	08/18/94								
OP2-6-3	08/18/94			3.0597E-07	1.8227E-07				
OP2-6-4	08/18/94	1.7412E-06	6.1671E-07	4.221E-07					
OP2-6-5	08/18/94	4.8802E-07	9.4458E-07	6.337E-07					
OP2-6-6	08/18/94			3.3833E-07	2.7623E-07				
OP2-6-7	08/18/94								

Assymetric, High MW PPO membranes from fractionnal factorial design optimization (7-)
filtered solutions

pure gas permeation rate ratio

coupons	date cast	H2/CH4 100 psi	H2/CO2 100 psi	CO2/CH4 100 psi	O2/N2 100 psi
12.5% HPPO in (7% additive, 93% CHCl3), at 40 C, no evap					
F0-6-1	07/20/94			119.10	
F0-6-2	07/20/94			16.98	
F0-6-3	07/20/94			1.83	
F0-6-4	07/20/94			2.39	
F0-6-5	07/20/94			11.82	
F0-6-6	07/20/94			0.76	
F0-6-7	07/20/94			23.32	
F0-6-8	08/08/94			1.87	
F0-6-9	08/08/94				
F0-6-10	08/08/94			4.34	
F0-6-11	08/08/94				
F0-6-12	08/08/94				
F0-6-13	08/08/94			21.11	
F0-6-14	08/08/94				
F0-6-15	08/08/94			5.12	
12.5 % HPPO, 8.75% additive in CHCl3, at 23 C, no evaporation					
OP1-6-1	08/16/94			3.31	
OP1-6-2	08/16/94				
OP1-6-3	08/16/94				
OP1-6-4	08/16/94			19.24	
OP1-6-5	08/16/94			14.41	
10% HPPO, 9.8% additive in CHCl3, no evap., 27 C					
OP2-6-1	08/18/94	2.576	3.706	0.70	
OP2-62	08/18/94				
OP2-6-3	08/18/94				
OP2-6-4	08/18/94	2.823	4.125	0.68	
OP2-6-5	08/18/94	0.517	0.770	0.67	
OP2-6-6	08/18/94				
OP2-6-7	08/18/94				

Extrapolation of the CO2 flow rate

date: 6/14/94
membrane: 7-F3-6-1 cell: 1 (cell area 9.62 cm2)

feed pressure (psig)	flowrate (ml/min)	atmospn. pressure (mmHg)	temp. (°C)	flowrate at STP (ml/min)
2.5	270.3	756.8	23.0	272.3
2.5	276.5	756.8	23.0	278.5
2.5	272.1	756.8	23.0	274.1
4.0	309.3	756.8	23.0	311.6
4.0	311.7	756.8	23.0	314.0
4.0	303.8	756.8	23.0	306.1
5.0	328.5	756.8	23.0	330.9
5.0	333.3	756.8	23.0	335.8
5.0	332.1	756.8	23.0	334.6
6.0	355.0	756.8	23.0	357.6
6.0	355.0	756.8	23.0	357.6
6.0	359.3	756.8	23.0	362.0
6.5	397.1	756.8	23.0	400.0
6.5	391.3	756.8	23.0	394.2
6.5	394.4	756.8	23.0	397.3
9.0	467.9	756.8	23.0	471.4
9.0	466.3	756.8	23.0	469.8
9.0	469.2	756.8	23.0	472.7
12.0	570.2	756.8	23.0	574.4
12.0	567.8	756.8	23.0	572.0
12.0	566.6	756.8	23.0	570.8
12.5	606.7	756.8	23.0	611.2
12.5	595.4	756.8	23.0	599.8
12.5	598.7	756.8	23.0	603.1
15.0	722.9	757.2	23.0	728.6
15.0	701.3	757.2	23.0	706.9
15.0	712.4	757.2	23.0	718.1
17.5	806.0	757.2	23.0	812.4
17.5	800.0	757.2	23.0	806.4
17.5	796.5	757.2	23.0	802.8
19.5	892.6	757.3	23.0	899.8
19.5	886.7	757.3	23.0	893.9
19.5	885.2	757.3	23.0	892.3

Regression Output:

Constant		152.98
Std Err of Y Est		16.788
R Squared		0.9936
No. of Observations		33
Degrees of Freedom		31
X Coefficient(s)	37.091	
Std Err of Coef.	0.535	

at 100 psig feed: 3862.1 ml/min

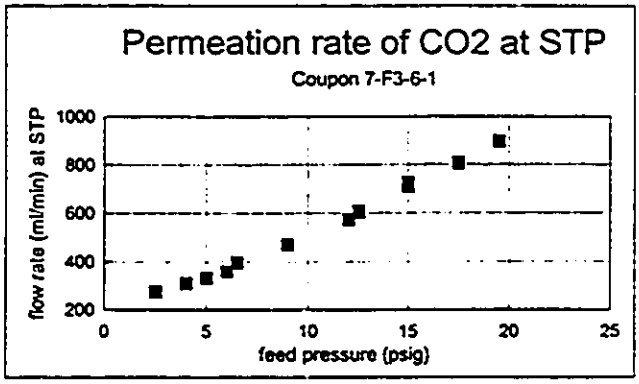

Extrapolation of the CH4 flow rate

date: 6/15/94
membrane: 7-F3-6-1 cell: 1 (cell area 9.62 cm2)

feed pressure (psig)	flowrate (ml/min)	atmosph. pressure (mmHg)	temp. (°C)	flowrate at STP (ml/min)
4.0	470.0	763.3	22.5	478.4
4.0	473.7	763.3	22.5	482.2
4.0	466.7	763.3	22.5	475.1
7.0	647.5	763.3	22.5	659.1
7.0	629.4	763.3	22.5	640.7
7.0	646.7	763.3	22.5	658.3
10.5	816.9	763.4	23.0	830.1
10.5	812.0	763.4	23.0	825.1
10.5	806.0	763.4	23.0	819.1
12.5	962.6	763.4	23.0	978.2
12.5	944.1	763.4	23.0	959.4
12.5	950.7	763.4	23.0	966.1
15.0	1090.9	763.4	23.0	1108.6
15.0	1080.0	763.4	23.0	1097.5
15.0	1086.5	763.4	23.0	1104.1
19.0	1436.2	763.4	23.0	1459.5
19.0	1406.3	763.4	23.0	1429.1
19.0	1421.1	763.4	23.0	1444.1
17.5	1252.9	763.4	23.0	1273.2
17.5	1261.7	763.4	23.0	1282.1
17.5	1235.7	763.4	23.0	1255.7
17.5	1276.6	763.4	23.0	1297.3

Regression Output:

Constant	205.95
Std Err of Y Est	33.678
R Squared	0.9897
No. of Observations	22
Degrees of Freedom	20
X Coefficient(s)	62.015
Std Err of Coef.	1.4169

at 100 psig feed: 6407.4 ml/min

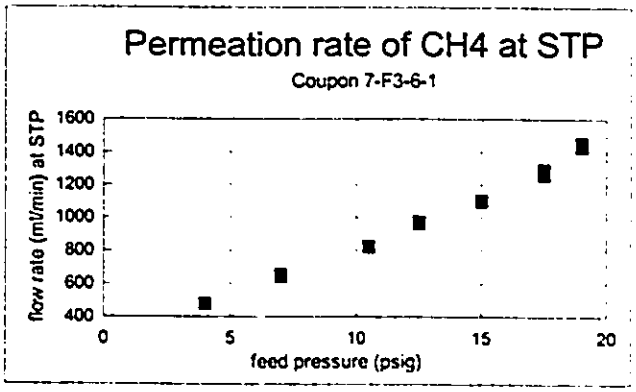

Extrapolation of the CO2 flow rate

date: 6/14/94
membrane: 7-F3-6-11 cell: 5 (cell area 9.62 cm2)

feed pressure (psig)	flowrate (ml/min)	atmosph. pressure (mmHg)	temp. (°C)	flowrate at STP (ml/min)
2.5	338.3	756.8	23.0	340.9
2.5	336.4	756.8	23.0	338.9
2.5	337.1	756.8	23.0	339.6
3.8	382.2	756.8	23.0	385.0
3.8	380.0	756.8	23.0	382.8
3.8	367.8	756.8	23.0	370.6
5.0	415.1	756.8	23.0	418.1
5.0	415.1	756.8	23.0	418.1
5.0	415.1	756.8	23.0	418.1
6.0	438.3	756.8	23.0	441.6
6.0	438.7	756.8	23.0	441.9
6.0	434.4	756.8	23.0	437.7
6.3	475.8	756.8	23.0	479.3
6.3	467.1	756.8	23.0	470.6
6.3	473.3	756.8	23.0	476.8
9.0	592.8	756.8	23.0	597.1
9.0	590.8	756.8	23.0	595.2
9.0	593.4	756.8	23.0	597.8
11.5	690.5	756.8	23.0	695.7
11.5	701.3	756.8	23.0	706.5
11.5	705.9	756.8	23.0	711.1
13.0	778.1	756.8	23.0	783.9
13.0	764.9	756.8	23.0	770.5
13.0	762.7	756.8	23.0	768.4
15.0	876.6	757.2	23.0	883.6
15.0	859.9	757.2	23.0	866.7
15.0	859.9	757.2	23.0	866.7
18.0	1058.8	757.2	23.0	1067.2
18.0	1018.9	757.2	23.0	1027.0
18.0	1036.5	757.2	23.0	1044.7
19.5	1102.0	757.3	23.0	1110.9
19.5	1095.3	757.3	23.0	1104.2
19.5	1088.7	757.3	23.0	1097.5

Regression Output:

Constant		190.81
Std Err of Y Est		20.102
R Squared		0.9943
No. of Observations		33
Degrees of Freedom		31
X Coefficient(s)	46.143	
Std Err of Coef.	0.6286	
at 100 psig feed:	4805.1	ml/min

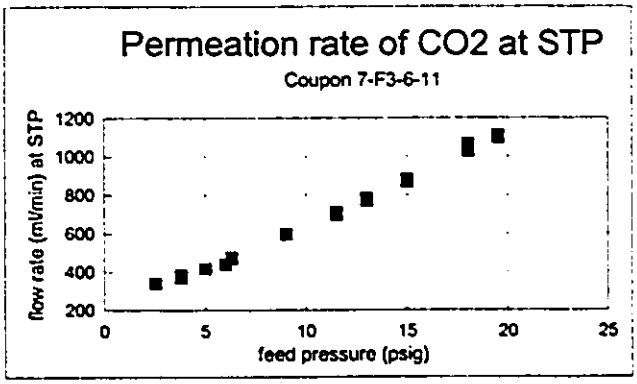

Extrapolation of the CH4 flow rate

date: 6/15/94
membrane: 7-F3-6-11 cell: 5 (cell area 9.62 cm2)

feed pressure (psig)	flowrate (ml/min)	atmosph. pressure (mmHg)	temp. (°C)	flowrate at STP (ml/min)
2.5	113.3	763.3	22.5	115.3
2.5	111.7	763.3	22.5	113.7
2.5	111.2	763.3	22.5	113.2
8.5	820.7	763.3	22.5	835.4
8.5	819.4	763.3	22.5	834.1
8.5	828.2	763.3	22.5	843.1
10.0	929.4	763.4	23.0	944.5
10.0	932.6	763.4	23.0	947.7
10.0	931.0	763.4	23.0	946.1
12.5	1221.7	763.4	23.0	1241.5
12.5	1179.0	763.4	23.0	1198.1
12.5	1213.5	763.4	23.0	1233.1
14.0	1247.1	763.4	23.0	1267.3
14.0	1232.9	763.4	23.0	1252.8
14.0	1230.1	763.4	23.0	1250.0
19.0	1888.1	763.4	23.0	1918.7
19.0	1818.2	763.4	23.0	1847.6
19.0	1862.1	763.4	23.0	1892.2
15.5	1343.3	763.4	23.0	1365.0
15.5	1360.2	763.4	23.0	1382.2
15.5	1402.6	763.4	23.0	1425.3

Regression Output:

Constant	-100.6
Std Err of Y Est	65.542
R Squared	0.985
No. of Observations	21
Degrees of Freedom	19
X Coefficient(s)	101.95
Std Err of Coef.	2.8901

at 100 psig feed: 10094.1 ml/min

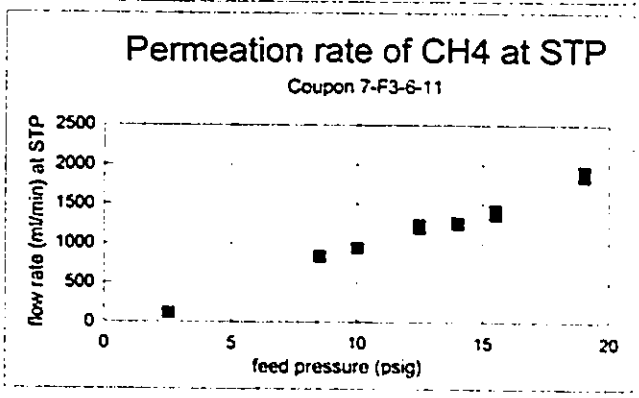

Extrapolation of the CO2 flow rate

date: 6/01/94
membrane: 7-F8-6-6 cell: 6 (cell area 11.34 cm2)

feed pressure (psig)	flowrate (ml/min)	atmosph. pressure (mmHg)	temp. (°C)	flowrate at STP (ml/min)
7.0	639.8	749.5	24.0	636.0
7.0	668.3	749.5	24.0	664.3
10.0	1016.9	749.5	24.0	1010.8
10.0	1058.8	749.5	24.0	1052.5
5.0	555.6	749.5	24.0	552.3
5.0	591.5	749.5	24.0	588.0
5.0	593.4	749.6	24.0	589.9
13.0	1090.9	749.6	24.0	1084.5
13.0	1084.3	749.6	24.0	1077.9
13.0	1075.7	749.7	24.0	1069.5
12.0	996.3	749.7	24.0	990.6
12.0	1007.5	749.7	24.0	1001.7
12.0	1046.5	749.7	24.0	1040.5

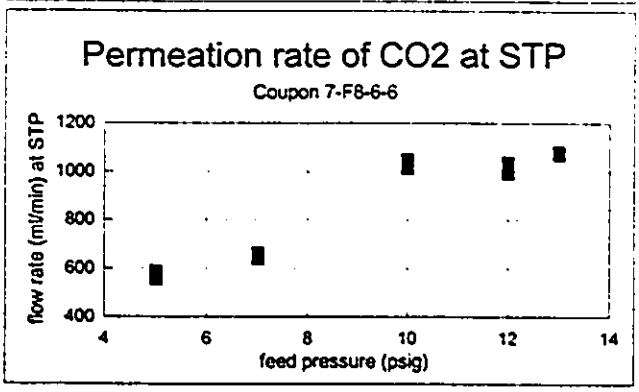

Regression Output:

Constant	249.86
Std Err of Y Est	64.779
R Squared	0.9229
No. of Observations	13
Degrees of Freedom	11
X Coefficient(s)	65.406
Std Err of Coef.	5.6984

at 100 psig feed: 6790 ml/min

Extrapolation of the CH4 flow rate

date: 6/02/94
membrane: 7-F8-6-6 cell: 6 (cell area 11.34 cm2)

feed pressure (psig)	flowrate (ml/min)	atmosph. pressure (mmHg)	temp. (°C)	flowrate at STP (ml/min)
3.0	533.6	753.7	23.0	535.4
3.0	543.8	753.7	23.0	545.6
3.0	546.0	753.7	23.0	547.8
7.5	923.1	753.7	23.0	926.1
7.5	913.7	753.7	23.0	916.7
7.5	921.5	754.0	23.5	923.2
10.0	1270.6	754.0	23.5	1272.9
10.0	1194.7	754.0	23.5	1196.9
10.0	1232.9	754.0	23.5	1235.1
8.0	1171.4	754.0	23.5	1173.5
8.0	1127.3	754.0	23.5	1129.4
8.0	1139.2	754.4	24.0	1139.8
12.0	1409.9	754.4	24.0	1410.6
12.0	1395.3	754.4	24.0	1396.0
12.0	1417.3	754.4	24.0	1418.0

Regression Output:

Constant	262.33
Std Err of Y Est	65.106
R Squared	0.9589
No. of Observations	15
Degrees of Freedom	13
X Coefficient(s)	97.383
Std Err of Coef.	5.591

at 100 psig feed: 10000.6 ml/min

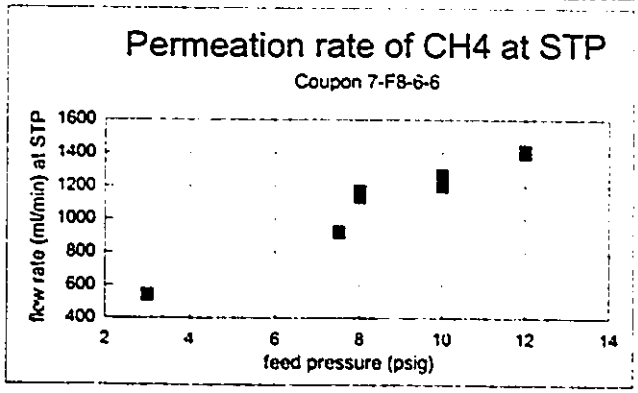

Extrapolation of the CO2 flow rate

date: 6/01/94
membrane: 7-F8-6-9 cell: 5 (cell area 9.62 cm2)

feed pressure (psig)	flowrate (ml/min)	atmosph. pressure (mmHg)	temp. (°C)	flowrate at STP (ml/min)
11.0	638.3	749.5	24.0	634.5
11.0	758.4	749.5	24.0	753.9
10.0	670.0	749.5	24.0	666.0
10.0	742.8	749.5	24.0	738.3
10.0	732.7	749.5	24.0	728.3
10.0	639.8	749.5	24.0	636.0
10.0	666.7	749.6	24.0	662.8
12.0	828.2	749.6	24.0	823.3
12.0	784.9	749.6	24.0	780.3
12.0	816.9	749.7	24.0	812.2
14.0	916.8	749.7	24.0	911.5
14.0	885.2	749.7	24.0	880.1
14.0	909.1	749.7	24.0	903.9

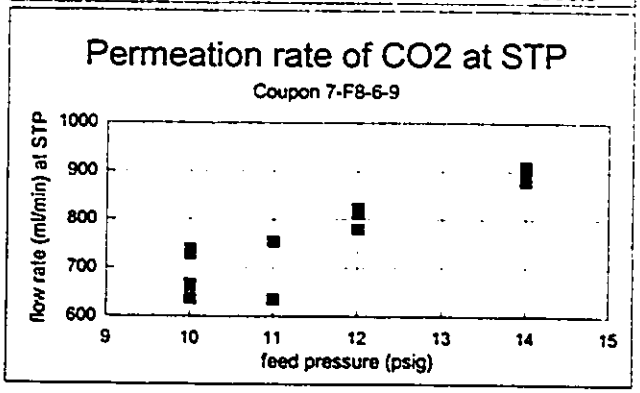

Regression Output:

Constant	127.13
Std Err of Y Est	43.554
R Squared	0.8201
No. of Observations	13
Degrees of Freedom	11
X Coefficient(s)	55.19
Std Err of Coef.	7.7936

at 100 psig feed: 5647 ml/min

Extrapolation of the CH4 flow rate

date: 6/02/94
membrane: 7-F8-6-9 cell: 5 (cell area 9.62 cm2)

feed pressure (psig)	flowrate (ml/min)	atmosph. pressure (mmHg)	temp. (°C)	flowrate at STP (ml/min)
3.0	612.2	753.7	23.0	614.2
3.0	611.6	753.7	23.0	613.6
6.5	878.0	753.7	23.0	880.9
6.5	883.8	753.7	23.0	886.7
6.5	869.6	753.7	23.0	872.5
10.0	1176.5	754.0	23.5	1178.6
10.0	1168.8	754.0	23.5	1170.9
10.0	1173.9	754.0	23.5	1176.0
7.5	957.4	754.0	23.5	959.1
7.5	971.2	754.0	23.5	973.0
7.5	971.2	754.0	23.5	973.0
12.0	1264.6	754.4	24.0	1265.2
12.0	1276.6	754.4	24.0	1277.2
12.0	1267.6	754.4	24.0	1268.2

Regression Output:

Constant		401.55
Std Err of Y Est		20.948
R Squared		0.992
No. of Observations		14
Degrees of Freedom		12
X Coefficient(s)	74.452	
Std Err of Coef.	1.9348	

at 100 psig feed: 7846.8 ml/min

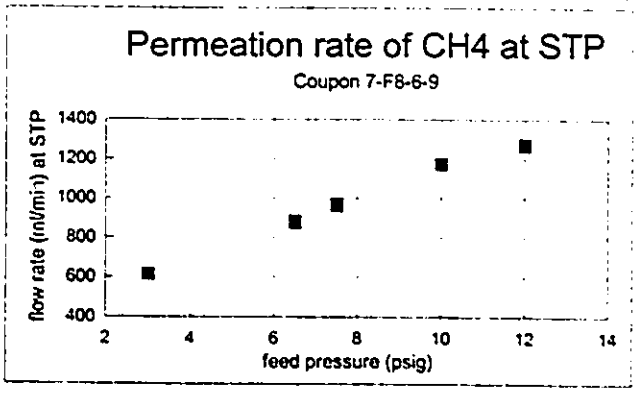

Gas seperation testing cell area is 10.46 cm2

membranes:

cell #3: 2-20C-6-19 assymetric, 20% PPO (BHPP 820) in chloroform
thickness 6 mil when casted
methanol coagulation bath
casted May 24/94
NOTE: PPO solution was filtered

gas: CH4 100 psig date: 06/08/94

time from start (min)	gas perm. (ml/min)	pressure (mmHg)	temperature (deg.C)	gas perm. at STP (ml/min)
0	0.010	756.9	23.0	0.009
28		757.2	23.0	
78	0.006	757.0	23.0	0.006
171	0.010	756.5	23.0	0.009
251	0.0110	755.7	23	0.010
333	0.002308847	754.6	23	0.002
			s.s. average:	0.008
			in moles/(m2 s Pa):	6.68127E-12

gas: CO2, 100 psi date: 06/15/94

time from start (min)	gas perm. (ml/min)	pressure (mmHg)	temperature (deg.C)	gas perm. at STP (ml/min)
0	0.476	763.0	22.5	0.442
60	0.566	763.4	23.0	0.525
136	0.561	762.8	23.0	0.519
196	0.604	762.[illegible]	23.0	0.559
			s.s. average:	0.534336824
			in moles/(m2 s Pa):	5.51273E-10

gas: 20.4% CO2 in CH4, 100 psi
date: 06/15/94

time from start (min)	gas perm. (ml/min)	pressure (mmHg)	temperature (deg.C)	gas perm. at STP (ml/min)
0	0.205	762.6	23.0	0.190
60	0.143	762.6	23.5	0.132
171	0.109	762.0	23.5	0.101
			s.s. average:	0.1163
			in moles/(m2 s Pa):	1.1997E-10
			2 x std. dev.	4.55426E-11

gas: 49.2% CO2 in CH4, 100 psi
date: 06/16/94

time from start (min)	gas perm. (ml/min)	pressure (mmHg)	temperature (deg.C)	gas perm. at STP (ml/min)
0	1.717	762.3	23.0	1.588
63	2.344	762.3	24.0	2.161
119	2.507	762.3	24.0	2.312
279	2.5775			
366	2.645	760.5	25	2.425
			s.s. average:	2.3682
			in moles/(m2 s Pa):	2.44328E-09

GC Analysis
gas: 20.4% CO2 in CH4, 100 psi
date: 06/15/94

injection time	CH4 area	CO2 area	corrected CH4 area	corrected CO2 area	%CH4 in permeate	%CO2 in permeate	separation factor	enrichment factor
14:43:32	788645	5698396	20811	121242	14.65	85.35	22.73	4.18
15:31:46	787922	5544513	20844	117968	15.02	84.98	22.06	4.17
						average:	22.4078	4.1748
						2 x std. de	0.9189	0.0254

GC Analysis
gas: 49.2% CO2 in CH4, 100 psi
date: 06/16/94

injection time	CH4 area	CO2 area	corrected CH4 area	corrected CO2 area	%CH4 in permeate	%CO2 in permeate	separation factor	enrichment factor	
									permeation rate is too high
11:37:47	5435098	8408635	143788	17[illegible]37	44.56	55.44	1.26	1.13	rupture or damage of membrane
14:19:09	5541557	8437804	146602	17[illegible]523	44.95	55.05	1.26	1.12	

Gas separation testing cell area 9.62 cm2

membrane:

cell #1 7 PD 6.1 [illegible] asymmetric, flat lateral design cast #C 12.5% HPPO in chloroform 7% additive no evaporation temp 60 C
film brass 6 mil when cooled
methanol coagulation bath
cooled July 20/94
NOTE: PPO solution was filtered

gas: CH4 100 psig date: 07/21/94

time from start (min)	gas perm. (mL/min)	pressure (mmHg)	temperature (deg C)	gas perm at STP (mL/min)
0	0.084	737.0	24.0	0.086
63	0.085	737.1	24.0	0.087
153	0.083	736.5	24.0	0.082
246	0.056	733.3	24.0	0.051
343	0.056	736.3	24.0	0.051
			s.s. average	0.051
			m moles/(m2 s Pa)	3.7254E-11
			2 x standard dev.	3.1162E-16

gas: CO2, 100 psig date: 07/22/94

time from start (min)	gas perm. (mL/min)	pressure (mmHg)	temperature (deg C)	gas perm at STP (mL/min)
0	6.100	732.7	23.0	5.972
107	6.457	732.2	23.5	5.994
220	6.368	732.4	23.5	6.003
281	6.702	731.8	24.0	6.062
428	6.738	731.6	24	6.123
			s.s. average	6.074429648
			m moles/(m2 s Pa)	6.814E-09

gas: 49.2% CO2 in CH4, 100 psig date: 07/26/94

time from start (min)	gas perm. (mL/min)	pressure (mmHg)	temperature (deg C)	gas perm at STP (mL/min)
0	2.353	730.0	22.0	2.330
66	2.361	730.1	23.0	2.331
130	2.465	730.2	23.0	2.375
216	2.253	748.9	23	2.060
			s.s. average	2.2437
			m moles/(m2 s Pa)	2.3192E-09
			2 x standard dev.	2.9882E-10

gas: 20.4% CO2 in CH4, 100 psig date: 07/26/94

time from start (min)	gas perm. (mL/min)	pressure (mmHg)	temperature (deg C)	gas perm at STP (mL/min)
0	1.005	730.3	23.0	0.915
77	0.925	748.8	23.0	0.842
110	0.882	748.8	23.0	0.812
			s.s. average	0.8230
			m moles/(m2 s Pa)	9.2755E-10
			2 x standard dev.	4.8319E-11

GC Analysis
gas: 20.4% CO2 in CH4, 100 psig date: 07/26/94

injection time	CH4 area	CO2 area	corrected CH4 area	corrected CO2 area	%CH4 in permeate	%CO2 in permeate	separation factor	correction factor
14:20:39	2030843	6277288	33729	133008	28.69	71.31	9.70	3.30
15:11:43	3884187	9167087	97730	185043	33.38	66.62	7.78	3.27
15:43:04	3746503	8002880	98115	191347	34.10	65.90	7.54	3.23
						average	7.68	3.23
						2 x std. dev.	2.3633	0.2992

GC Analysis

gas: 49.2% CO2 in CH4, 100 psig date: 07/26/94

injection time	CH4 area	CO2 area	corrected CH4 area	corrected CO2 area	%CH4 in permeate	%CO2 in permeate	separation factor	correction factor
10:02:29	837000	8838382	22673	196031	10.76	89.24	8.56	1.81
10:34:29	771144	10233324	20401	217773	8.57	91.43	11.02	1.86
11:05:49	800882	10491308	21167	223224	8.67	91.33	10.69	1.86
11:35:49	829888	10523178	21957	223840	8.93	91.07	10.53	1.85
12:16:30	866245	10432605	22917	222386	9.34	90.66	10.02	1.84
13:04:37	962738	10795720	25469	229484	9.86	90.02	9.31	1.83
						average	10.33	1.85
						2 x std. dev.	1.3864	0.0233

gas: CH4, 100 psig

Gas separation testing membrane area 11.34 cm2

membranes:

cell #4 7-F6-6-8 Factorial design test #6, 15% HPPO in chloroform 3 min evap., at room temp
thickness 6 mil when casted
methanol coagulation bath
casted January 6/94
NOTE: PPO solution was filtered

gas: CH4, 100 psi date: 06/01/94
no top filter paper cell: 4

time from start (min)	gas perm. (ml/min)	pressure (mmHg)	temperature (deg.C)	gas perm. at STP (ml/min)
0	0.0265	748.0	23.5	0.024
50	0.0217	749.1	24.0	0.020
113	0.0235	749.4	24.0	0.021
			s.s. average:	0.020
			in moles/(m2 s Pa):	2.2965E-11

gas: 20.4% CO2 in CH4, 100 date: 06/01/94
no top filter paper cell: 4

time from start (min)	gas perm. (ml/min)	pressure (mmHg)	temperature (deg.C)	gas perm. at STP (ml/min)
0	0.1491	749.5	24.0	0.135
56	0.1723	749.7	24.0	0.156
124	0.1834	750.8	24.5	0.166
161	0.1869	750.9	24.5	0.169
			s.s. average:	0.166
			in moles/(m2 s Pa):	1.5976E-10

gas: 49.2% CO2 in CH4, 100 date: 06/02/94
no top filter paper cell: 4

time from start (min)	gas perm. (ml/min)	pressure (mmHg)	temperature (deg.C)	gas perm. at STP (ml/min)
0	0.4020	753.3	23.0	0.366
94	0.3979	754.0	23.5	0.363
253	0.3260	755.5	24.0	0.298
343	0.3061	756.2	25.0	0.281
			s.s. average:	0.289
			in moles/(m2 s Pa):	3.246E-10

GC analysis
gas: 20.4% CO2 in CH4, 100 date: 06/01/94
not top filter paper cell: 4

injection time	CH4 area	CO2 area	corrected CH4 area	corrected CO2 area	%CH4 in permeate	%CO2 in permeate	separation factor	enrichment factor
14:44:31	726445	4781742	19218.1	101739.2	15.89	84.11	20.7	4.1
15:15:40	475866	2977223	12589.0	63345.2	16.58	83.42	19.6	4.1
15:46:50	710682	4750439	18801.1	101073.2	15.68	84.32	21.0	4.1

GC analysis
gas: 49.2% CO2 in CH4, 100 date: 06/02/94
no top filter paper cell: 4

injection time	CH4 area	CO2 area	corrected CH4 area	corrected CO2 area	%CH4 in permeate	%CO2 in permeate	separation factor	enrichment factor
13:42:30	784488	15514589	16678.3	352904.5	5.03	94.97	19.5	1.9
15:01:47	791433	15468414	16843.6	351554.9	5.09	94.91	19.3	1.9

Appendix B

SAS® Programs

```
*************************************************************************
* SYLVIE GAGNE                                                          *
*                                                                       *
* ANOVA PROCEDURE FOR ANALYSIS OF VARIANCE ON EFFECT OF CASTING         *
* CONDITIONS ON THE CO2/CH4 PURE GAS PERMEATION RATE RATIO FOR          *
* HIGH MOLECULAR WEIGHT PPO MEMBRANES                                   *
*                                                                       *
*************************************************************************;
*:
    OPTIONS PAGESIZE=80 LINESIZE=100 NODATE;
    TITLE ANOVA PROCEDURE FOR THE MAIN EFFECTS ON CO2/CH4 PERMEATION;
    TITLE2 RATE RATIO OF MEMBRANES FROM HIGH MOLECULAR WEIGH PPO;
    FOOTNOTE DATA USED IN ANOVA IS AVERAGE OF 1 TO 3 COUPONS;
DATA HPPO;
    INPUT T A B C D PERM RATIO;
    LABEL T='RUN NUMBER'
          A='POLYMER CONC., SCALED'
          B='ADDITIVE CONC., SCALED'
          C='EVAPORATION TIME, SCALED'
          D='TEMP.OF CASTING SOL., SCALED'
          PERM='CO2 PERM. RATE, (MMOLES/(MIN M2 KPA))'
          RATIO='CO2/CH4, PURE GAS PERM. RATIO';
    CARDS;
1 -1 -1 -1 -1 1.1232E-1 1.668392E2
2 1 -1 -1 1 9.42024E-2 2.295
3 -1 1 -1 1 2.91486147E2 5.4E-1
4 1 1 -1 -1 4.16856 2.44666667
5 -1 -1 1 1 6.3726E-2 1.25895E2
6 1 -1 1 -1 5.46207E-2 1.099E2
7 -1 1 1 -1 1.0944E1 1.40
8 1 1 1 1 4.1828712E2 7.0E-1
;
PROC PRINT;
    * TO PRINT DATA;
    TITLE DATA FOR HIGH MOLECULAR WEIGHT PPO MEMBRANES (AVERAGED);
PROC ANOVA;
    CLASS A B C D;
    MODEL RATIO= A B C D A*C A*D C*D;
```

```
*************************************************************************
* SYLVIE GAGNE                                                          *
*                                                                       *
* ANOVA PROCEDURE FOR ANALYSIS OF VARIANCE ON EFFECT OF CASTING         *
* CONDITIONS ON THE CO2 PURE GAS PERMEATION RATE FOR                    *
* HIGH MOLECULAR WEIGHT PPO MEMBRANES                                   *
*                                                                       *
*************************************************************************;
*;
    OPTIONS PAGESIZE=80 LINESIZE=100 NODATE NONUMBER;
    TITLE ANOVA PROCEDURE FOR THE MAIN EFFECTS ON CO2 PERMEATION;
    TITLE2 RATE OF MEMBRANES FROM HIGH MOLECULAR WEIGH PPO;
    FOOTNOTE DATA USED IN ANOVA IS AVERAGE OF 1 TO 3 COUPONS;
DATA HPPO;
    INPUT T A B C D PERM RATIO;
    LABEL T='RUN NUMBER'
          A='POLYMER CONC., SCALED'
          B='ADDITIVE CONC., SCALED'
          C='EVAPORATION TIME, SCALED'
          D='TEMP.OF CASTING SOL., SCALED'
          PERM='CO2 PERM. RATE, (MMOLES/(MIN M2 KPA))'
          RATIO='CO2/CH4, PURE GAS PERM. RATIO';
    CARDS;
1 -1 -1 -1 -1 1.1232E-1 1.668392E2
2 1 -1 -1 1 9.42024E-2 2.295
3 -1 1 -1 1 2.91486147E2 5.4E-1
4 1 1 -1 -1 4.16856 2.44666667
5 -1 -1 1 1 6.3726E-2 1.25895E2
6 1 -1 1 -1 5.46207E-2 1.099E2
7 -1 1 1 -1 1.0944E1 1.40
8 1 1 1 1 4.1828712E2 7.0E-1
;
PROC PRINT;
    * TO PRINT DATA;
    TITLE DATA FOR HIGH MOLECULAR WEIGHT PPO MEMBRANES (AVERAGED);
PROC ANOVA;
    CLASS A B C D;
    MODEL PERM= A B C D A*C A*D C*D;
```

```
*****************************************************************
* SYLVIE GAGNe                                                  *
*                                                               *
* HALF NORMAL PLOT TO DETERMINE MAIN EFFECTS OF CASTING CONDITIONS *
* ON THE CO2/CH4 PURE GAS PERMEATION RATE RATIO OF HIGH MOLECULAR *
* WEIGHT PPO MEMBRANES                                          *
*                                                               *
*****************************************************************;
*;
   OPTIONS PAGESIZE=80 LINESIZE=100 NODATE NONUMBER;
* DATA OBTAINED FROM ANOVA PROCEDURE:
DATA;
    INPUT EFFECT $ ASS;
    LABEL EFFECT= 'EFFECT NAME'
          ASS='ANOVA SUM OF SQUARES';
    X = SQRT(ASS);
    ABSX= ABS(X);
    CARDS;
A 4020.01968882
B 19984.25643247
C 540.77957691
D 2856.01200359
E 2662.40287935
F 570.33253169
G 4128.94500645
;
PROC RANK OUT=RANKS;
    VAR ABSX;
    RANKS R;
DATA PLOTDATA;
    LABEL V=PROBABILITY FOR NORMAL DISTRIBUTION
    ABSX= SQUARE ROOT OF ANOVA SUM OF SQUARES;
    SET RANKS;
    RSTAR=(R-.5)/7;
    P=RSTAR/2+.5;
    V=PROBIT(P);
PROC PRINT;
    TITLE DATA FOR HALF-NORMAL PLOT OF THE EFFECTS ON THE RATIO;
PROC PLOT;
    PLOT V*ABSX = EFFECT/VREF = 1;
    TITLE HALF-NORMAL PLOT OF THE EFFECTS ON THE RATIO;
    TITLE2 ALL EFFECTS;
    FOOTNOTE E-AC EFFECT  F-BC EFFECT  G-AB EFFECT;
```

```
*************************************************************************
* SYLVIE GAGNe                                                          *
*                                                                       *
* HALF NORMAL PLOT TO DETERMINE MAIN EFFECTS OF CASTING CONDITIONS      *
* ON THE CO2 PURE GAS PERMEATION RATE OF HIGH MOLECULAR                 *
* WEIGHT PPO MEMBRANES                                                  *
*                                                                       *
*************************************************************************;
*;
    OPTIONS PAGESIZE=80 LINESIZE=100 NODATE NONUMBER;
* DATA OBTAINED FROM ANOVA PROCEDURE:
DATA;
    INPUT EFFECT $ ASS;
    LABEL EFFECT= 'EFFECT NAME'
          ASS='ANOVA SUM OF SQUARES';
    X = SQRT(ASS);
    ABSX= ABS(X);
    CARDS;
A 1799.94930336
B 65623.57271412
C 2227.38868718
D 60317.62211870
E 60320.75236404
F 2233.27778404
G 1801.58302490
;
PROC RANK OUT=RANKS;
    VAR ABSX;
    RANKS R;
DATA PLOTDATA;
    LABEL V=PROBABILITY FOR NORMAL DISTRIBUTION
    ABSX= SQUARE ROOT OF ANOVA SUM OF SQUARES;
    SET RANKS;
    RSTAR=(R-.5)/7;
    P=RSTAR/2+.5;
    V=PROBIT(P);
PROC PRINT;
    TITLE DATA FOR HALF-NORMAL PLOT OF THE EFFECTS ON CO2 PERMEATION;
PROC PLOT;
    PLOT V*ABSX = EFFECT/VREF = 1.0 HAXIS= 25 TO 275 BY 25
                                VAXIS= 0.0 TO 1.8 BY 0.2;
    TITLE HALF-NORMAL PLOT OF THE EFFECTS ON CO2 PERMEATION;
    TITLE2 WITH ALL EFFECTS;
    FOOTNOTE E-AC EFFECT  F-BC EFFECT  G-AB EFFECT;
```

```
*****************************************************************
* SYLVIE GAGNE                                                  *
*                                                               *
* MODELLING OF CO2/CH4 PURE GAS PERMEATION RATE RATIO FOR       *
* HIGH MOLECULAR WEIGHT PPO MEMBRANES                           *
*                                                               *
*****************************************************************;
*;
    OPTIONS PAGESIZE=80 LINESIZE=100 NODATE NONUMBER;
DATA FACT;
    INPUT N A B C D PERM RATIO VARP VARR;
    BC= B*C;
    AC= A*C;
    AB= A*B;
    WP=1/VARP;
    WR=1/VARR;
    LABEL N='OBSERVATIONS'
          PERM = 'CO2 PERM. (MMOL/(MIN M2 KPA))'
          RATIO = 'CO2/CH4 PERMEATION RATE RATIO'
          A='POLYMER CONCENTRATION, SCALED'
          B='PRESENCE OF ADDITIVE, SCALED'
          C='EVAPORATION TIME BEFORE GELATION, SCALED'
          D='TEMP. OF CASTING SOLUTION, SCALED'
          WP='INVERSE PERMEATION COUPON VARIANCE'
          WR='INVERSE OF THE RATIO COUPON VARIANCE';
    CARDS;
1 -1 -1 -1 -1 1.5444E-1 124.75 0.0035481888 3543.0159
2 -1 -1 -1 -1 7.02E-2 2.08928571E2 0.0035481888 3543.0159
3 1 -1 -1 1 6.90168E-2 1.03 0.00126862889 0.06845
4 1 -1 -1 1 1.19388E-1 1.40 0.00126862889 0.06845
5 -1 1 -1 1 2.597721E2 0.6 2011.55812912 0.0072
6 -1 1 -1 1 3.2320014E2 0.48 2011.55812912 0.0072
7 1 1 -1 -1 4.788 2.49 0.81102912480 0.0129333333
8 1 1 -1 -1 4.5822 2.43 0.81102912480 0.0129333333
9 1 1 -1 -1 3.13548 2.65 0.81102912480 0.0129333333
10 -1 -1 1 1 6.5532E-2 34.79 6.523272E-6 1.11744843E4
11 -1 -1 1 1 6.192E-2 1.84285714E2 6.523272E-6 1.11744843E4
12 1 -1 1 -1 5.03034E-2 176 3.72781586E-5 8.73842E3
13 1 -1 1 -1 5.8938E-2 43.80 3.72781586E-5 8.73842E3
14 -1 1 1 -1 1.0944E1 1.40 1 1
15 1 1 1 1 4.5676122E2 0.68 2.96051274E3 8E-4
16 1 1 1 1 3.7981302E2 0.72 2.96051274E3 8E-4
;
PROC STEPWISE;
    MODEL RATIO= A B C D AC AB BC/ BACKWARD SLSTAY=0.5 DETAILS;
*   WEIGHT WR;
PROC REG;
    MODEL RATIO = A B D AC AB/ALL;
*   WEIGHT WR;
    OUTPUT OUT=BOB
    P=PREDICT
    R=RESID;
PROC PRINT;
    TITLE DATA FOR MODEL FITTING OF CO2/CH4 RATIO FOR HPPO;
    TITLE2 PARAMETERS B AND CD;
```

FILE: HPPOR SAS * VM/SP CONVERSATIONAL MONITOR SYSTEM

```
PROC PLOT;
    PLOT RESID * PREDICT;
    TITLE PLOT OF RESIDUALS VS. PREDICTED VALUE OF RATIO;
```

```
**********************************************************************
* SYLVIE GAGNE                                                       *
*                                                                    *
* MODELLING OF CO2 PURE GAS PERMEATION RATE FOR                      *
* HIGH MOLECULAR WEIGHT PPO MEMBRANES                                *
*                                                                    *
**********************************************************************;
*;
    OPTIONS PAGESIZE=80 LINESIZE=100 NODATE NONUMBER;
DATA FACT;
    INPUT N A B C D PERM RATIO VARP VARR;
    BC= B*C;
    AC= A*C;
    AB= A*B;
    WP=1/VARP;
    WR=1/VARR;
    LABEL N='OBSERVATIONS'
          PERM = 'CO2 PERM. (MMOL/(MIN M2 KPA))'
          RATIO = 'CO2/CH4 PERMEATION RATE RATIO'
          A='POLYMER CONCENTRATION, SCALED'
          B='PRESENCE OF ADDITIVE, SCALED'
          C='EVAPORATION TIME BEFORE GELATION, SCALED'
          D='TEMP. OF CASTING SOLUTION, SCALED'
          WP='INVERSE PERMEATION COUPON VARIANCE'
          WR='INVERSE OF THE RATIO COUPON VARIANCE';
    CARDS;
1 -1 -1 -1 -1 1.5444E-1 124.75 0.0035481888 3543.0159
2 -1 -1 -1 -1 7.02E-2 2.08928571E2 0.0035481888 3543.0159
3 1 -1 -1 1 6.90168E-2 1.03 0.00126862889 0.06845
4 1 -1 -1 1 1.19388E-1 1.40 0.00126862889 0.06845
5 -1 1 -1 1 2.597721E2 0.6 2011.55812912 0.0072
6 -1 1 -1 1 3.2320014E2 0.48 2011.55812912 0.0072
7 1 1 -1 -1 4.788 2.49 0.81102912480 0.0129333333
8 1 1 -1 -1 4.5822 2.43 0.81102912480 0.0129333333
9 1 1 -1 -1 3.13548 2.65 0.81102912480 0.0129333333
10 -1 -1 1 1 6.5532E-2 34.79 6.523272E-6 1.11744843E4
11 -1 -1 1 1 6.192E-2 1.84285714E2 6.523272E-6 1.11744843E4
12 1 -1 1 -1 5.03034E-2 176 3.72781586E-5 8.73842E3
13 1 -1 1 -1 5.8938E-2 43.80 3.72781586E-5 8.73842E3
14 -1 1 1 -1 1.0944E1 1.40 1 1
15 1 1 1 1 4.5676122E2 0.68 2.96051274E3 8E-4
16 1 1 1 1 3.7981302E2 0.72 2.96051274E3 8E-4
;
PROC STEPWISE;
    MODEL PERM= A B C D AC AB BC/ BACKWARD SLSTAY=0.1 DETAILS;
*   WEIGHT WR;
PROC REG;
    MODEL PERM = A B C D AC AB BC/ALL;
*   WEIGHT WP;
    OUTPUT OUT=BOB
    P=PREDICT
    R=RESID;
PROC PRINT;
    TITLE DATA FOR MODEL FITTING OF CO2 PERMEATION FOR HPPO;
    TITLE2 ALL PARAMETERS;
```

FILE: HPPOP SAS * VM/SP CONVERSATIONAL MONITOR SYSTEM

```
PROC PLOT;
    PLOT RESID * PREDICT;
    TITLE PLOT OF RESIDUALS VS. PREDICTED VALUE OF CO2 PERMEATION;
```

```
FILE: PLOT     SAS      *                    VM/SP CONVERSATIONAL MONITOR SYSTEM

*************************************************************************
*  SYLVIE GAGNE                                                         *
*                                                                       *
*  CONTOUR PLOTS FOR OPTIMIZATION OF CO2/CH4 PURE GAS PERMEATION        *
*  RATE RATIO FOR HIGH MOLECULAR WEIGHT PPO MEMBRANES                   *
*                                                                       *
*************************************************************************;
*;
OPTIONS PAGESIZE=80 LINESIZE=100 NODATE NONUMBER;
DATA AREA;
    C=-1;
    A=0;
    DO B =-1 TO 1 BY 0.1;
    DO D=-1 TO 1 BY 0.1;
    RATIO=49.11633924-20.51455353*A-47.75669638*B-21.11812499*D+
+   20.37848213*B*D+20.80098210*A*B;
    OUTPUT;
    END;
END;
PROC PLOT DATA=AREA;
    PLOT D*B=RATIO/ CONTOUR;
    TITLE1 CONTOUR PLOT OF THE RATIO AS A FUNCTION OF;
    TITLE2 ADDITIVE CONCENTRATION (B), CASTING SOLUTION TEMPERATURE (D);
    TITLE3 WITH POLYMER CONCENTRATION (A)=0 AND EVAPORATION TIME C=-1;
    FOOTNOTE ALL VARIABLES ARE CODED;
RUN;
```

```
FILE: PLOT2    SAS      *                    VM/SP CONVERSATIONAL MONITOR SYSTEM

*************************************************************************
*  SYLVIE GAGNE                                                         *
*                                                                       *
*  CONTOUR PLOTS FOR OPTIMIZATION OF CO2 PERMEATION RATE FOR            *
*  HIGH MOLECULAR WEIGHT PPO MEMBRANES                                  *
*                                                                       *
*************************************************************************;
*;
OPTIONS PAGESIZE=80 LINESIZE=100 NODATE NONUMBER;
DATA AREA;
    C=-1;
    D=1;
    DO B =-1 TO 1 BY 0.1;
    DO A=-1 TO 1 BY 0.1;
    PERM=90.65133364+14.99979214*A+90.57011636*B+16.68603304*C+
+   86.83145846*D+86.83371154*B*D+15.00659786*A*B+16.70807696*B*C;
    OUTPUT;
    END;
END;
PROC PLOT DATA=AREA;
    PLOT A*B=PERM/ CONTOUR;
   TITLE1 CONTOUR PLOT OF THE CO2 PERMEATION RATE AS A FUNCTION OF;
  TITLE2 ADDITIVE CONCENTRATION (B) AND POLYMER CONCENTRATION (A);
   TITLE3 WITH CASTING SOL. TEMP. (D)=1 AND EVAPORATION TIME (C)=-1;
FOOTNOTE ALL VARIABLES ARE CODED, PERMEATION RATE IN MMOLES/(M2 MIN KPA);
RUN;
```

```
*****************************************************************
* SYLVIE GAGNE                                                  *
*                                                               *
* MODELLING OF CO2 PURE GAS PERMEATION RATE FOR                 *
* HIGH MOLECULAR WEIGHT PPO MEMBRANES                           *
* BY BEATON-TUKEY BIWEIGHT (ITERATIVELY REWEIGHED LEAST SQUARES)*
*                                                               *
*****************************************************************;
*;
    OPTIONS PAGESIZE=80 LINESIZE=100 NODATE NONUMBER;
DATA FACT;
    INPUT N A B C D PERM RATIO;
    BC= B*C;
    AC= A*C;
    AB= A*B;
    LABEL N='OBSERVATIONS'
          PERM = 'CO2 PERM. (MMOL/(MIN M2 KPA))'
          RATIO = 'CO2/CH4 PERMEATION RATE RATIO'
          A='POLYMER CONCENTRATION, SCALED'
          B='PRESENCE OF ADDITIVE, SCALED'
          C='EVAPORATION TIME BEFORE GELATION, SCALED'
          D='TEMP. OF CASTING SOLUTION, SCALED';
    CARDS;
1 -1 -1 -1 -1 1.5444E-1 124.75
2 -1 -1 -1 -1 7.02E-2 2.08928571E2
3 1 -1 -1 1 6.90168E-2 1.03
4 1 -1 -1 1 1.19388E-1 1.40
5 -1 1 -1 1 2.597721E2 0.6
6 -1 1 -1 1 3.2320014E2 0.48
7 1 1 -1 -1 4.788 2.49
8 1 1 -1 -1 4.5822 2.43
9 1 1 -1 -1 3.13548 2.65
10 -1 -1 1 1 6.5532E-2 34.79
11 -1 -1 1 1 6.192E-2 1.84285714E2
12 1 -1 1 -1 5.03034E-2 176
13 1 -1 1 -1 5.8938E-2 43.80
14 -1 1 1 -1 1.0944E1 1.40
15 1 1 1 1 4.5676122E2 0.68
16 1 1 1 1 3.7981302E2 0.72
;
PROC NLIN NOHALVE;
    PARMS B0=90.7 B1=15 B2=90.6 B3=16.7 B4=86.8 B5=86.8 B6=15 B7=16.7;
* GUESSES FOR PARMS OBTAINED BY REGULAR LEAST SQUARES;
    MODEL PERM= B0+B1*A+B2*B+B3*C+B4*D+B5*AB+B6*AC+B7*BC;
* PARTIAL DERIVATIVES;
    DER.B0=1;
    DER.B1=A;
    DER.B2=B;
    DER.B3=C;
    DER.B4=D;
    DER.B5=AB;
    DER.B6=AC;
    DER.B7=BC;
    RESID=PERM-MODEL.PERM;
    SIGMA=162;
```

```
* SIGMA IS MEASURE OF SCALE OF ERROR STANDARD DEVIATION;
    T= 0.8;
*T IS TUNING CONSTANT;
    R= ABS(RESID/SIGMA);
    IF R<=T THEN _WEIGHT_=(1-(R/T)**2)**2;
    ELSE _WEIGHT_=0;
    OUTPUT OUT=SORTIE
           R=RBI;
DATA SORTIE;
SET SORTIE;
    SIGMA = 162;
    T=0.8;
    R=ABS(RBI/SIGMA);
    IF R<=T THEN _WEIGHT_=(1-(R/T)**2)**2;
    ELSE _WEIGHT_=0;
PROC PRINT;
    TITLE DATA FOR MODEL FITTING OF CO2 PERMEATION FOR HPPO;
    TITLE2 BY TUKEY BIWEIGHT ROBUST REGRESSION;
PROC STEPWISE;
    MODEL PERM=A B C D AC AB BC/BACKWARD SLSTAY=0.05 DETAILS;
    WEIGHT _WEIGHT_;
```

Appendix C

SAS® Outputs

DATA FOR HIGH MOLECULAR WEIGHT PPO MEMBRANES (AVERAGED)

OBS	T	A	B	C	D	PERM	RATIO
1	1	-1	-1	-1	-1	0.112	166.839
2	2	1	-1	-1	1	0.094	2.295
3	3	-1	1	-1	1	291.486	0.540
4	4	1	1	-1	-1	4.169	2.447
5	5	-1	-1	1	1	0.064	125.895
6	6	1	-1	1	-1	0.055	109.900
7	7	-1	1	1	-1	10.944	1.400
8	8	1	1	1	1	418.287	0.700

DATA USED IN ANOVA IS AVERAGE OF 1 TO 3 COUPONS

DATA FOR HIGH MOLECULAR WEIGHT PPO MEMBRANES (AVERAGED)

Analysis of Variance Procedure

Dependent Variable: PERM CO2 PERM. RATE, (MMOLES/(MIN M2 KPA))

Source	DF	Sum of Squares	Mean Square	F Value	Pr > F
Model	7	194324.14599634	27760.59228519	.	.
Error	0	.	.		
Corrected Total	7	194324.14599634			

R-Square	C.V.	Root MSE	PERM Mean
1.000000	0	0	90.65133701

Source	DF	Anova SS	Mean Square	F Value	Pr > F
A	1	1799.94930336	1799.94930336	.	.
B	1	65623.57271412	65623.57271412	.	.
C	1	2227.38868718	2227.38868718	.	.
D	1	60317.62211870	60317.62211870	.	.
A*C	1	60320.75236404	60320.75236404	.	.
A*D	1	2233.27778404	2233.27778404	.	.
C*D	1	1801.58302490	1801.58302490	.	.

DATA USED IN ANOVA IS AVERAGE OF 1 TO 3 COUPONS

DATA FOR HALF-NORMAL PLOT OF THE EFFECTS ON CO2 PERMEATION

OBS	V	ABSX	EFFECT	ASS	X	R	RSTAR	P
1	0.08964	42.426	A	1799.95	42.426	1	0.07143	0.53571
2	1.80274	256.171	B	65623.57	256.171	7	0.92857	0.96429
3	0.46371	47.195	C	2227.39	47.195	3	0.35714	0.67857
4	0.92082	245.596	D	60317.62	245.596	5	0.64286	0.82143
5	1.24187	245.603	E	60320.75	245.603	6	0.78571	0.89286
6	0.67449	47.258	F	2233.28	47.258	4	0.50000	0.75000
7	0.27188	42.445	G	1801.58	42.445	2	0.21429	0.60714

DATA FOR HALF-NORMAL PLOT OF THE EFFECTS ON CO2 PERMEATION

OBS	V	ABSX	EFFECT	ASS	X	R	RSTAR	P
1	0.15731	42.4258	A	1799.95	42.4258	1	0.125	0.5625
2	0.88715	47.1952	C	2227.39	47.1952	3	0.625	0.8125
3	1.53412	47.2576	F	2233.28	47.2576	4	0.875	0.9375
4	0.48878	42.4451	G	1801.58	42.4451	2	0.375	0.6875

DATA FOR HIGH MOLECULAR WEIGHT PPO MEMBRANES (AVERAGED)

Analysis of Variance Procedure

Dependent Variable: RATIO CO2/CH4, PURE GAS PERM. RATIO

Source	DF	Sum of Squares	Mean Square	F Value	Pr > F
Model	7	34762.74811929	4966.10687418	.	.
Error	0	.	.		
Corrected Total	7	34762.74811929			

R-Square	C.V.	Root MSE	RATIO Mean
1.000000	0	0	51.25198333

Source	DF	Anova SS	Mean Square	F Value	Pr > F
A	1	4020.01968882	4020.01968882	.	.
B	1	19984.25643247	19984.25643247	.	.
C	1	540.77957691	540.77957691	.	.
D	1	2856.01200359	2856.01200359	.	.
A*C	1	2662.40287935	2662.40287935	.	.
A*D	1	570.33253169	570.33253169	.	.
C*D	1	4128.94500645	4128.94500645	.	.

DATA USED IN ANOVA IS AVERAGE OF 1 TO 3 COUPONS

DATA FOR HALF-NORMAL PLOT OF THE EFFECTS ON THE RATIO

OBS	V	ABSX	EFFECT	ASS	X	R	RSTAR	P
1	0.92082	63.404	A	4020.02	63.404	5	0.64286	0.82143
2	1.80274	141.366	B	19984.25	141.366	7	0.92857	0.96429
3	0.08964	23.255	C	540.78	23.255	1	0.07143	0.53571
4	0.67449	53.442	D	2856.01	53.442	4	0.50000	0.75000
5	0.46371	51.598	E	2662.40	51.598	3	0.35714	0.67857
6	0.27188	23.882	F	570.33	23.882	2	0.21429	0.60714
7	1.24187	64.257	G	4128.95	64.257	6	0.78571	0.89286

DATA FOR HALF-NORMAL PLOT OF THE EFFECTS ON THE RATIO
WITHOUT EFFECTS B AND CD(AB)

OBS	V	ABSX	EFFECT	ASS	X	R	RSTAR	P
1	1.64485	63.4036	A	4020.02	63.4036	5	0.9	0.95
2	0.12566	23.2547	C	540.78	23.2547	1	0.1	0.55
3	1.03643	53.4417	D	2856.01	53.4417	4	0.7	0.85
4	0.67449	51.5985	E	2662.40	51.5985	3	0.5	0.75
5	0.38532	23.8816	F	570.33	23.8816	2	0.3	0.65

The SAS System

Backward Elimination Procedure for Dependent Variable PERM

Step 0 All Variables Entered R-square = 0.98740023 C(p) = 8.00000000

	DF	Sum of Squares	Mean Square	F	Prob>F
Regression	7	389771.41224126	55681.63032018	89.56	0.0001
Error	8	4973.69778961	621.71222370		
Total	15	394745.11003087			

Variable	Parameter Estimate	Standard Error	Type II Sum of Squares	F	Prob>F
INTERCEP	90.65133364	6.48807356	121368.58028688	195.22	0.0001
A	14.99979214	6.48807356	3322.98482464	5.34	0.0495
B	90.57011636	6.48807356	121151.20213539	194.87	0.0001
C	16.68603304	6.48807356	4112.10385519	6.61	0.0330
D	86.83145846	6.48807356	111355.60140886	179.11	0.0001
AC	86.83371154	6.48807356	111361.38032312	179.12	0.0001
AB	15.00659786	6.48807356	3326.00092662	5.35	0.0495
BC	16.70807696	6.48807356	4122.97603621	6.63	0.0323

Bounds on condition number: 1.083333, 52.60937

Statistics for Removal: Step 1
DF = 1,8

Variable	Partial R**2	Model R**2
A	0.0084	0.9790
B	0.3069	0.6805
C	0.0104	0.9770
D	0.2821	0.7053
AC	0.2821	0.7053
AB	0.0084	0.9790
BC	0.0104	0.9770

All variables left in the model are significant at the 0.0500 level.

The SAS System

Model: MODEL1
Dependent Variable: PERM CO2 PERM. (MMOL/(MIN M2 KPA))

Analysis of Variance

Source	DF	Sum of Squares	Mean Square	F Value	Prob>F
Model	7	389771.41224	55681.63032	89.562	0.0001
Error	8	4973.69779	621.71222		
C Total	15	394745.11003			

Root MSE	24.93416	R-square	0.9874
Dep Mean	90.22787	Adj R-sq	0.9764
C.V.	27.63465		

Parameter Estimates

Variable	DF	Parameter Estimate	Standard Error	T for H0: Parameter=0	Prob > |T|
INTERCEP	1	90.651334	6.48807356	13.972	0.0001
A	1	14.999792	6.48807356	2.312	0.0495
B	1	90.570116	6.48807356	13.959	0.0001
C	1	16.686033	6.48807356	2.572	0.0330
D	1	86.831458	6.48807356	13.383	0.0001
AC	1	86.833712	6.48807356	13.384	0.0001
AB	1	15.006598	6.48807356	2.313	0.0495
BC	1	16.708077	6.48807356	2.575	0.0329

Variable	DF	Variable Label
INTERCEP	1	Intercept
A	1	POLYMER CONCENTRATION, SCALED
B	1	PRESENCE OF ADDITIVE, SCALED
C	1	EVAPORATION TIME BEFORE GELATION, SCALED
D	1	TEMP. OF CASTING SOLUTION, SCALED
AC	1	
AB	1	
BC	1	

The SAS System

Backward Elimination Procedure for Dependent Variable RATIO

Step 0 All Variables Entered R-square = 0.73541005 C(p) = 8.00000000

	DF	Sum of Squares	Mean Square	F	Prob>F
Regression	7	65194.44559897	9313.49222842	3.18	0.0638
Error	8	23456.02247665	2932.00280958		
Total	15	88650.46807563			

Variable	Parameter Estimate	Standard Error	Type II Sum of Squares	F	Prob>F
INTERCEP	49.08193448	14.08974888	35579.61293121	12.13	0.0083
A	-20.49735115	14.08974888	6205.16535132	2.12	0.1838
B	-47.79110115	14.08974888	33732.76576588	11.51	0.0095
C	6.30252977	14.08974888	586.66163464	0.20	0.6665
D	-21.08372023	14.08974888	6565.26659006	2.24	0.1729
AC	20.41288690	14.08974888	6154.13097485	2.10	0.1854
AB	20.81818448	14.08974888	6400.93742782	2.18	0.1778
BC	-6.54336310	14.08974888	632.35348745	0.22	0.6547

Bounds on condition number: 1.083333, 52.60937

Step 1 Variable C Removed R-square = 0.72879236 C(p) = 6.20008904

	DF	Sum of Squares	Mean Square	F	Prob>F
Regression	6	64607.78396433	10767.96399406	4.03	0.0306
Error	9	24042.68411129	2671.40934570		
Total	15	88650.46807563			

Variable	Parameter Estimate	Standard Error	Type II Sum of Squares	F	Prob>F
INTERCEP	48.11231451	13.28892658	35016.53236730	13.11	0.0056
A	-20.01254116	13.40919081	5950.31251389	2.23	0.1698
B	-48.76072111	13.28892658	35966.72349313	13.46	0.0052
D	-20.11410026	13.28892658	6120.14706364	2.29	0.1644
AC	21.38250686	13.28892658	6916.36456487	2.59	0.1421
AB	21.30299446	13.40919081	6742.43251356	2.52	0.1466
BC	-7.02817309	13.40919081	733.87179445	0.27	0.6128

Bounds on condition number: 1.060096, 38.12019

Step 2 Variable BC Removed R-square = 0.72051410 C(p) = 4.45038614

	DF	Sum of Squares	Mean Square	F	Prob>F
Regression	5	63873.91216988	12774.78243398	5.16	0.0135
Error	10	24776.55590575	2477.65559057		
Total	15	88650.46807563			

Variable	Parameter Estimate	Standard Error	Type II Sum of Squares	F	Prob>F

DATA FOR MODEL FITTING OF CO2 PERMEATION FOR HPPO
ALL PARAMETERS

OBS	N	A	B	C	D	PEPM	RATIO	VARP	VARR
1	1	-1	-1	-1	-1	0.154	124.750	0.00	3543.02
2	2	-1	-1	-1	-1	0.070	208.929	0.00	3543.02
3	3	1	-1	-1	1	0.069	1.030	0.00	0.07
4	4	1	-1	-1	1	0.119	1.400	0.00	0.07
5	5	-1	1	-1	1	259.772	0.600	2011.56	0.01
6	6	-1	1	-1	1	323.200	0.480	2011.56	0.01
7	7	1	1	-1	-1	4.788	2.490	0.81	0.01
8	8	1	1	-1	-1	4.582	2.430	0.81	0.01
9	9	1	1	-1	-1	3.135	2.650	0.81	0.01
10	10	-1	-1	1	1	0.066	34.790	0.00	11174.48
11	11	-1	-1	1	1	0.062	184.286	0.00	11174.48
12	12	1	-1	1	-1	0.050	176.000	0.00	8738.42
13	13	1	-1	1	-1	0.059	43.800	0.00	8738.42
14	14	-1	1	1	-1	10.944	1.400	1.00	1.00
15	15	1	1	1	1	456.761	0.680	2960.51	0.00
16	16	1	1	1	1	379.813	0.720	2960.51	0.00

OBS	BC	AC	AB	WP	WR	PREDICT	RESID
1	1	1	1	281.83	0.00	0.112	0.0421
2	1	1	1	281.83	0.00	0.112	-0.0421
3	1	-1	-1	788.25	14.61	0.094	-0.0252
4	1	-1	-1	788.25	14.61	0.094	0.0252
5	-1	1	-1	0.00	138.89	291.486	-31.7140
6	-1	1	-1	0.00	138.89	291.486	31.7140
7	-1	-1	1	1.23	77.32	4.169	0.6194
8	-1	-1	1	1.23	77.32	4.169	0.4136
9	-1	-1	1	1.23	77.32	4.169	-1.0331
10	-1	-1	1	153297.30	0.00	0.064	0.0018
11	-1	-1	1	153297.30	0.00	0.064	-0.0018
12	-1	1	-1	26825.36	0.00	0.055	-0.0043
13	-1	1	-1	26825.36	0.00	0.055	0.0043
14	1	-1	-1	1.00	1.00	10.944	-0.0000
15	1	1	1	0.00	1250.00	418.287	38.4741
16	1	1	1	0.00	1250.00	418.287	-38.4741

PLOT OF RESIDUALS VS. PREDICTED VALUE OF CO2 PERMEATION

Plot of RESID*PREDICT. Legend: A = 1 obs, B = 2 obs, etc.

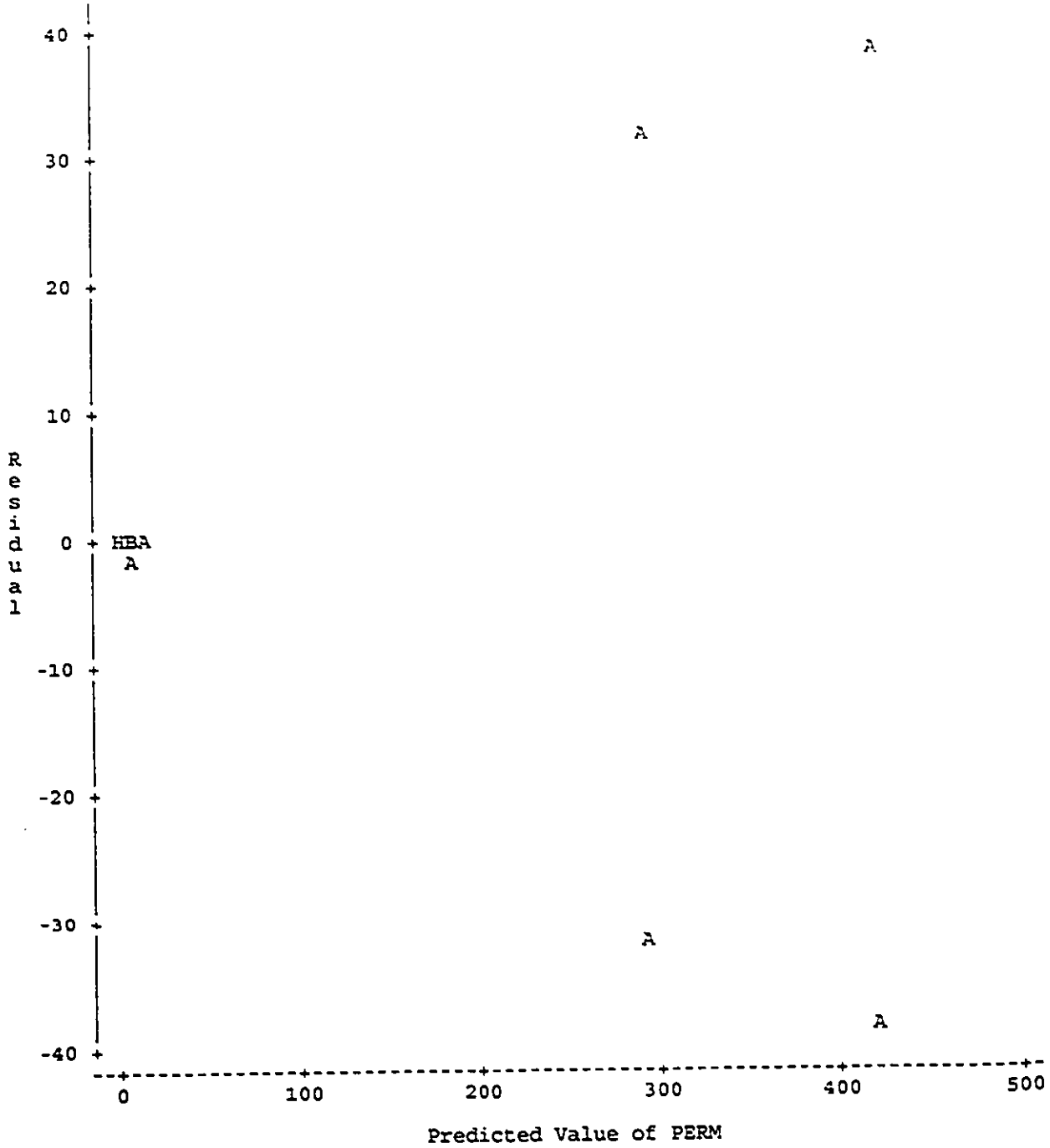

DATA FOR HALF-NORMAL PLOT OF THE EFFECTS ON CO2 PERMEATION

OBS	V	ABSX	EFFECT	ASS	X	R	RSTAR	P
1	0.10463	42.426	A	1799.95	42.426	1	0.08333	0.54167
2	0.54852	47.195	C	2227.39	47.195	3	0.41667	0.70833
3	1.15035	245.596	D	60317.62	245.596	5	0.75000	0.87500
4	1.73166	245.603	E	60320.75	245.603	6	0.91667	0.95833
5	0.81222	47.258	F	2233.28	47.258	4	0.58333	0.79167
6	0.31864	42.445	G	1801.58	42.445	2	0.25000	0.62500

INTERCEP	49.11633924	12.66427873	37267.64902203	15.04	0.0031
A	-20.51455353	12.88077781	6284.64713562	2.54	0.1423
B	-47.75669638	12.66427873	35232.91441997	14.22	0.0037
D	-21.11812499	12.66427873	6889.54796573	2.78	0.1264
AC	20.37848213	12.66427873	6415.39914721	2.59	0.1387
AB	20.80098210	12.88077781	6461.36745334	2.61	0.1374

Bounds on condition number: 1.054687, 26.08259

All variables left in the model are significant at the 0.2500 level.

Summary of Backward Elimination Procedure for Dependent Variable RATIO

Step	Variable Removed	Number In	Partial R**2	Model R**2	C(p)	F	Prob>F
	Label						
1	C	6	0.0066	0.7288	6.2001	0.2001	0.6665
	EVAPORATION TIME BEFORE GELATION, SCALED						
2	BC	5	0.0083	0.7205	4.4504	0.2747	0.6128

The SAS System

Model: MODEL1
Dependent Variable: RATIO CO2/CH4 PERMEATION RATE RATIO

Analysis of Variance

Source	DF	Sum of Squares	Mean Square	F Value	Prob>F
Model	5	63873.91217	12774.78243	5.156	0.0135
Error	10	24776.55591	2477.65559		
C Total	15	88650.46808			

Root MSE	49.77605	R-square	0.7205
Dep Mean	49.15214	Adj R-sq	0.5808
C.V.	101.26935		

Parameter Estimates

Variable	DF	Parameter Estimate	Standard Error	T for H0: Parameter=0	Prob > |T|
INTERCEP	1	49.116339	12.66427873	3.878	0.0031
A	1	-20.514554	12.88077781	-1.593	0.1423
B	1	-47.756696	12.66427873	-3.771	0.0037
D	1	-21.118125	12.66427873	-1.668	0.1264
AC	1	20.378482	12.66427873	1.609	0.1387
AB	1	20.800982	12.88077781	1.615	0.137[illegible]

Variable	DF	Variable Label
INTERCEP	1	Intercept
A	1	POLYMER CONCENTRATION, SCALED
B	1	PRESENCE OF ADDITIVE, SCALED
D	1	TEMP. OF CASTING SOLUTION, SCALED
AC	1	
AB	1	

DATA FOR MODEL FITTING OF CO2/CH4 RATIO FOR HPPO
PARAMETERS B AND CD

OBS	N	A	B	C	D	PERM	RATIO	VARP	VARR
1	1	-1	-1	-1	-1	0.154	124.750	0.00	3543.02
2	2	-1	-1	-1	-1	0.070	208.929	0.00	3543.02
3	3	1	-1	-1	1	0.069	1.030	0.00	0.07
4	4	1	-1	-1	1	0.119	1.400	0.00	0.07
5	5	-1	1	-1	1	259.772	0.600	2011.56	0.01
6	6	-1	1	-1	1	323.200	0.480	2011.56	0.01
7	7	1	1	-1	-1	4.788	2.490	0.81	0.01
8	8	1	1	-1	-1	4.582	2.430	0.81	0.01
9	9	1	1	-1	-1	3.135	2.650	0.81	0.01
10	10	-1	-1	1	1	0.066	34.790	0.00	11174.48
11	11	-1	-1	1	1	0.062	184.286	0.00	11174.48
12	12	1	-1	1	-1	0.050	176.000	0.00	8738.42
13	13	1	-1	1	-1	0.059	43.800	0.00	8738.42
14	14	-1	1	1	-1	10.944	1.400	1.00	1.00
15	15	1	1	1	1	456.761	0.680	2960.51	0.00
16	16	1	1	1	1	379.813	0.720	2960.51	0.00

OBS	BC	AC	AB	WP	WR	PREDICT	RESID
1	1	1	1	281.83	0.00	179.685	-54.9352
2	1	1	1	281.83	0.00	179.685	29.2434
3	1	-1	-1	788.25	14.61	14.061	-13.0309
4	1	-1	-1	788.25	14.61	14.061	-12.6609
5	-1	1	-1	0.00	138.89	0.334	0.2664
6	-1	1	-1	0.00	138.89	0.334	0.1464
7	-1	-1	1	1.23	77.32	2.386	0.1043
8	-1	-1	1	1.23	77.32	2.386	0.0443
9	-1	-1	1	1.23	77.32	2.386	0.2643
10	-1	-1	1	153297.30	0.00	96.692	-61.9020
11	-1	-1	1	153297.30	0.00	96.692	87.5937
12	-1	1	-1	26825.36	0.00	97.054	78.9459
13	-1	1	-1	26825.36	0.00	97.054	-53.2541
14	1	-1	-1	1.00	1.00	1.813	-0.4129
15	1	1	1	0.00	1250.00	0.906	-0.2264
16	1	1	1	0.00	1250.00	0.906	-0.1864

PLOT OF RESIDUALS VS. PREDICTED VALUE OF RATIO

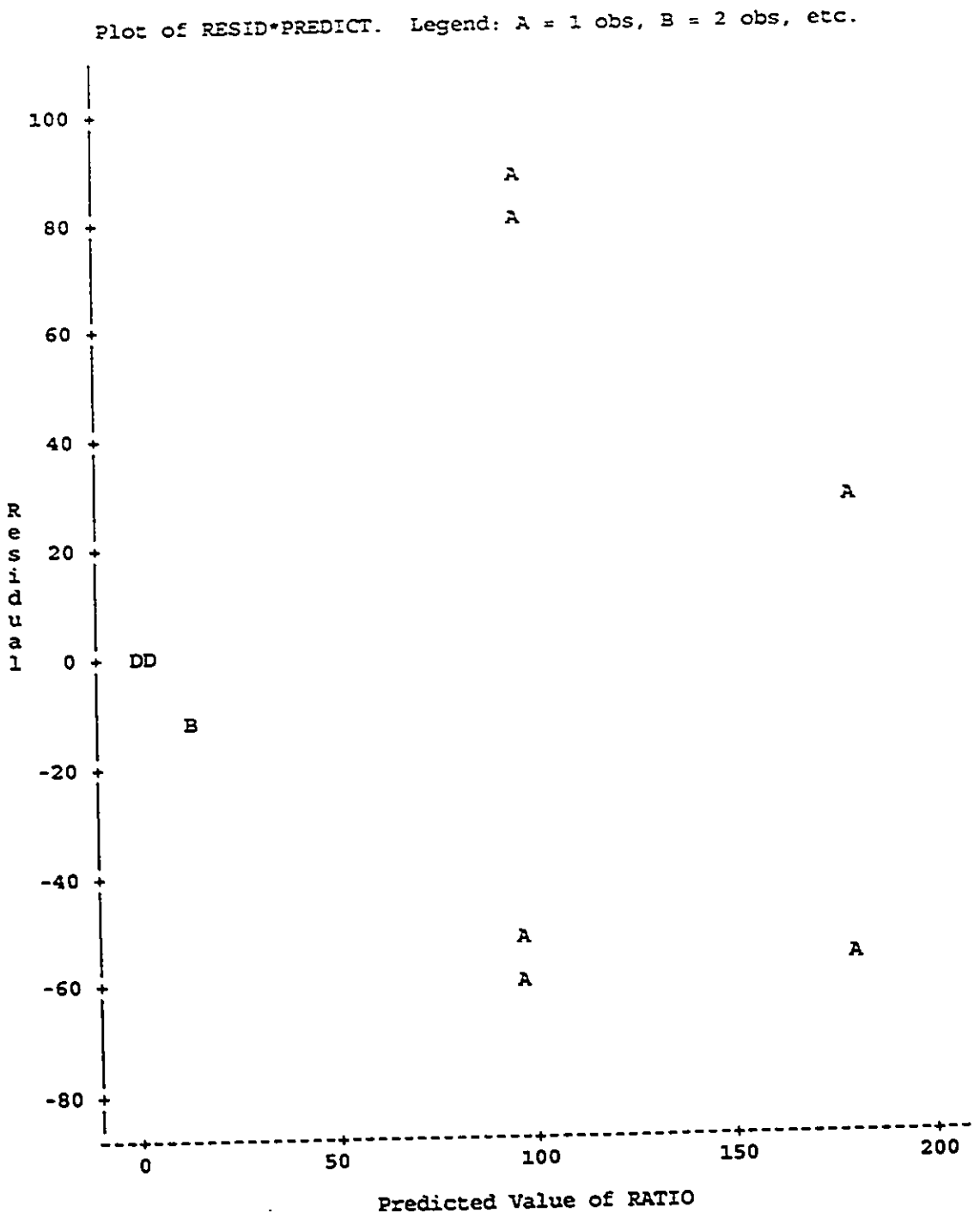

The SAS System

Non-Linear Least Squares Iterative Phase
Dependent Variable PERM Method: Gauss-Newton

Iter	B0 B4	B1 B5	B2 B6	B3 B7	Weighted SS
0	90.700000 86.800000	15.000000 86.800000	90.600000 15.000000	16.700000 16.700000	3274.678270
1	90.660655 86.800000	15.032495 86.841554	146.571444 15.000000	-39.314050 16.700000	6557.056524
2	88.565018 86.800000	15.031732 73.126181	146.571444 28.714610	-39.314814 18.794873	4287.006221
3	90.141747 86.799705	15.031732 71.549157	146.571149 30.291338	-39.314814 17.217850	4242.691813
4	90.545157 86.799705	15.031618 71.145519	146.571035 30.694863	-39.314814 16.814326	4239.753360
5	90.647998 86.799661	15.031618 71.042633	146.570991 30.797704	-39.314814 16.711440	4239.562348
6	90.674201 86.799644	15.031618 71.016414	146.570974 30.823906	-39.314814 16.685221	4239.549948
7	90.680877 86.799637	15.031618 71.009731	146.570967 30.830582	-39.314814 16.678538	4239.549143
8	90.682578 86.799634	15.031618 71.008028	146.570965 30.832283	-39.314814 16.676835	4239.549090
9	90.683010 86.799634	15.031617 71.007593	146.570964 30.832717	-39.314814 16.676401	4239.549087

NOTE: Convergence criterion met.

Non-Linear Least Squares Summary Statistics Dependent Variable PERM

Source	DF	Weighted SS	Weighted MS
Regression	6	441273.51718	73545.58620
Residual	5	4239.54909	847.90982
Uncorrected Total	11	445513.06627	
(Corrected Total)	10	302269.30338	

NOTE: The Jacobian is singular.

Parameter	Estimate	Asymptotic Std. Error	Asymptotic 95 % Confidence Interval Lower	Upper
B0	90.6830101	11.660571573	60.70899104	120.65702911
B1	15.0316167	0.000000000	15.03161674	15.03161674
B2	146.5709636	11.741177126	116.38974441	176.75218281
B3	-39.3148136	0.000000000	-39.31481359	-39.31481359
B4	86.7996345	11.741177126	56.61841529	116.98085368
B5	71.0075933	10.716392479	43.46062869	98.55455785
B6	30.8327167	11.660571573	0.85869771	60.80673578
B7	16.6764011	10.716392479	-10.87056343	44.22336573

Asymptotic Correlation Matrix

Corr	B0	B1	B2	B3
B0	1	.	0.1935388316	.
B1	.	.	.	.
B2	0.1935388316	.	1	.
B3	.	.	.	.
B4	-0.580616658	.	-0.153261163	.
B5	-0.027873203	.	0.4638552606	.
B6	-0.169260444	.	-0.580616658	.
B7	-0.451966327	.	0.0426735897	.

Corr	B4	B5	B6	B7
B0	-0.580616658	-0.027873203	-0.169260444	-0.451966327
B1	.	.	.	.
B2	-0.153261163	0.4638552606	-0.580616658	0.0426735897
B3	.	.	.	.
B4	1	0.0426735897	0.1935388316	0.4638552606
B5	0.0426735897	1	-0.451966327	0.0770833704
B6	0.1935388316	-0.451966327	1	-0.027873203
B7	0.4638552606	0.0770833704	-0.027873203	1

DATA FOR MODEL FITTING OF CO2 PERMEATION FOR HPPO
BY TUKEY BIWEIGHT ROBUST REGRESSION

OBS	N	A	B	C	D	PERM	RATIO	BC	AC	AB	RBI	SIGMA	T	R	_WEIGHT_
1	1	-1	-1	-1	-1	0.154	124.750	1	1	1	0.042	162	0.8	0.00026	1.00000
2	2	-1	-1	-1	-1	0.070	208.929	1	1	1	-0.042	162	0.8	0.00026	1.00000
3	3	1	-1	-1	1	0.069	1.030	1	-1	-1	-0.025	162	0.8	0.00016	1.00000
4	4	1	-1	-1	1	0.119	1.400	1	-1	-1	0.025	162	0.8	0.00016	1.00000
5	5	-1	1	-1	1	259.772	0.600	-1	1	-1	-31.713	162	0.8	0.19576	0.88383
6	6	-1	1	-1	1	323.200	0.480	-1	1	-1	31.715	162	0.8	0.19577	0.88382
7	7	1	1	-1	-1	4.788	2.490	-1	-1	1	-223.511	162	0.8	1.37970	0.00000
8	8	1	1	-1	-1	4.582	2.430	-1	-1	1	-223.717	162	0.8	1.38097	0.00000
9	9	1	1	-1	-1	3.135	2.650	-1	-1	1	-225.164	162	0.8	1.38990	0.00000
10	10	-1	-1	1	1	0.066	34.790	-1	-1	1	0.002	162	0.8	0.00001	1.00000
11	11	-1	-1	1	1	0.062	184.286	-1	-1	1	-0.002	162	0.8	0.00001	1.00000
12	12	1	-1	1	-1	0.050	176.000	-1	1	-1	223.872	162	0.8	1.38193	0.00000
13	13	1	-1	1	-1	0.059	43.800	-1	1	-1	223.881	162	0.8	1.38198	0.00000
14	14	-1	1	1	-1	10.944	1.400	1	-1	-1	-0.000	162	0.8	0.00000	1.00000
15	15	1	1	1	1	456.761	0.680	1	1	1	38.474	162	0.8	0.23749	0.83151
16	16	1	1	1	1	379.813	0.720	1	1	1	-38.474	162	0.8	0.23749	0.83151

DATA FOR MODEL FITTING OF CO2 PERMEATION FOR HPPO
BY TUKEY BIWEIGHT ROBUST REGRESSION

Backward Elimination Procedure for Dependent Variable PERM

Step 0 All Variables Entered R-square = 0.98597427 C(p) = 6.00000000
NOTE: The model is not of full rank. A subset of the model which is of full rank is chosen.

	DF	Sum of Squares	Mean Square	F	Prob>F
Regression	5	298029.75429027	59605.95085805	70.30	0.0001
Error	5	4239.54908670	847.90981734		
Total	10	302269.30337697			

Variable	Parameter Estimate	Standard Error	Type II Sum of Squares	F	Prob>F
INTERCEP	107.35941084	11.74117713	70893.53350143	83.61	0.0003
A	31.70790709	10.71639248	7423.13904998	8.75	0.0316
B	75.56348075	11.66057157	35606.87793132	41.99	0.0013
C	31.69266889	10.71639248	7416.00593352	8.75	0.0316
D	70.12334375	11.66057157	30664.45279606	36.16	0.0018
AC	101.84030964	11.74117713	63791.93947606	75.23	0.0003

Bounds on condition number: 1.692951, 36.91512

All variables left in the model are significant at the 0.0500 level.

Half-normal plot of the effects on the CO2 permeation rate

Effect	v (probability)	absx (square root of anova sum of squares)
B	1.80274	256.171
AC	1.24187	245.603
D	0.92082	245.596
BC	0.67449	47.258
C	0.46371	47.195
AB	0.27188	42.445
A	0.08964	42.426

Half-normal plot of the effects on the CO2 permeation rate, without main effects

Effect	v (probability)	absx (square root of anova sum of squares)
BC	1.53412	47.2576
C	0.88715	47.1952
AB	0.48878	42.4451
A	0.15731	42.4258

Half-normal plot of the effects on the CO2 permeation rate, without B effect

Effect	v (probability)	absx (square root of anova sum of squares)
AC	0.95833	245.603
D	0.875	245.596
BC	1.53412	47.2576
C	0.88715	47.1952
AB	0.48878	42.4451
A	0.15731	42.4258

Half-normal plot of the effects on the CO2/CH4 permeation rate ratio

Effect	v (probability)	absx (square root of anova sum of squares)
A	0.92082	63.404
B	1.80274	141.366
C	0.08964	23.255
D	0.67449	53.442
BD	0.46371	51.598
BC	0.27188	23.882
AB	1.24187	64.257

Half-normal plot of the effects on the CO2/CH4 permeation rate ratio, without B and C

Effect	v (probability)	absx (square root of anova sum of squares)	Best fit line	
		100	1.940034369586	for graph
C	0.12566	23.2547	0.451149172544	
BC	0.38532	23.8816	0.463311248007	
AC	0.67449	51.5985	1.001028634191	
D	1.03643	53.4417	1.036787347691	
A	1.64485	63.4036	1.230051631555	
		0	0	for graph

Linear regression to determine the variance

Regression Output:

Constant		0
Std Err of Y Est		0.312534450097
R Squared		0.722617854035
No. of Observations		5
Degrees of Freedom		4
X Coefficient(s)	0.019400343696	
Std Err of Coef.	0.003028532859	

variance estimate at probability = 1 variance = 51.55

Backward Elimination Procedure for Dependent Variable PERM

Step 0 All Variables Entered R-square = 0.97869490 C(p) = 10.00000000

	DF	Sum of Squares	Mean Square	F	Prob>F
Regression	9	418930.90427241	46547.87825249	71.46	0.0001
Error	14	9119.65919568	651.40422826		
Total	23	428050.56346808			

Variable	Parameter Estimate	Standard Error	Type II Sum of Squares	F	Prob>F
INTERCEP	36.17965264	14.05807904	4314.46944537	6.62	0.0221
A	15.08101158	6.64110910	3359.15690719	5.16	0.0395
B	91.44441338	6.63102916	123880.52992274	190.17	0.0001
C	17.18458214	6.63789238	4365.84298649	6.70	0.0214
D	83.52792261	6.49452412	107750.49282918	165.41	0.0001
AC	66.19256214	16.69574070	10239.00073969	15.72	0.0014
AB	14.64715865	6.63947936	3170.21921536	4.87	0.0446
BB	54.70572691	15.15661940	8486.16495568	13.03	0.0028
BD	19.82733494	17.09541720	876.23349745	1.35	0.2655
BC	16.56637496	6.64092989	4053.66408157	6.22	0.0257

Bounds on condition number: 7.969977, 215.8759

Step 1 Variable BD Removed R-square = 0.97664787 C(p) = 9.34514555

	DF	Sum of Squares	Mean Square	F	Prob>F
Regression	8	418054.67077495	52256.83384687	78.42	0.0001
Error	15	9995.89269313	666.39284621		
Total	23	428050.56346808			

Variable	Parameter Estimate	Standard Error	Type II Sum of Squares	F	Prob>F
INTERCEP	28.89179668	12.71941898	3438.30880600	5.16	0.0383
A	17.51362944	6.37327887	5032.18726935	7.55	0.0149
B	90.33341281	6.63653302	123465.22251650	185.27	0.0001
C	17.36850598	6.71190979	4462.34382282	6.70	0.0206
D	84.87823934	6.46240425	114956.83762138	172.51	0.0001
AC	84.06961131	6.48906872	111851.97534545	167.85	0.0001
AB	15.70850235	6.65134031	3716.90577302	5.58	0.0321
BB	61.32732694	14.20082881	12428.27954586	18.65	0.0006
BC	17.19504344	6.69448630	4396.45230738	6.60	0.0214

Bounds on condition number: 1.390848, 75.69724

Step 2 Variable AB Removed R-square = 0.96796454 C(p) = 13.05113518

	DF	Sum of Squares	Mean Square	F	Prob>F
Regression	7	414337.76500194	59191.10928599	69.06	0.0001
Error	16	13712.79846615	857.04990413		
Total	23	428050.56346808			

Variable	Parameter Estimate	Standard Error	Type II Sum of Squares	F	Prob>F
INTERCEP	27.59791585	14.41125917	3143.07559010	3.67	0.0735
A	16.97657396	7.22310934	4734.32243166	5.52	0.0319
B	92.45960784	7.45668702	131770.55508666	153.75	0.0001
C	18.64211049	7.58713267	5174.17256652	6.04	0.0258
D	82.87662680	7.26548577	111516.96221106	130.12	0.0001
AC	81.06464381	7.21617168	108157.17988363	126.20	0.0001
BB	64.88962624	16.01355763	14072.81576313	16.42	0.0009
BC	18.61087139	7.56147927	5191.89612661	6.06	0.0256

Bounds on condition number: 1.375157, 57.75364

Step 3 Variable A Removed R-square = 0.95690434 C(p) = 18.31900700

	DF	Sum of Squares	Mean Square	F	Prob>F
Regression	6	409603.44257027	68267.24042838	62.91	0.0001
Error	17	18447.12089781	1085.12475869		
Total	23	428050.56346808			

Variable	Parameter Estimate	Standard Error	Type II Sum of Squares	F	Prob>F
INTERCEP	23.57667061	16.10112571	2326.65581775	2.14	0.1614
B	94.42408291	8.33752284	139178.17900342	128.26	0.0001
C	20.18871623	8.50501007	6114.30945337	5.63	0.0297
D	81.07750212	8.12975620	107925.81805044	99.46	0.0001
AC	76.76585456	7.85461936	103649.10663245	95.52	0.0001
BB	71.21001373	17.76286016	17439.57985901	16.07	0.0009
BC	20.49214430	8.46050970	6365.92368868	5.87	0.0269

Bounds on condition number: 1.336376, 41.62251

Step 4 Variable C Removed R-square = 0.94262026 C(p) = 25.70535911

	DF	Sum of Squares	Mean Square	F	Prob>F
Regression	5	403489.13311691	80697.82662338	59.14	0.0001
Error	18	24561.43035118	1364.52390840		
Total	23	428050.56346808			

Variable	Parameter Estimate	Standard Error	Type II Sum of Squares	F	Prob>F
INTERCEP	2.85201247	15.17048628	48.22641574	0.04	0.8530
B	91.64946960	9.25715092	133747.71574779	98.02	0.0001
D	83.79721108	9.02551273	117624.15401392	86.20	0.0001
AC	79.02618940	8.74300634	111481.20261605	81.70	0.0001
BB	89.21000217	18.01257341	33470.07780883	24.53	0.0001
BC	19.28198194	9.47016115	5656.78607155	4.15	0.0567

Bounds on condition number: 1.092831, 26.54655

Step 5 Variable BC Removed R-square = 0.92940503 C(p) = 32.38934645

	DF	Sum of Squares	Mean Square	F	Prob>F
Regression	4	397832.34704536	99458.08676134	62.54	0.0001
Error	19	30218.21642272	1590.43244330		
Total	23	428050.56346808			

Variable	Parameter Estimate	Standard Error	Type II Sum of Squares	F	Prob>F
INTERCEP	0.16619678	16.31618071	0.16501501	0.00	0.9920
B	88.97753885	9.89318598	128648.18315553	80.89	0.0001
D	86.58326925	9.63140170	128529.90713735	80.81	0.0001
AC	80.71261773	9.39658782	117343.14886820	73.78	0.0001
BB	89.37672020	19.44635971	33595.98849491	21.12	0.0002

Bounds on condition number: 1.092809, 16.80129

All variables left in the model are significant at the 0.0100 level.

Summary of Backward Elimination Procedure for Dependent Variable PERM

Step	Variable Removed	Number In	Partial R**2	Model R**2	C(p)	F	Prob>F
1	BD	8	0.0020	0.9766	9.3451	1.3451	0.2655
2	AB	7	0.0087	0.9680	13.0511	5.5776	0.0321
3	A	6	0.0111	0.9569	18.3190	5.5240	0.0319
4	C	5	0.0143	0.9426	25.7054	5.6347	0.0297
5	BC	4	0.0132	0.9294	32.3893	4.1456	0.0567

Model: MODEL1
Dependent Variable: PERM

Analysis of Variance

Source	DF	Sum of Squares	Mean Square	F Value	Prob>F
Model	4	397832.34705	99458.08676	62.535	0.0001
Error	19	30218.21642	1590.43244		
C Total	23	428050.56347			

Root MSE	39.88023	R-square	0.9294
Dep Mean	65.22750	Adj R-sq	0.9145
C.V.	61.14021		

Parameter Estimates

Variable	DF	Parameter Estimate	Standard Error	T for H0: Parameter=0	Prob > |T|
INTERCEP	1	0.166197	16.31618071	0.010	0.9920
B	1	88.977539	9.89318598	8.994	0.0001
D	1	86.583269	9.63140170	8.990	0.0001
AC	1	80.712618	9.39656782	8.590	0.0001
BB	1	89.376720	19.44635971	4.596	0.0002

DATA FOR MODEL FITTING OF CO2 PERMEATION FOR HPPO
WITH NEW DATA FROM OPTIMIZATION

OBS	N	A	B	C	D	PERM	RATIO	VARP	VARR	BC
1	1	-1	-1.00	-1	-1.00	0.154	124.750	0.00	3543.02	1.00
2	2	-1	-1.00	-1	-1.00	0.070	208.929	0.00	3543.02	1.00
3	3	1	-1.00	-1	1.00	0.069	1.030	0.00	0.07	1.00
4	4	1	-1.00	-1	1.00	0.119	1.400	0.00	0.07	1.00
5	5	-1	1.00	-1	1.00	259.772	0.600	2011.56	0.01	-1.00
6	6	-1	1.00	-1	1.00	323.200	0.480	2011.56	0.01	-1.00
7	7	1	1.00	-1	-1.00	4.788	2.490	0.81	0.01	-1.00
8	8	1	1.00	-1	-1.00	4.582	2.430	0.81	0.01	-1.00
9	9	1	1.00	-1	-1.00	3.135	2.650	0.81	0.01	-1.00
		-1	-1.00	1	1.00	0.066	34.790	0.00	11174.48	-1.00
			-1.00	1	1.00	0.062	184.286	0.00	11174.48	-1.00
			-1.00	1	-1.00	0.050	176.000	0.00	8738.42	-1.00
			1.00	1	-1.00	0.059	43.800	0.00	8738.42	-1.00
			1.00	1	-1.00	10.944	1.400	1.00	1.00	1.00
15			1.00	1	1.00	456.761	0.680	2960.51	0.00	1.00
16			1.00	1	1.00	379.813	0.720	2960.51	0.00	1.00
17	1		0.00	-1	0.00	0.409	119.000	1.00	1.00	0.00
18	18	0	0.00	-1	0.00	0.714	17.000	1.00	1.00	0.00
19	19	0	0.00	-1	0.00	0.412	21.100	1.00	1.00	0.00
20	20	0	0.25	-1	-0.85	0.553	19.200	1.00	1.00	-0.25
21	21	0	0.25	-1	-0.85	0.966	14.400	1.00	1.00	-0.25
22	22	-1	0.40	-1	-0.65	55.400	0.700	1.00	1.00	-0.40
23	23	-1	0.40	-1	-0.65	25.320	0.700	1.00	1.00	-0.40
24	24	-1	0.40	-1	-0.65	38.040	0.700	1.00	1.00	-0.40

OBS	AC	AB	BB	BD	WP	WR	PREDICT	RESID
1	1	1.0	1.0000	1.0000	281.83	0.00	-5.305	5.460
2	1	1.0	1.0000	1.0000	281.83	0.00	-5.305	5.375
3	-1	-1.0	1.0000	-1.0000	788.25	14.61	6.436	-6.367
4	-1	-1.0	1.0000	-1.0000	788.25	14.61	6.436	-6.317
5	1	-1.0	1.0000	1.0000	0.00	138.89	345.816	-86.044
6	1	-1.0	1.0000	1.0000	0.00	138.89	345.816	-22.616
7	-1	1.0	1.0000	-1.0000	1.23	77.32	11.225	-6.437
8	-1	1.0	1.0000	-1.0000	1.23	77.32	11.225	-6.642
9	-1	1.0	1.0000	-1.0000	1.23	77.32	11.225	-8.089
10	-1	1.0	1.0000	-1.0000	153297.30	0.00	6.436	-6.370
11	-1	1.0	1.0000	-1.0000	153297.30	0.00	6.436	-6.374
12	1	-1.0	1.0000	1.0000	26825.36	0.00	-5.305	5.356
13	1	-1.0	1.0000	1.0000	26825.36	0.00	-5.305	5.364
14	-1	-1.0	1.0000	-1.0000	1.00	1.00	11.225	-0.281
15	1	1.0	1.0000	1.0000	0.00	1250.00	345.816	110.945
16	1	1.0	1.0000	1.0000	0.00	1250.00	345.816	33.997
17	0	0.0	0.0000	0.0000	1.00	1.00	0.166	0.242
18	0	0.0	0.0000	0.0000	1.00	1.00	0.166	0.548
19	0	0.0	0.0000	0.0000	1.00	1.00	0.166	0.246
20	0	0.0	0.0625	-0.2125	1.00	1.00	-45.599	46.152
21	0	0.0	0.0625	-0.2125	1.00	1.00	-45.599	46.565
22	1	-0.4	0.1600	-0.2600	1.00	1.00	74.491	-19.091
23	1	-0.4	0.1600	-0.2600	1.00	1.00	74.491	-49.171
24	1	-0.4	0.1600	-0.2600	1.00	1.00	74.491	-36.451

PLOT OF RESIDUALS VS. PREDICTED VALUE OF CO2 PERMEATION

Plot of RESID*PREDICT. Legend: A = 1 obs, B = 2 obs, etc.

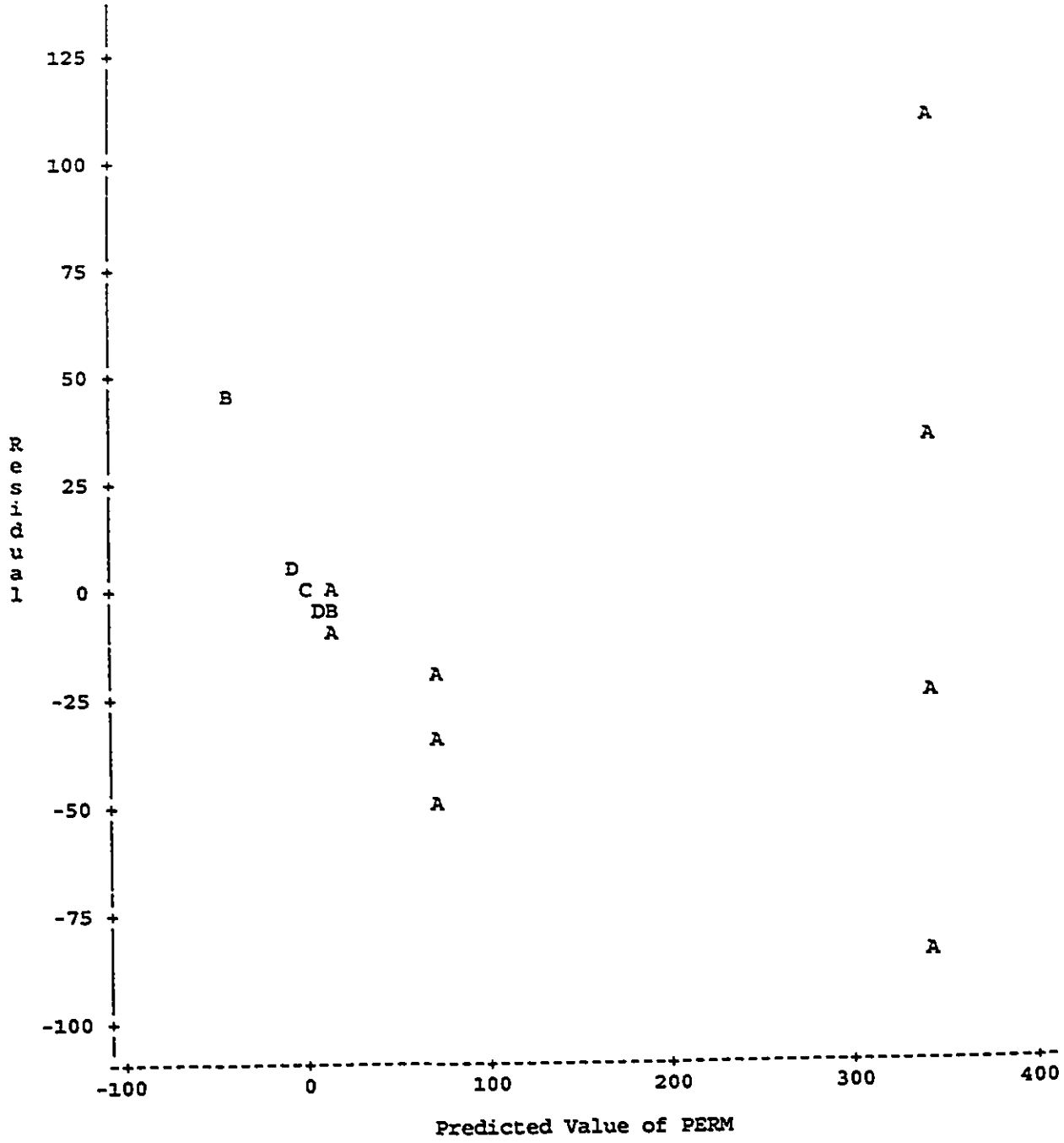

The SAS System

Backward Elimination Procedure for Dependent Variable RATIO

Step 0 All Variables Entered R-square = 0.69608290 C(p) = 10.00000000

	DF	Sum of Squares	Mean Square	F	Prob>F
Regression	9	71573.97311452	7952.66367939	3.56	0.0166
Error	14	31249.94754509	2232.13911036		
Total	23	102823.92065961			

Variable	Parameter Estimate	Standard Error	Type II Sum of Squares	F	Prob>F
INTERCEP	48.23925385	26.02323733	7670.07790611	3.44	0.0850
A	-20.54197833	12.29351164	6232.37931074	2.79	0.1169
B	-48.27149616	12.27485242	34519.95475389	15.46	0.0015
C	6.02859482	12.28755709	537.30681911	0.24	0.6313
D	-19.26854513	12.02216478	5733.94804531	2.57	0.1313
AC	-36.73920172	30.90587424	3154.26823235	1.41	0.2543
AB	21.01568351	12.29049479	6526.33799372	2.92	0.1093
BB	0.71408076	28.05677097	1.44590760	0.00	0.9801
BD	57.59925063	31.64572471	7394.77274437	3.31	0.0902
BC	-6.46550291	12.29317990	617.44376014	0.28	0.6072

Bounds on condition number: 7.969977, 215.8759

Step 1 Variable BB Removed R-square = 0.69606884 C(p) = 8.00064777

	DF	Sum of Squares	Mean Square	F	Prob>F
Regression	8	71572.52720692	8946.56590086	4.29	0.0074
Error	15	31251.39345270	2083.42623018		
Total	23	102823.92065961			

Variable	Parameter Estimate	Standard Error	Type II Sum of Squares	F	Prob>F
INTERCEP	48.83491955	10.99225794	41121.15069389	19.74	0.0005
A	-20.53226783	11.87121409	6232.49149686	2.99	0.1042
B	-48.26994506	11.85876224	34518.58724381	16.57	0.0010
C	6.13947275	11.10002353	637.37126586	0.31	0.5883
D	-19.24510359	11.58064772	5753.77576347	2.76	0.1173
AC	-37.04476466	27.51363252	3776.90397340	1.81	0.1982
AB	21.02992761	11.86170370	6548.76702567	3.14	0.0965
BD	57.90264020	28.32141525	8708.53211364	4.18	0.0589
BC	-6.47459115	11.87160336	619.70367202	0.30	0.5935

Bounds on condition number: 6.767278, 159.5944

Step 2 Variable BC Removed R-square = 0.69004200 C(p) = 6.27827548

	DF	Sum of Squares	Mean Square	F	Prob>F
Regression	7	70952.82353490	10136.11764784	5.09	0.0034
Error	16	31871.09712471	1991.94357029		
Total	23	102823.92065961			

Variable	Parameter Estimate	Standard Error	Type II Sum of Squares	F	Prob>F
INTERCEP	49.76155310	10.61904588	43741.52191334	21.96	0.0002
A	-21.02463354	11.57404337	6573.00087339	3.30	0.0881
B	-47.26878600	11.45571488	33914.19680295	17.03	0.0008
C	6.70651599	10.80587098	767.27563087	0.39	0.5436
D	-20.24015617	11.18212797	6526.13168786	3.28	0.0891
AC	-36.86703265	26.90090670	3741.27439687	1.88	0.1895
AB	20.53866961	11.56486851	6282.61215579	3.15	0.0948
BD	56.72359710	27.61184639	8406.46987504	4.22	0.0567

Bounds on condition number: 6.766329, 131.2324

Step 3 Variable C Removed R-square = 0.68257996 C(p) = 4.62201554

	DF	Sum of Squares	Mean Square	F	Prob>F
Regression	6	70185.54790403	11697.59131734	6.09	0.0015
Error	17	32638.37275558	1919.90427974		
Total	23	102823.92065961			

Variable	Parameter Estimate	Standard Error	Type II Sum of Squares	F	Prob>F
INTERCEP	47.63155027	9.86577729	44751.37621515	23.31	0.0002
A	-20.39385696	11.31893283	6232.57264212	3.25	0.0893
B	-48.32860061	11.12100608	36257.66739794	18.89	0.0004
D	-18.99798783	10.80078559	5939.96789421	3.09	0.0966
AC	-38.82617523	26.22752839	4207.40254866	2.19	0.1571
AB	21.20252475	11.30515214	6753.08027362	3.52	0.0780
BD	59.73801409	26.68527721	9621.38739174	5.01	0.0388

Bounds on condition number: 6.673158, 103.3171

Step 4 Variable AC Removed R-square = 0.64166144 C(p) = 4.50693504

	DF	Sum of Squares	Mean Square	F	Prob>F
Regression	5	65978.14535537	13195.62907107	6.45	0.0013
Error	18	36845.77530424	2046.98751690		
Total	23	102823.92065961			

Variable	Parameter Estimate	Standard Error	Type II Sum of Squares	F	Prob>F
INTERCEP	42.10907548	9.43072334	40810.94001362	19.94	0.0003
A	-12.88593465	10.44864021	3113.34675622	1.52	0.2333
B	-51.88520500	11.21200429	43836.48845044	21.42	0.0002
D	-14.29000529	10.65809595	3679.77040678	1.80	0.1967
AB	25.45038782	11.29102968	10400.08540073	5.08	0.0369
BD	23.72069900	11.31824748	8991.07847481	4.39	0.0505

Bounds on condition number: 1.024721, 25.35834

Step 5 Variable A Removed R-square = 0.61138301 C(p) = 3.90171673

	DF	Sum of Squares	Mean Square	F	Prob>F
Regression	4	62864.79859915	15716.19964979	7.47	0.0009
Error	19	39959.12206047	2103.11168739		
Total	23	102823.92065961			

Variable	Parameter Estimate	Standard Error	Type II Sum of Squares	F	Prob>F
INTERCEP	42.76512603	9.54391485	42226.85501897	20.08	0.0003
B	-52.47304124	11.35439551	44916.58942062	21.36	0.0002
D	-14.26125492	10.80319357	3664.99601601	1.74	0.2025
AB	24.62998167	11.42489059	9774.31688848	4.65	0.0441
BD	24.63247756	11.44785812	9737.10944624	4.63	0.0445

Bounds on condition number: 1.021164, 16.20328

Step 6 Variable D Removed R-square = 0.57573960 C(p) = 3.54363770

	DF	Sum of Squares	Mean Square	F	Prob>F
Regression	3	59199.80258314	19733.26752771	9.05	0.0005
Error	20	43624.11807647	2181.20590382		
Total	23	102823.92065961			

Variable	Parameter Estimate	Standard Error	Type II Sum of Squares	F	Prob>F
INTERCEP	44.82892664	9.58820652	47680.25682575	21.86	0.0001
B	-51.73861819	11.54939490	43773.15533055	20.07	0.0002
AB	25.46640618	11.61716916	10481.69120329	4.81	0.0404
BD	24.13064601	11.65203613	9354.72267139	4.29	0.0515

Bounds on condition number: 1.018024, 9.109558

All variables left in the model are significant at the 0.1000 level.

Summary of Backward Elimination Procedure for Dependent Variable RATIO

Step	Variable Removed	Number In	Partial R**2	Model R**2	C(p)	F	Prob>F
1	BB	8	0.0000	0.6961	8.0006	0.0006	0.9801
2	BC	7	0.0060	0.6900	6.2783	0.2974	0.5935
3	C	6	0.0075	0.6826	4.6220	0.3852	0.5436
4	AC	5	0.0409	0.6417	4.5069	2.1915	0.1571
5	A	4	0.0303	0.6114	3.9017	1.5209	0.2333
6	D	3	0.0356	0.5757	3.5436	1.7427	0.2025

Model: MODEL1
Dependent Variable: RATIO

Analysis of Variance

Source	DF	Sum of Squares	Mean Square	F Value	Prob>F
Model	3	59199.80258	19733.26753	9.047	0.0005
Error	20	43624.11808	2181.20590		
C Total	23	102823.92066			

Root MSE	46.70338	R-square	0.5757
Dep Mean	40.80143	Adj R-sq	0.5121
C.V.	114.46507		

Parameter Estimates

Variable	DF	Parameter Estimate	Standard Error	T for H0: Parameter=0	Prob > |T|
INTERCEP	1	44.828927	9.58820652	4.675	0.0001
B	1	-51.738618	11.54939490	-4.480	0.0002
AB	1	25.466406	11.61716916	2.192	0.0404
BD	1	24.130646	11.65203613	2.071	0.0515

DATA FOR MODEL FITTING OF CO2/CH4 RATIO FOR HPPO
WITH THE NEW DATA FROM OPTIMISATION

OBS	N	A	B	C	D	PERM	RATIO	VARP	VARR	BC
1	1	-1	-1.00	-1	-1.00	0.154	124.750	0.00	3543.02	1.00
2	2	-1	-1.00	-1	-1.00	0.070	208.929	0.00	3543.02	1.00
3	3	1	-1.00	-1	1.00	0.069	1.030	0.00	0.07	1.00
4	4	1	-1.00	-1	1.00	0.119	1.400	0.00	0.07	1.00
5	5	-1	1.00	-1	1.00	259.772	0.600	2011.56	0.01	-1.00
6	6	-1	1.00	-1	1.00	323.200	0.480	2011.56	0.01	-1.00
7	7	1	1.00	-1	-1.00	4.788	2.490	0.81	0.01	-1.00
8	8	1	1.00	-1	-1.00	4.582	2.430	0.81	0.01	-1.00
9	9	1	1.00	-1	-1.00	3.135	2.650	0.81	0.01	-1.00
10	10	-1	-1.00	1	1.00	0.066	34.790	0.00	11174.48	-1.00
11	11	-1	-1.00	1	1.00	0.062	184.286	0.00	11174.48	-1.00
12	12	1	-1.00	1	-1.00	0.050	176.000	0.00	8738.42	-1.00
13	13	1	-1.00	1	-1.00	0.059	43.800	0.00	8738.42	-1.00
14	14	-1	1.00	1	-1.00	10.944	1.400	1.00	1.00	1.00
15	15	1	1.00	1	1.00	456.761	0.680	2960.51	0.00	1.00
16	16	1	1.00	1	1.00	379.813	0.720	2960.51	0.00	1.00
17	17	0	0.00	-1	0.00	0.409	119.000	1.00	1.00	0.00
18	18	0	0.00	-1	0.00	0.714	17.000	1.00	1.00	0.00
19	19	0	0.00	-1	0.00	0.412	21.100	1.00	1.00	0.00
20	20	0	0.25	-1	-0.85	0.553	19.200	1.00	1.00	-0.25
21	21	0	0.25	-1	-0.85	0.966	14.400	1.00	1.00	-0.25
22	22	-1	0.40	-1	-0.65	55.400	0.700	1.00	1.00	-0.40
23	23	-1	0.40	-1	-0.65	25.320	0.700	1.00	1.00	-0.40
24	24	-1	0.40	-1	-0.65	38.040	0.700	1.00	1.00	-0.40

OBS	AC	AB	BB	BD	WP	WR	PREDICT	RESID
1	1	1.0	1.0000	1.0000	281.83	0.00	146.165	-21.4146
2	1	1.0	1.0000	1.0000	281.83	0.00	146.165	62.7640
3	-1	-1.0	1.0000	-1.0000	788.25	14.61	46.970	-45.9405
4	-1	-1.0	1.0000	-1.0000	788.25	14.61	46.970	-45.5705
5	1	-1.0	1.0000	1.0000	0.00	138.89	-8.245	8.8455
6	1	-1.0	1.0000	1.0000	0.00	138.89	-8.245	8.7255
7	-1	1.0	1.0000	-1.0000	1.23	77.32	-5.574	8.0639
8	-1	1.0	1.0000	-1.0000	1.23	77.32	-5.574	8.0039
9	-1	1.0	1.0000	-1.0000	1.23	77.32	-5.574	8.2239
10	-1	1.0	1.0000	-1.0000	153297.30	0.00	97.903	-63.1133
11	-1	1.0	1.0000	-1.0000	153297.30	0.00	97.903	86.3824
12	1	-1.0	1.0000	1.0000	26825.36	0.00	95.232	80.7682
13	1	-1.0	1.0000	1.0000	26825.36	0.00	95.232	-51.4318
14	-1	-1.0	1.0000	-1.0000	1.00	1.00	-56.507	57.9067
15	1	1.0	1.0000	1.0000	0.00	1250.00	42.687	-42.0074
16	1	1.0	1.0000	1.0000	0.00	1250.00	42.687	-41.9674
17	0	0.0	0.0000	0.0000	1.00	1.00	44.829	74.1711
18	0	0.0	0.0000	0.0000	1.00	1.00	44.829	-27.8289
19	0	0.0	0.0000	0.0000	1.00	1.00	44.829	-23.7289
20	0	0.0	0.0625	-0.2125	1.00	1.00	26.767	-7.5665
21	0	0.0	0.0625	-0.2125	1.00	1.00	26.767	-12.3665
22	1	-0.4	0.1600	-0.2600	1.00	1.00	7.673	-6.9729
23	1	-0.4	0.1600	-0.2600	1.00	1.00	7.673	-6.9729
24	1	-0.4	0.1600	-0.2600	1.00	1.00	7.673	-6.9729

PLOT OF RESIDUALS VS. PREDICTED VALUE OF RATIO

Plot of RESID*PREDICT. Legend: A = 1 obs, B = 2 obs, etc.

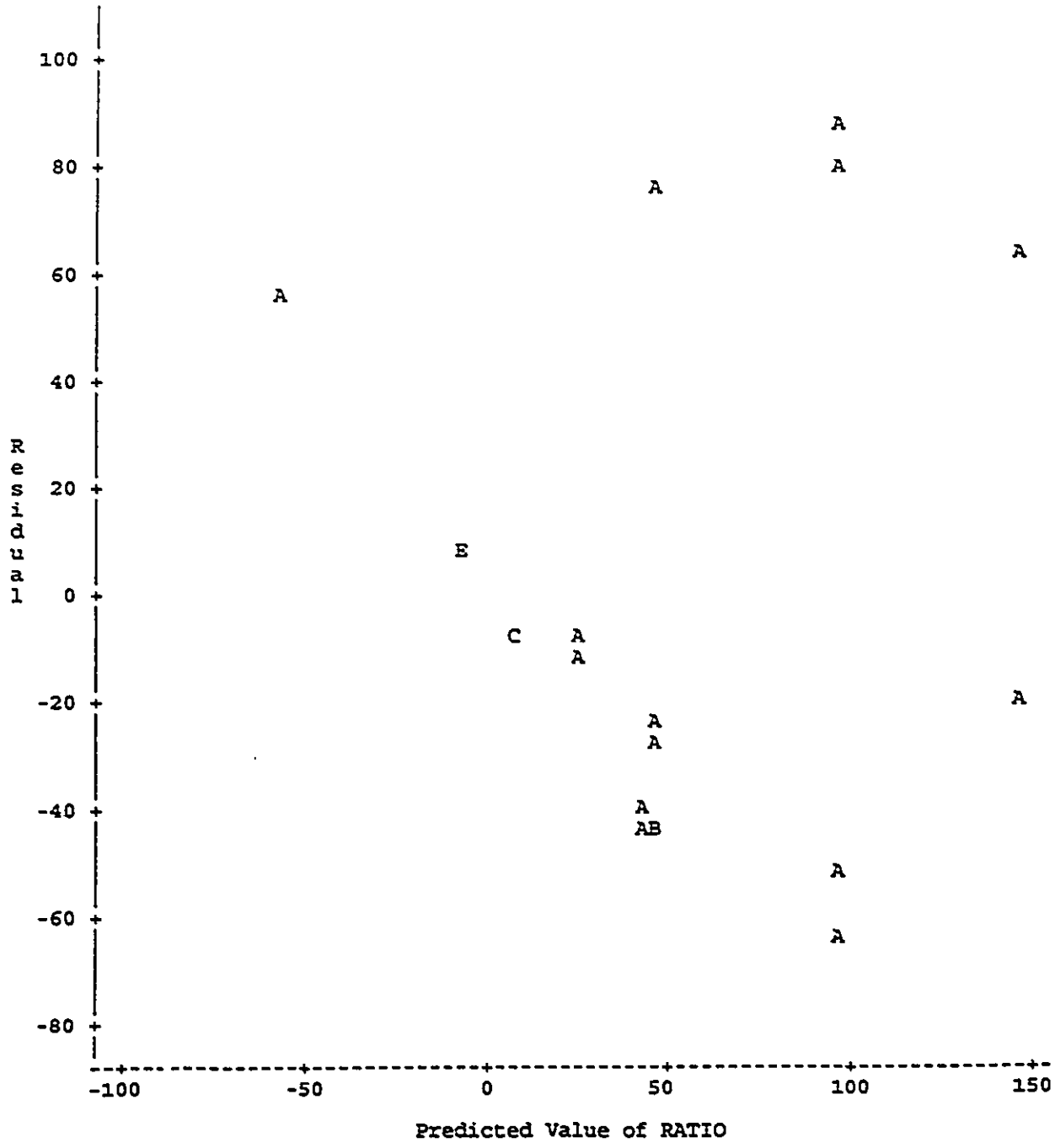

Appendix D

Gas Chromatograph Settings

initial column temperature: 50 °C

initial column hold: 3 min

final temperature: 210 °C

rate: 26.6 °C/min

hold: 8 min

injection temperature: 60 °C

detector temperature: 160 °C

detector: A

attenuation: 256

attenuation range: 0.5

autozero: yes

filament temperature: 250 °C

polarity: positive

TCD time: 17 min